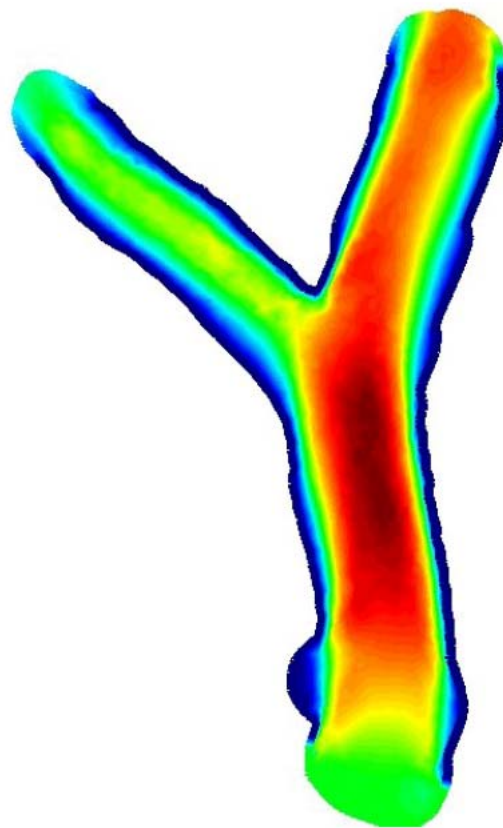


Numerical Validation of Hemodynamic Factors in Vascular Diseases

M. Bordone
E. Oñate
E. Soudah



Numerical Validation of Hemodynamic Factors in Vascular Diseases

M. Bordone
E. Oñate
E. Soudah

Publication CIMNE N°-315, February 2008

Index of contents

Chapter 1.	Introduction	9
1.1	Hemodynamic and mathematical investigation	9
1.2	Medical background.....	10
1.3	Predictive medicine	12
1.4	Project structure	12
Chapter 2.	Mathematical and physical theory	14
2.1	Governing Equations	15
2.2	The Womersley velocity solution.....	16
Chapter 3.	The cases.....	20
Chapter 4.	Aorta modeling like long and straight artery (Womersley’s solution).....	22
4.1	Geometry, Mesh and Data.....	22
4.2	Results.....	26
Chapter 5.	Steady Flow in an End to Side Anastomosis (graft bifurcation)	31
5.1	Geometry, Mesh and Data.....	32

5.2	Results.....	38
Chapter 6.	Pulsatile Flow in an End to Side Anastomosis (graft bifurcation)	54
6.1	Data: the pulsatile blood flow	54
6.2	Results.....	57
Chapter 7.	Carotid bifurcation (pulsatile flow)	62
7.1	Geometry, Mesh and Data.....	63
7.2	The pulsatile blood flow.....	67
7.3	Results.....	71
Chapter 8.	Idealized abdominal Aorta	75
8.1	Geometry, Mesh and Data.....	77
8.2	Weak blood flow	80
8.3	The flow rate.....	81
8.4	Results.....	81
Chapter 9.	Real Carotid.....	85
9.1	Data and conditions.....	87
9.2	Results.....	88
Chapter 10.	Real Aorta reconstruction	93
10.1	Data and Geometry	94
10.2	Results.....	96
Chapter 11.	Conclusions	99
Appendix A.	MatLab Programs.....	114
Appendix B.	TCL Statement	118
Appendix C.	Tdyn Graphics.....	123
References		126
11.1	Books, newspaper and journal	126
11.2	Web sites.....	128

Index of illustrations

Fig. 1.1 Example of obstructed vessel.....	11
Fig. 2.1 Womersley velocity profiles in 4 different instants	18
Fig. 4.1 Geometrical representation of the vessel	23
Fig. 4.2 Mesh visualization of the vessel.....	24
Fig. 4.3 Flow profile.....	25
Fig. 4.4 Comparison of the Womersley velocity solution with the results of 2 different meshes.....	27
Fig. 4.5 Visualization of the external portion of the fluid.....	27
Fig. 4.6 Variation of the error expressed in percent, varying in the diameter	28
Fig. 4.7 Variation of the error in absolute value, varying in the diameter.....	29
Fig. 4.8 Evolution of the error in the time (4 different cases).....	30
Fig. 5.1 Geometry of the graft model.....	32
Fig. 5.2 Graft model geometry representation.....	32

Fig. 5.3 Mesh visualization in the plane XY	33
Fig. 5.4 3D representation of the graft model (mesh visualization)	34
Fig. 5.5 Representation of the velocity in the inner section.....	35
Fig. 5.6 Representations of the velocities profiles in the Distal Outgoing Section (upside) and in the Proximal Outgoing Section (downside)	36
Fig. 5.7 Positions of the cuts realized (zero point is marked with a red cross).....	37
Fig. 5.8 Series of the results of the velocity varying the point of cut.....	43
Fig. 5.9 Velocity profile in X direction, this is the principal direction of the velocity	45
Fig. 5.10 Velocity profile in Y direction, this is the vertical direction	45
Fig. 5.11 Series of results obtained changing the pressure imposed.....	49
Fig. 5.12 Series of results obtained changing the elements dimension.....	53
Fig. 6.1 Polynomial interpolation: best polinomy choice	56
Fig. 6.2 Evolution of the flow velocity profile at 45°, 90°,120° and	58
Fig. 6.3 X and Y Velocity profile in the 2 section for the 4 time instants	60
Fig. 6.4 3D representations of velocity profiles	61
Fig. 7.1 Carotid anatomy	63
Fig. 7.2 Geometry model of idealized carotid vessel.....	64
Fig. 7.3 Geometry model realized for carotid test.....	65
Fig. 7.4 3D mesh representation of carotid model.....	66
Fig. 7.5 Angles changed to obtain larger ones	67
Fig. 7.6 Test results for best polinomy choice	68
Fig. 7.7 Interpolation of the first part of the flow	70
Fig. 7.8 The arrow shows the negative velocity and blood reflow. The white line shows the cut effectuated.....	72
Fig. 7.9 Representation of the Y velocity profile (principal direction) in the cut zone.....	74
Fig. 8.1 Abdominal Aorta anatomy	77
Fig. 8.2 Geometry visualization of the Idealized Aorta Model.....	78
Fig. 8.3 Mesh visualization of the Idealized Aorta model.....	79
Fig. 8.4 Blood flow rate profile in aorta test.....	80
Fig. 8.5 Studied exit surfaces.....	82
Fig. 8.6 Representation of the 3 flow rate registered at the exit surfaces.....	84
Fig. 9.1 3D visualization of the geometry obtained by the Voxelization	86
Fig. 9.2 Velocity registered in different places of the model.....	89

Fig. 9.3 Velocity profile at 90°, 180°, 270° and 360° 92

Fig. 10.1 Geometry of the reconstructed aorta, geometry and mesh visualization 94

Fig. 10.2 Representation of the absolute value of velocities 95

Fig. 10.3 Representation of the velocity profiles in the ascending zone..... 96

Fig. 10.4 Representation of the velocity profiles in the aortic arc..... 97

Fig. 10.5 Representation of the velocity profiles in the descendent zone..... 98

1. Introduction

1.1. Hemodynamic and mathematical investigation

Hemodynamic forces are very important determinants of the structure and function of the vascular system, during growth and development, as well as during adult life.

Blood flow factors also play an important role in the localization of the atherosclerotic plaques, which can obstruct the lumen and prevent blood flow, and generates in artery wall the plaque degenerative processes.

Understanding the nature and the interaction of the forces on the artery wall could make a significant contribution to prevent and to diagnostic a vascular disease

The human vascular system is composed by the heart and blood vessels, and functions in such a way as to supply each organ demands.

The arteries, supplying blood, must respond to local changes in the organs while maintaining overall homeostasis of the circulatory system. Normally the artery can adapt itself to the changes in blood flow or pressure. However the adaptive and healing processes fail and the arteries are unable to respond to the imposed forces and, in some worst cases, are unable to provide blood to important organs.

Various methods have been applied in an effort to understand vascular function, ranging from dissection and animal experiments to the development of physical and mathematical models. Recently was introduced the numerical methods for solving the equations resulting from a mathematical model of hemodynamic situation.

The mayor factor of problems is the difficulty to create models, the problem of the discretization, the algorithms solutions and the visualization of the results to insufficient computing power, so the study of the hemodynamic have been limited in scope to simple problems of flow in a single, often over-idealized, vascular branch.

1.2. Medical background

The modern surgical techniques sometimes use graft or bypass to resolve some cardiovascular problem; is so important to see how this practice can change the normal way of propagation of the blood flow, and what problems can source by them.

Surgical bypass treats narrowed arteries by creating a bypass around a section of the artery that is blocked. These arteries are normally smooth and unobstructed on the inside but they can become blocked through a process called arteriosclerosis, which means hardening of the arteries. As you age, a sticky substance called plaque can build up in the walls of your arteries. Cholesterol, calcium, and fibrous tissue make up the plaque.

Blockage in right coronary artery

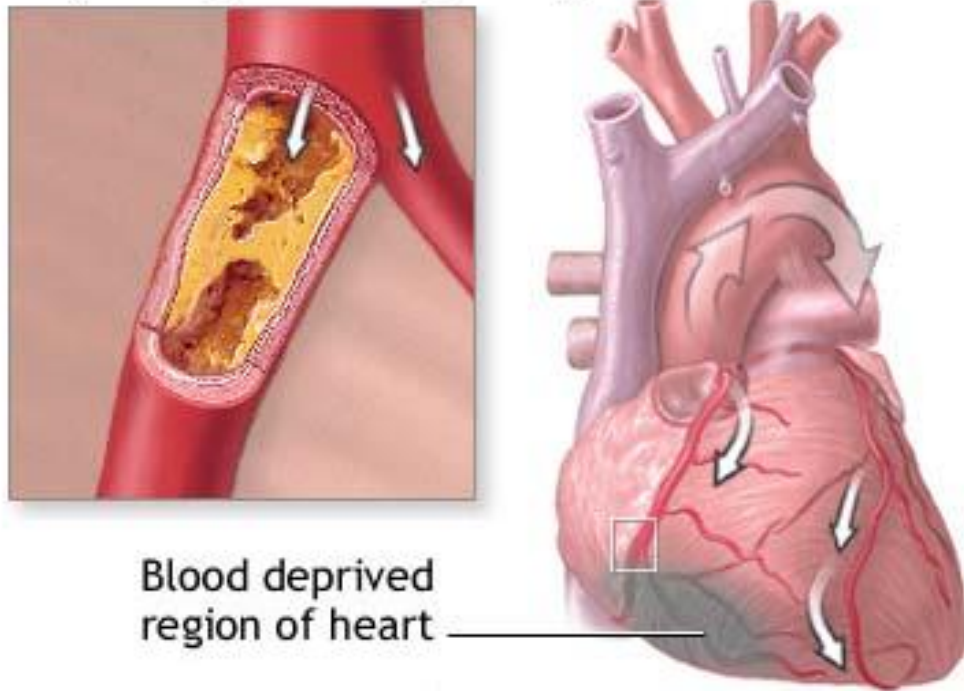


Figure 1 Example of obstructed vessel

As more plaque builds up, arteries can narrow and stiffen. Eventually, as the process progresses, the blood vessels can no longer supply the oxygen demands of the organs or muscles and symptoms may develop.

During a bypass, vascular surgeon creates a new pathway for blood flow using a graft. A graft is a portion of one of your veins or a man-made synthetic tube that your surgeon connects above and below a blockage to allow blood to pass around it.

We can find different places where apply this surgical operation: heart vessel and peripheral arterial like leg vessel.

We surely say that another phenomenon of considerable clinical importance is the pulsatile flow in a carotid artery. We can note that plaques localized in the carotid sinus region where wall shear stress is low and particle residence time is high.

In the carotid artery, atherosclerotic lesions localize in the carotid sinus, the enlarged region just beyond the bifurcation, and can might, restrict cerebral flow. Ultimately carotid

bifurcation arteriosclerosis can result in plaque disruption and clot formation resulting in stroke.

1.3. Predictive medicine

Computer technology, pervasive in our society, is gaining wide spread use in medical field.

Medical professionals use computers to access and store data, informations or important medical or scientific results. Is also possible to find another important development in the use of computer technology for acquiring and storing raw data, as well as extracting anatomic and physiologic information.

Another application of the computers, with big implications in the medical fields, is the use of hardware and software technology to evaluate, support and predict medical decision.

The opportunity exists to develop software to augment the information available from medical diagnostic imaging of individual patient and employ diagnostic information to initialize predictive patient-specific computer models of surgical planning.

It is expected that the additional information which can be obtained from predictive versus exclusively diagnostic or experience based approaches will lead to improved patient care with fewer short-term and long-term complications In the predictive medicine paradigm, a surgeon would decide which corrective procedure to perform based on experience, diagnostic information from different medical imaging data sources, and predictive physiologic computer simulations.

1.4. Project structure

Here is presented the plan of the project and a little explication of the works realized in every single chapter of this thesis for the obtainment of the objects proposed

- In the chapter 2 is illustrated the mathematical and physical theory used in the development of the project: the Navier-Stokes equations and the form of the Womersley velocity solution, finally a little introduction to the f.e.m. softwares.
- In the chapter 3 we have a panoramic vision on the experiments made and a little overview of the single characteristics.
- The chapter numbered by 4 to 10 are dedicated to the explication of the experiments made, the ways to realized them, the problems met and the results are showed with plots and comments.
- The chapter 11 illustrates the conclusions , the future plans of research and the possible applications of the results obtained in this work.
- The appendixes, in the last part of this document, show the informatic procedures used to solve the problem that we encountered, like matlab code, tcl code and the question of design with graphic tools of Tdyn.
- Finally are showed the bibliography and the sources used to write this work and to resolve the problems of the project.

2. Mathematical and physical theory

The problems of computational modeling of flow require solving, generally, three dimensional, transient flow equations in deforming blood vessels.

The appropriate framework for problems of this type is the arbitrary Lagrangian-Eulerian description of continuous media (ALE), in which the fluid and solid domains are allowed to move to follow the distensible vessel walls. This description of fluid motion simplifies to the classical Eulerian description of flow problem.

The governing equations, (Navier-Stokes) and initial and boundary conditions constitute the strong form of the problems considered in the remainder of this thesis.

The Womersley solution, the canonical analytical solution for pulsatile flow, is presented. At the end the relevance of the Womersley solution to the pulsatile flow boundary conditions employed is discussed.

2.1. Governing Equations

It was observed that the vessel diameter can change approximately 5-10% during a normal cardiac cycle in most of the major arteries and, as a first approximation, the vessel are often treated as rigid elements. In addition, in diseased vessels, which are often the subject of interest, the arteries are even less compliant and wall motion is further reduced. Under the assumption of zero wall motion, the ALE description of incompressible flow in deforming fluid domain reduces to the incompressible Navier-Stokes equations.

The strong form of the problem governing incompressible, Newtonian fluid flow in a fixed domain consists of the governing equations and suitable initial and boundary conditions. This problem is posed as follows for a domain $\Omega \rightarrow \mathfrak{R}_{sd}^\pi$ where n_{sd} is the number of spatial dimensions.

Given $f : \Omega \times (0, T) \rightarrow \mathfrak{R}_{sd}^\pi$, $g : \Gamma \times (0, T) \rightarrow \mathfrak{R}_{sd}^\pi$, $h : \Gamma_h \times (0, T) \rightarrow \mathfrak{R}_{sd}^\pi$ and

$$u_0 : \Omega \rightarrow \mathfrak{R}_{sd}^\pi .$$

We seek $u(x, t)$, and $p(x, t) \forall x \in \Omega, \forall t \in [0, T]$ such that

$$\begin{aligned}
 \rho(u_s + (u \cdot \nabla)u) &= \nabla \cdot \sigma + f & (x, t) \in \Omega \times (0, T) \\
 \nabla \cdot u &= 0 & (x, t) \in \Omega \times (0, T) \\
 u(x, 0) &= u_0(x) & x \in \Omega \\
 u &= g & (x, t) \in \Gamma_g \times (0, T) \\
 t &= h & (x, t) \in \Gamma_h \times (0, T)
 \end{aligned}
 \tag{Equation 0-1}$$

The boundary conditions described above, involving the specification of velocity on part of the boundary and traction on the remaining part, results in a well-posed problem, but it is not the only suitable of variables.

Other well-posed boundary conditions involving other combination of velocity, vorticity, traction, and pressure have been formulated.

2.2. The Womersley velocity solution

The solutions of fluid-dynamic problems can be calculated by analytical way only in a few cases, with restrictive geometry and boundary conditions but these are necessary to validate numerical solutions.

The solution is based on Navier-Stokes equations. The results give this equation:

$$\frac{\partial w}{\partial t} - \nu \left(\frac{\partial^2 w}{\partial r^2} + \frac{1}{r} \frac{\partial w}{\partial r} \right) = \frac{1}{\rho} \frac{\partial p}{\partial z} \quad \text{Equation 0-2}$$

Where w is the velocity in the axial direction, r the radius, ρ the density of the fluid, p the pressure and z the orthogonal component the direction of gravity.

Assuming the pressure gradient so:

$$\frac{\partial p}{\partial z} = A e^{i\omega t} \quad \text{Equation 0-3}$$

With A algebraically coefficient.

And we put this expression for the velocity:

$$w = u(r) e^{i\omega t} \quad \text{Equation 0-2}$$

Putting them in the *equation 1* we obtain this:

$$r^2 \frac{d^2 u}{dr^2} + r \frac{du}{dr} - i \frac{\omega}{\nu} r^2 u = -\frac{1}{\mu} A \quad \text{Equation 0-3}$$

With this signification of the symbols: ω the pulsation ν the viscosity and ν the cinematic viscosity.

Now, the equation is in the Bessel standard form of order zero, defining

$$\frac{\partial p}{\partial z} \approx \sum_{n=0}^N A_n e^{in\pi t} \quad \text{Equation 0-4}$$

And

$$x = r\sqrt{\omega/\nu}i^{3/2} \quad \text{Equation 0-5}$$

Where A_n are the algebraically coefficients of the series N the level of approximation

The solution which is bounded for $r = 0$ and satisfies the no slip boundary condition for $r = R$ is

$$u(r) = \frac{A}{i\rho\omega} \left(1 - \frac{J_0\left(\frac{\alpha r}{R}i^{3/2}\right)}{J_0(\alpha_n i^{3/2})} \right) \quad \text{Equation 0-6}$$

With α a non dimensional number called *Womersley number*, and J_0 is the Bessel coefficient of grade zero:

$$\alpha_n = \alpha\sqrt{n} \quad \text{Equation 0-7}$$

Putting the pressure gradient like a periodic function we can decompose it in Fourier coefficients. So we have this expression for the velocity where J_0 is the Bessel function of order zero.

$$w(r,t) = \sum_{n=0}^N \frac{iA_n}{\rho n \varpi} \left(1 - \frac{J_0\left(\frac{\alpha_n r}{R} i^{3/2}\right)}{J_0(\alpha_n i^{3/2})} \right) \quad \text{Equation 0-8}$$

Now we have to define the flow $Q(t)$ decomposable with Fourier's series, and we obtain its expression integrated the velocity expression. So developing the Fourier series we set A_0 how the first element of the series and the other are put in the sequent equation, obtaining the ultimate formula that we use:

$$w(r,t) = \frac{2A_0}{\pi R^2} \left[1 - \left(\frac{r}{R}\right)^2 \right] + \sum_{n=1}^N \frac{B_n}{\pi R^2} \left(\frac{1 - \frac{J_0\left(\frac{\alpha_n r}{R} i^{3/2}\right)}{J_0(\alpha_n i^{3/2})}}{1 - \frac{2J_1(\alpha_n i^{3/2})}{\alpha_n i^{3/2} J_0(\alpha_n i^{3/2})}} \right) \quad \text{Equation 0-9}$$

Solving the equations for four specific time instants we obtain the profiles shown below. The time was chosen parting the real time by the period and taking

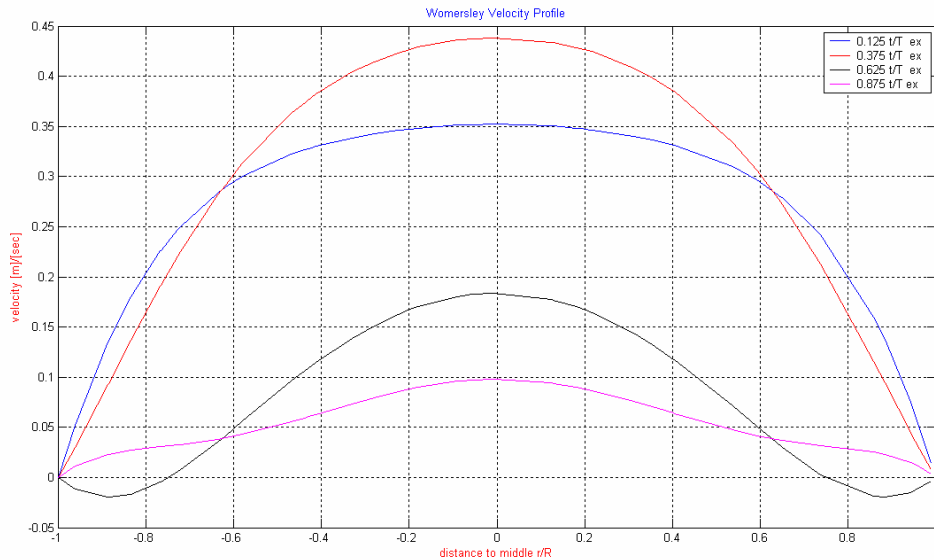


Figure 2 Womersley velocity profiles in 4 different instants

F.E.M. software

The tests that were run, were constructed with a finite elements method (F.E.M.) software. The F.E.M. software that was used was Tdyn, software developed in Compass.

Tdyn is a fluid dynamic (CFD) simulation environment based on the stabilized Finite Element Method. *Tdyn* can work with number of different turbulence models. It also uses sophisticated tools for simulating problems of many different cases: species advection, heat transfer in all kinds of materials, as well as free surface among others.

Tdyn also includes fully integrated pre/post-processing modules. *Tdyn* have a very high flexibility in defining physical properties of the model, boundary conditions, through user-defined functions that can make *Tdyn* a tool with large variety of applications. Moreover, *Tdyn* includes wizard-type utilities to take analyses definitions fast and easy to do. Finally, *Tdyn* can be easily adapted to specific needs allowing a simple and automated analysis process.

The processes of design are based on CAD tools and many options of visualization; once the geometry definition is finished, the problem data is entered in the same environment of Tdyn. The problem data definition includes the general definitions of the problem, boundary conditions and the mesh generation necessary for the analysis. With Tdyn you have the important control of the mesh generation process, by having the capability to control the size and quality of the elements. When the pre-processing phase is finished, the Tdyn calculating component is executed in the same user environment.

Likewise the results of the analysis are visualized automatically after the calculations are finished. Tdyn includes different calculating modules covering number of different areas of fluid-dynamic and heat-transfer field. Moreover, Tdyn includes a basic calculation model allowing you to simulate heat-transfer problems in solids.

Once the calculation phase is finished, the results are displayed in the post-processing module allowing you to work with the analysis. With Tdyn you can obtain the maps of a fluid pressures and velocities of a fluid on a surface, or user defined cut planes.

3. The cases

The primary target of this work is to evaluate the grade of precision that finite element method software, like Tdyn, can reach. The simulations are divided in five different cases, starting with the simpler till the more complex in geometry and methods of extrapolate the results to confront.

The Womersley velocity profile is the starting point for the test of valuation of TDyn. So the first step of this evaluation is comparing the level of precision that TDyn resolves this kind of problem; this is the simplest case, because the geometry is only constituted by a cylinder.

Another fundamental point that we have to specify is that all the testes were designed with the same geometry proposed by other researchers. Another step of research was to modify all the meshes trying to increase to number of its elements, so to see what differences can occur, how the results can receive improvements and when complicate the computation couldn't be necessary.

These procedures were utilized with all the five testes that were:

1. *Aorta modeling like long and straight artery (Womersley velocity)*
2. *Steady Flow in an End to Side Anastomosis (graft bifurcation)*
3. *Pulsatile Flow in an End to Side Anastomosis (graft bifurcation)*
4. *Carotid bifurcation (pulsatile flow)*
5. *Idealized abdominal Aorta (weak pulsatile flows)*
6. *Real Carotid geometry*
7. *Real Aorta geometry with pulsatile flow*

Note that all the testes run are imposed that the wall of the vessel can not move or expand itself.

4. Aorta modelling like long and straight artery (Womersley' s solution)

The first problem was the simulation of a sinusoidal flow in a long and straight channel. The goal is simulate the velocity profile and obtain results comparable to the solution calculated with the theoretical equations. After the attention was moved to the variation of the result in a cyclic sinusoid, so run a few cycles of the flow it's possible to how the solution converge in a stabile shape. The ultimate step was to perfect the mesh with very high number of elements and to study how the flow gets laminar close to the lateral walls.

4.1. Geometry, Mesh and Data

The construction of the geometries was done with GID software, the preprocess of Tdyn. The initial step was to define the starting points of construction of the body. After continuing with joint this points with lines and curves.

So it is possible to obtain the structure of the body. The successive step is create surfaces, the tool create Nurbs Surfaces permit us to create this ones, it is important to create regular areas to allow a good process of meshing.

Finally selecting the surfaces, those make as frontier to the body; it was possible to create the volume.

These steps were the same for all the testes. The different things were only in the difficulties to create regular and good surfaces in the geometry with particular crossing or division, with rapid variations of diameter or angles. Other important theme is the right curvature of some surfaces: to obtain good profiles, sometimes is better divide the surfaces in little ones, so the surfaces can be generated with a curvature that follow the entire profile of the body, and the program can use a regular boundary limit when has to generate and construct the volume.

Now are showed, the geometry and the data of every single test.

The geometry of this test is the simplest one. It is only a long tube with four surfaces: two lateral, an entering surface and an outgoing one. The dimensions are shown below.

- Length: 0.03 m (on X axis)
- Radius: 0.002 m

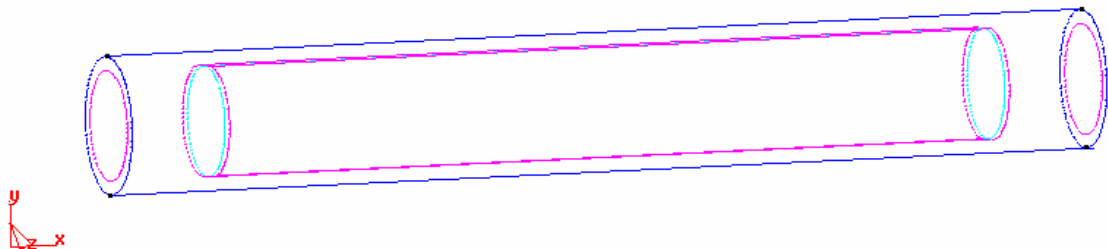


Figure 3 Geometrical representation of the vessel

The mesh was created with these proprieties and the external layer appear like shown.

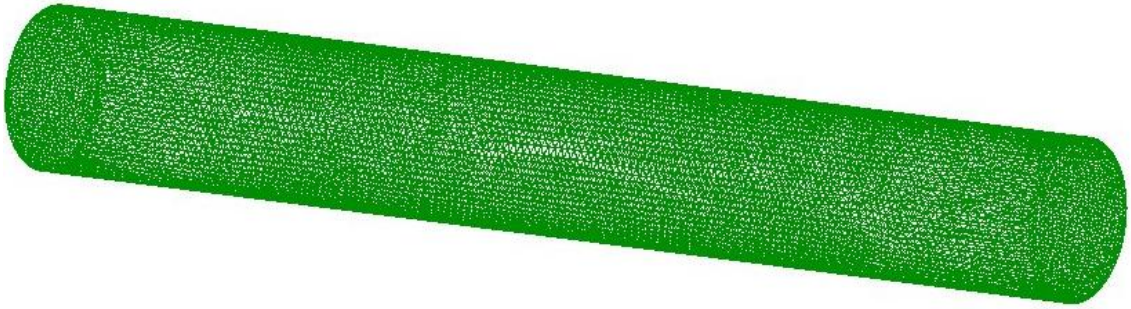


Figure 4 Mesh visualization of the vessel

Element size (m)	Triangles number	Tetraedras number
0.000163	189924	962757

The fluid body takes the same aspect in all the testes; the only different the first one, where Taylor set a different value of the density.

The model for blood flow was expressed by a regular sinusoidal wave with the next expression:

$$\bullet V(t) = V_m * (1 + \sin(2\pi t / T)) \quad m/sec$$

Where V is the velocity, V_m is the mean velocity, t the time and T the period.

Integrating this in the section of the vessel, that have a cylindrical form, is obtained this expression for the flow:

$$\bullet Q(t) = A_{vess} * V_m * (1 + \sin(2\pi t / T)) \quad m^3/sec$$

Where Q is the flow, V_m is the mean velocity, A_{vess} the area of the vessel section, t the time and T the period.

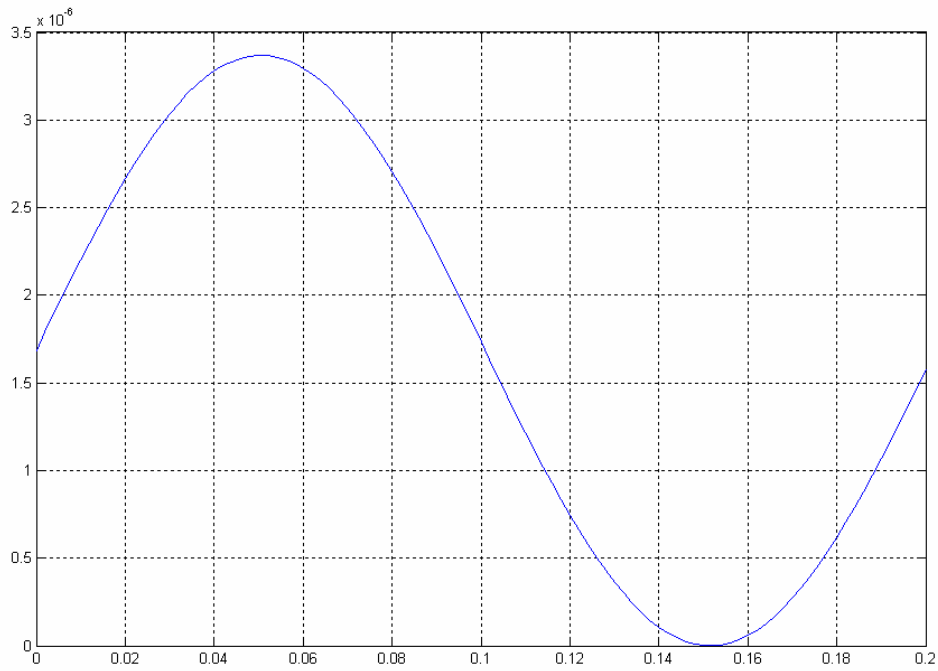


Figure 5 Flow profile

The fluid characteristics, inserted in the software Tdyn, were the most similar like the blood ones, like showed now.

Density	<i>1000</i>	<i>Kg / m³</i>
Viscosity	<i>0.004</i>	<i>Kg / m · s</i>
Compressibility	<i>0.0</i>	<i>s² / m²</i>

The boundary condition so was imposed like a fix velocity field in the inner section and a null value of field pressure in the section where the blood go out.

The no slip boundary condition for the vessel walls was imposed by a VfixWall in the “fluid body ransol boundary condition”, so doing we can put a fix null value of velocity in all the points of the surfaces that substituting the artery walls.

This one will become the standard procedure to fix the velocity in the boundary of the body, in all the cases that we’ll run. The problem data of the simulation was resumed in this table.

Step number	Time increment	Max iteration	Output step
800	0.001	3	50

4.2. Results

The plots show that the two ways of computation, the exact solution and the simulation with Tdyn, give similar solutions, comparable in form and dimension.

The first results are given us to the calculation effectuated by Tdyn, and we take the result of mayor importance at the end of the channel, where the velocity became regular and the condition of length and straight tube are satisfied.

All the solution was calculated in 4 different instants of time. This to emulate the Taylor's chooses. The instants of time selected are:

- 0.25 sec that correspond to $0.125 t/T$
- 0.75 sec that correspond to $0.375 t/T$
- 1.25 sec that correspond to $0.625 t/T$
- 1.75 sec that correspond to $0.875 t/T$

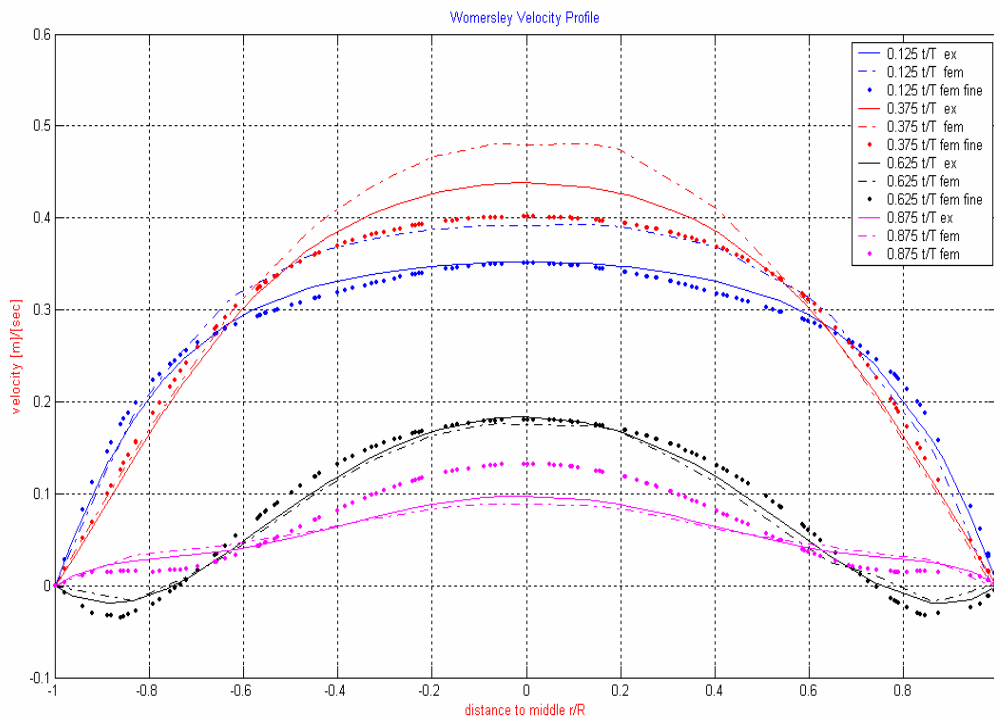


Figure 6 Comparison of the Womersley velocity solution with the results of 2 different meshes

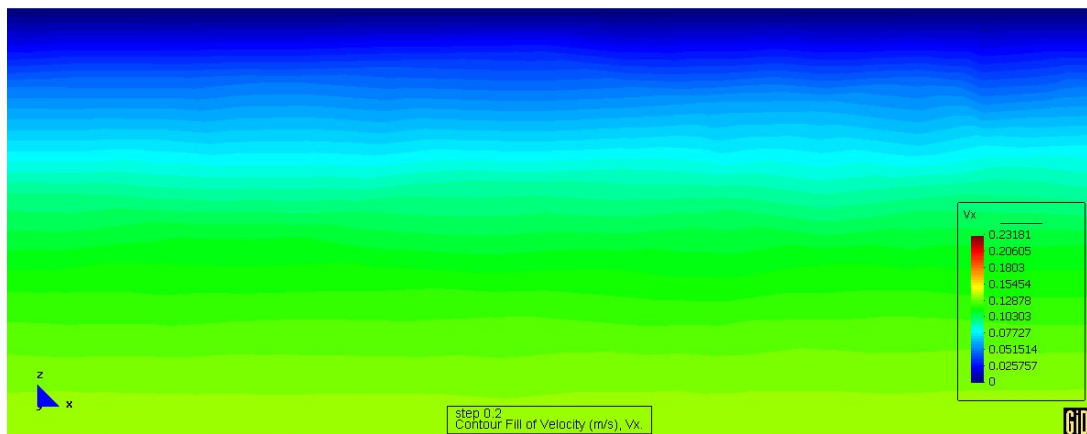


Figure 7 Visualization of the external portion of the fluid

We plot six graphics with MatLab, the first shows the results calculated with MatLab (exact solution) and with the F.E.M. software (F.E.M. solution).

We can see that the errors are bigger when velocity became higher and very small in the tracts with low speed, this tendency leave for all the tests that we do and is confirmed by the successive plots that are explicated in the next paragraphs.

To understand more the quality and the entity of the approximations, we plot, in the figure 2 of the program (figure 4.6 here), the error along all the length of the diameter, expressed in per cent reported to the exact analytical solution; we see that the bigger per cent error is found in the extremes of the radius, where the F.E.M. solutions come to zero because we put fixed velocity wall in Tdyn program, here instead the computational data are different to zero even if very small, so the ratio go to very high values. The central zone stays approximately all below the value 10%, giving so a good approximation, the high values registered in the lateral side are also acceptable for the reason written above. The next plot show the absolute error along the diameter, here we confirm that the most important error are localized in the middle of the diameter and the high values that compare in the lateral position of the last picture are only caused by the very little values calculated compared to the zero value of the F.E.M. simulation.

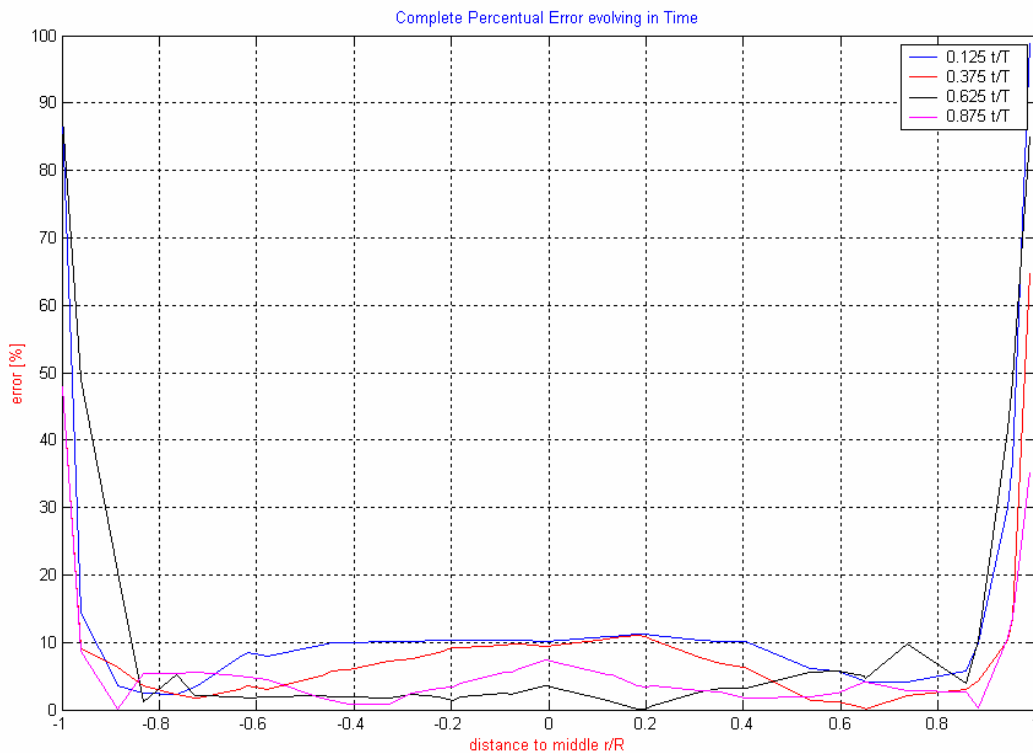


Figure 8 Variation of the error expressed in percent, varying in the diameter

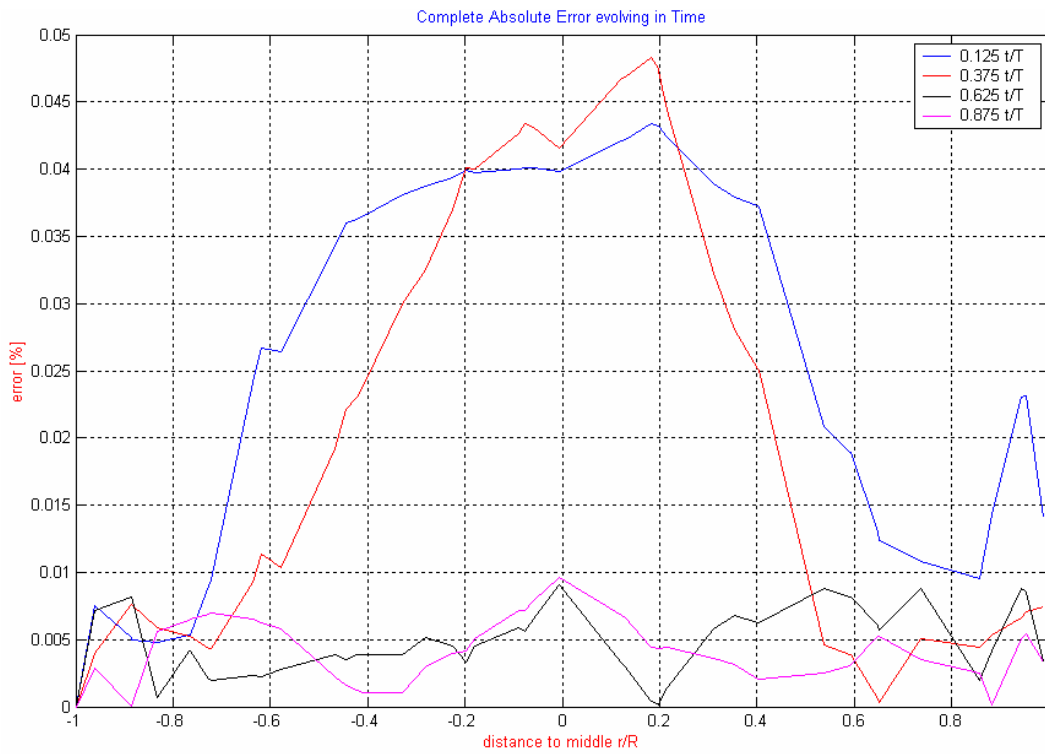


Figure 9 Variation of the error in absolute value, varying in the diameter

We can see confirmed the tendency that the bigger error corresponds to the high-speed moment of time and central position.

Other way to see the errors is make it by the two others plots printed by the program. The first one shows the ratio, respect the exact solution, of the larger error between the two kinds of result (F.E.M. and calculated).

The second one shows these values in absolute unity of measure, expressed in m/sec (figure 4.8).

Both give good results considering the low complexity of computation, chose to accelerate the calculating time.

Also here we note the increasing of the error when the velocity becomes greater.

Increasing the complexity and the precision of the calculation is right to attend more similar results.

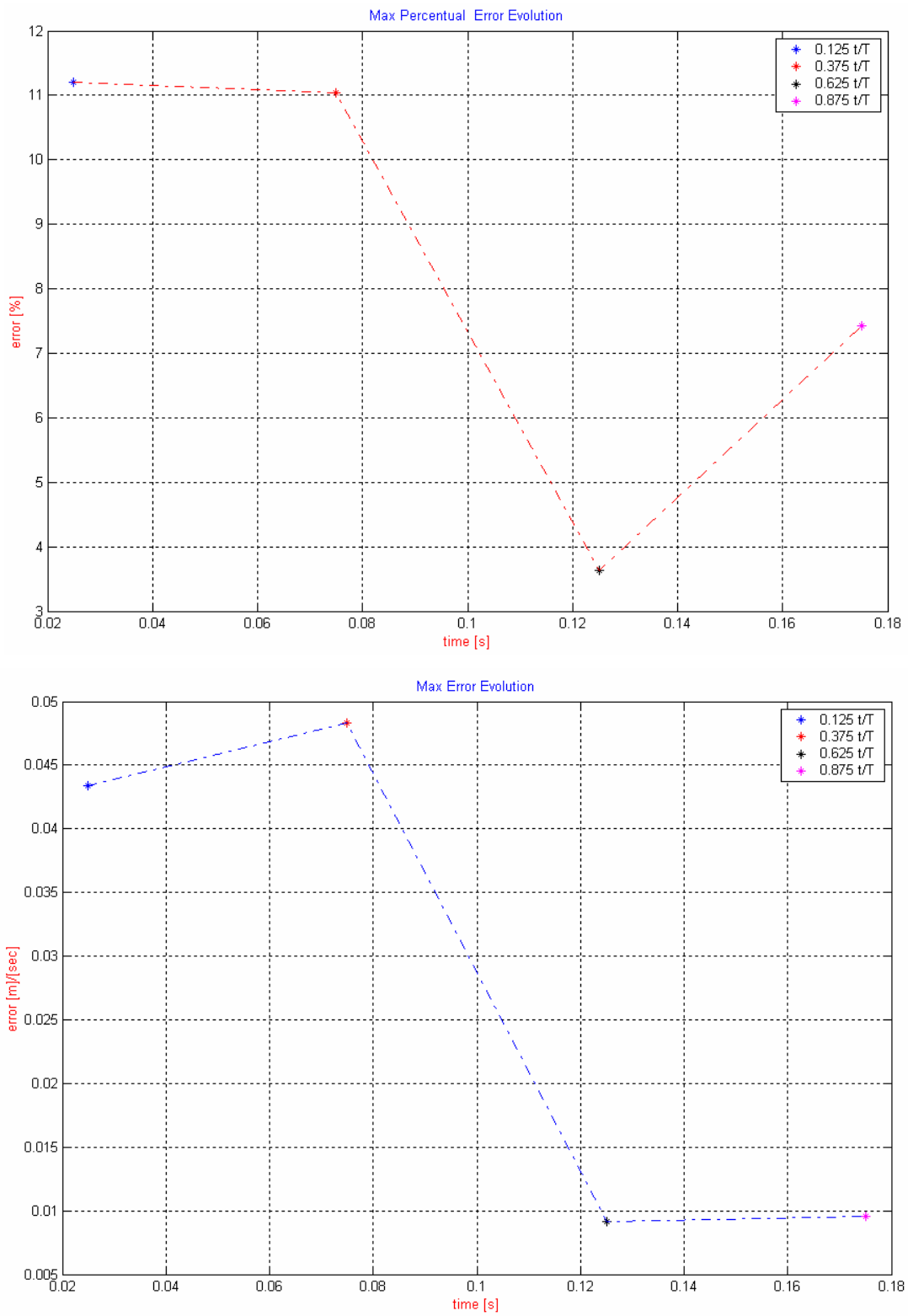


Figure 10 Evolution of the error in the time (4 different cases)

5. Steady Flow in an End to Side Anastomosis (graft bifurcation)

This is the second step of the study. The geometry represents a graft insertion, like the by-pass ones, a large channel come to upside and inserts him in a littler one that has a simple geometry like a straight and long vessel. The bloody flow is steady type and the problem is to visualize the return of the flow in the proximal out coming channel, and how much can go in the right direction. The reflux can become dangerous if reach a high level, because can occur thrombosis or other serious injury. The last step of the test was to evaluate the time that the simulation need to take a regular results, to be precise the internal time of the simulation that permits to see a steady flow in the fluid body.

5.1. Geometry, Mesh and Data

Taking the Taylor's second experiment, was reconstructed the geometry of the anastomosis, described by Loth, he designed the geometry so as to correspond to the dimensions of a real canine ilio-femoral anastomosis. The geometry is shown in the next picture.

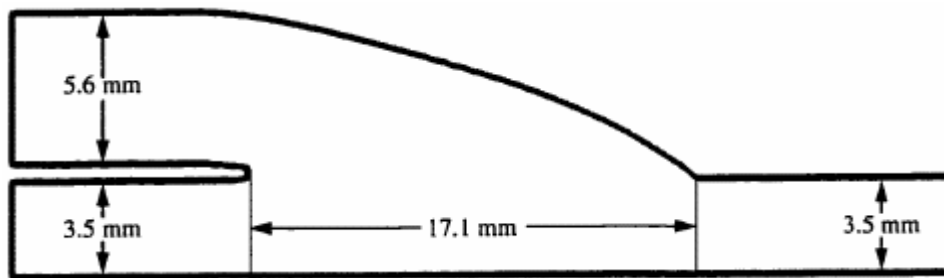


Figure 11 Geometry of the graft model

To plot the Taylor's data was made a data fitting, so obtained a series of plots to use like base-point, these ones was inserted in the MatLab program, joint with the calculated ones.

This data fitting can be results better disposing by the original data; we instead use the plots divulgated and take all the necessary informations from them.

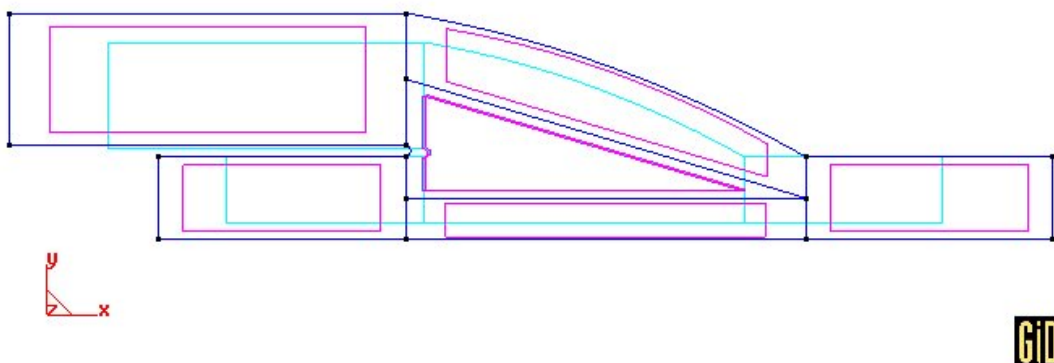


Figure 12 Graft model geometry representation

Geometry obtained was constituted by a cylinder in the low zone and curved cylinder inserted upstairs.

It is possible denote that the ingoing tube is longer that the Taylor's one; the difference is caused by the different condition imposed: Taylor imposes a Womersley profile velocity, our case supply this condition with a longer vessel, that stabilizes the blood flow till he takes the profile wanted.

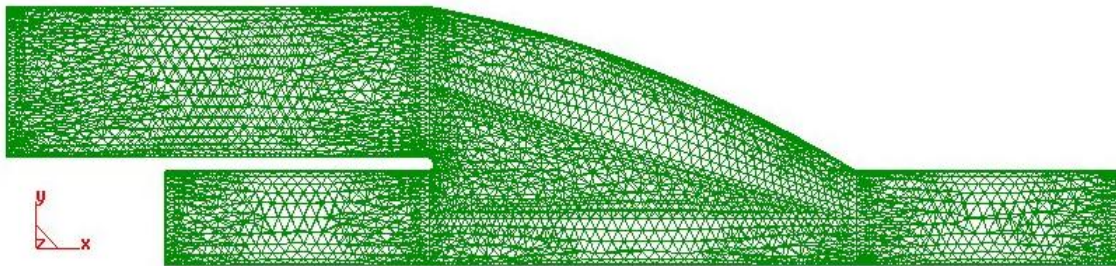


Figure 13 Mesh visualization in the plane XY

The major problem founded was the choice of the correct geometry of the body; it was necessary divide it in some different surfaces and then to create a unique volume.

Only with this way we can choose all the possible dimensions of the mesh elements and all the velocities that we have, to make the finite element meshing.

The mesh is described by these data that resumes the quality of the mesh constructed.

The same elements dimensions and velocity of transition were used for the two testes, because the pulsatile flow case is only a variation of the example run before.

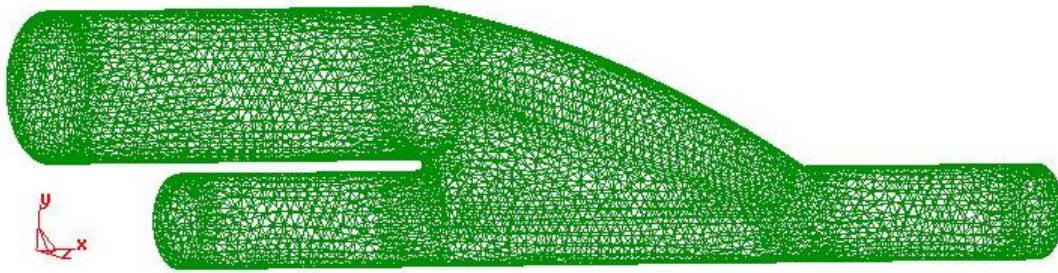


Figure 14 3D representation of the graft model (mesh visualization)

Element size (m)	Triangles number	Tetrahedras number
0.00027	31174	483366

This second experiment puts a modification in the properties of the blood.

Density	1050	Kg / m^3
Viscosity	0.0035	$Kg / m \cdot s$
Compressibility	0.0	s^2 / m^2

The profile of the velocity was selected as steady in the time, so it is possible to see how many time the blood flow use to reach a steady velocity without changes or variation in its shape. A variation in the flow profile are denoting by the insertion of a paraboloid profile, so the boundary condition are better respected.

The maximum of the velocity is in the center of the vessel and have a value of 0.154 m/sec, and the zones that touch the lateral walls get null velocity value. This is important because the no-slip boundary condition imposes null velocity in the external surfaces and the change of fluid velocity can increase without discontinuity.

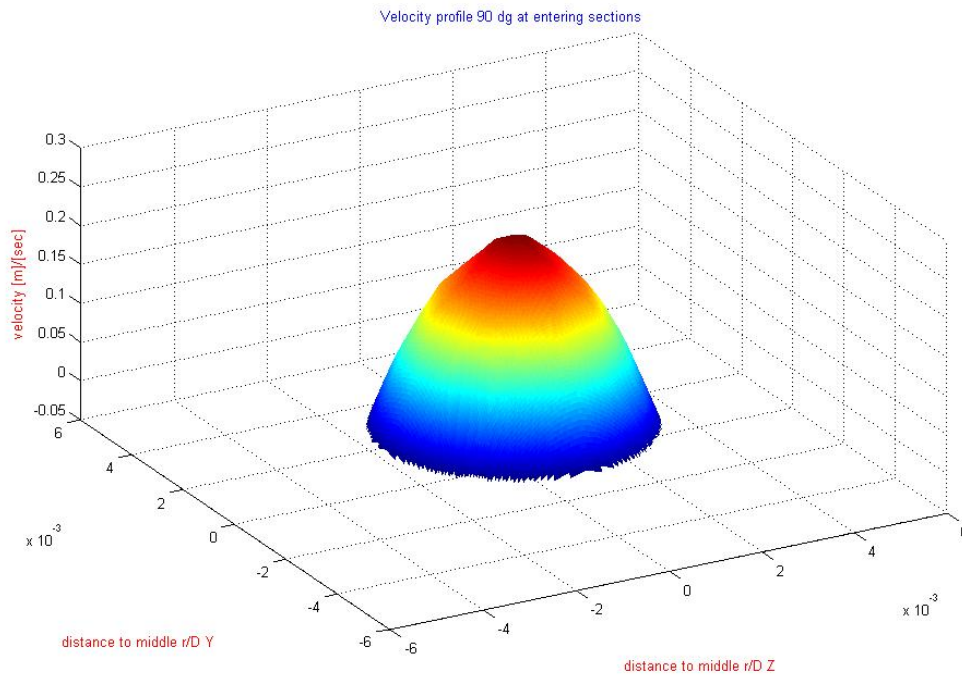


Figure 15 Representation of the velocity in the inner section

The boundary conditions are the same of the precedent example. Another different in the setting of the data test, are caused by the presence of two way of exit.

The proximal exit, the one that go below the inner section, and the distal section, the one that is situated far to the blood enter zone, both take the condition of null pressure value.

The outgoing profiles remain with a paraboloid profiles, even if the maximum value of the flow can be moved a little bit far to the geometrical center of the vessel.

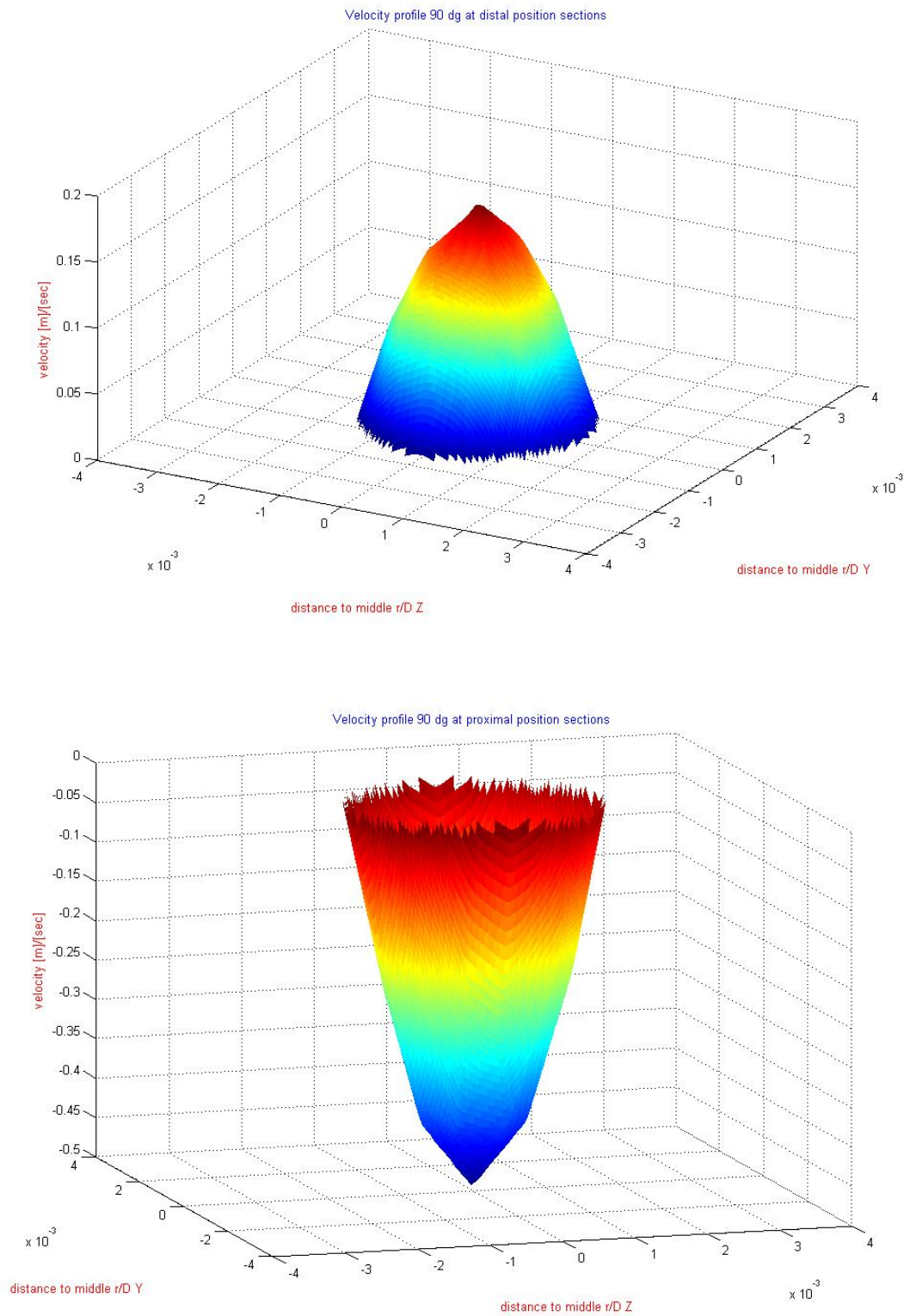


Figure 16 Representations of the velocities profiles in the Distal Outgoing Section (upside) and in the Proximal Outgoing Section (downside)

We do five different tests to compare when the results go to be stable and don't need other more precision in the meshing, starting with the bigger and faster to come to the slower and thinner one.

When we obtain these results, we take and plot only the data of interest, we extract them sectioning the body and taking only five sections posed like in the figure 5.7, and plotting them. After we take these data and plot them divided by position.

The first we compared the accuracy of the results, changing the mesh dimension; in a second time we move the section with a good mesh.

So we make 4 tests to set up the best condition in velocity and quality of the results and we chose 4 dimensions for the mesh elements.

	Test 1	Test 2	Test 3	Test 4
Dimension	<i>0.0015</i>	<i>0.001</i>	<i>0.0006</i>	<i>0.0003</i>
N. of triangles	<i>1946</i>	<i>4000</i>	<i>6692</i>	<i>36672</i>
N. of tetrahedral	<i>4721</i>	<i>14501</i>	<i>48173</i>	<i>477959</i>
N. of nodes	<i>1348</i>	<i>3522</i>	<i>9917</i>	<i>60451</i>

After passing to the second step of the test, we selected 5 sections to find the position of the cuts produced in the Taylor and Loth's experiments.

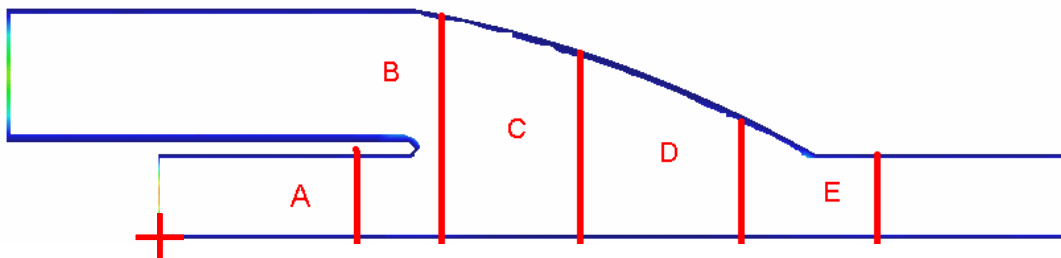


Figure 17 Positions of the cuts realized (zero point is marked with a red cross)

Section	A	B	C	D	E
Position	0.0085	0.0125	0.0175	0.0325	0.0295

Finally trying to change the pressure boundary conditions in the outgoing sections and show how the blood changes his velocity direction.

In the program the unity of measure of the pressure is expressed in m^2/s^2 , because we have to work with a *dynamic pressure* so we must translate the conventional mmHg utilized to measure the blood pressure in this new unity and make the tests.

Remembering these equivalences, we put 3 different values of pressure.

psi (pound-force per square inch) (lbf/in ²)	Pascal (Pa)	6894.757
torr (Torr)	Pascal (Pa)	133.3224
atmosphere (atm)	mmHg	760
millimeter of mercury conventional (mmHg)	Pascal (Pa)	133.3224
millimeter of mercury conventional (mmHg)	psi (lbf/in ²)	1.93368 E-02

So taking the usually normal values of pressure: 140 mmHg, 120 mmHg and 60 mmHg, related with the density of the blood (1050 kg/m^3), was obtained 3 different values of this dynamic pressure: $17'776 \text{ m}^2/\text{s}^2$, $15'236 \text{ m}^2/\text{s}^2$ and $7'618 \text{ m}^2/\text{s}^2$; we use them to see the variation confronting with the null condition of pressure.

Step number	Time increment	Max iteration	Output step
3000	0.001	3	50

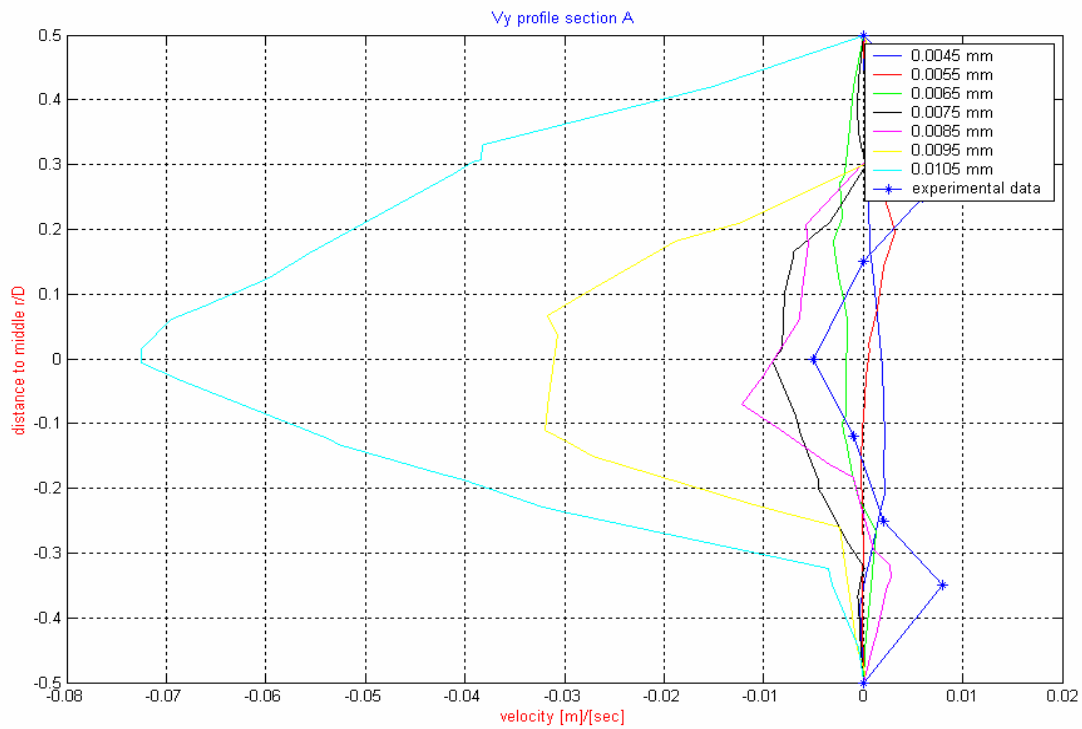
5.2. Results

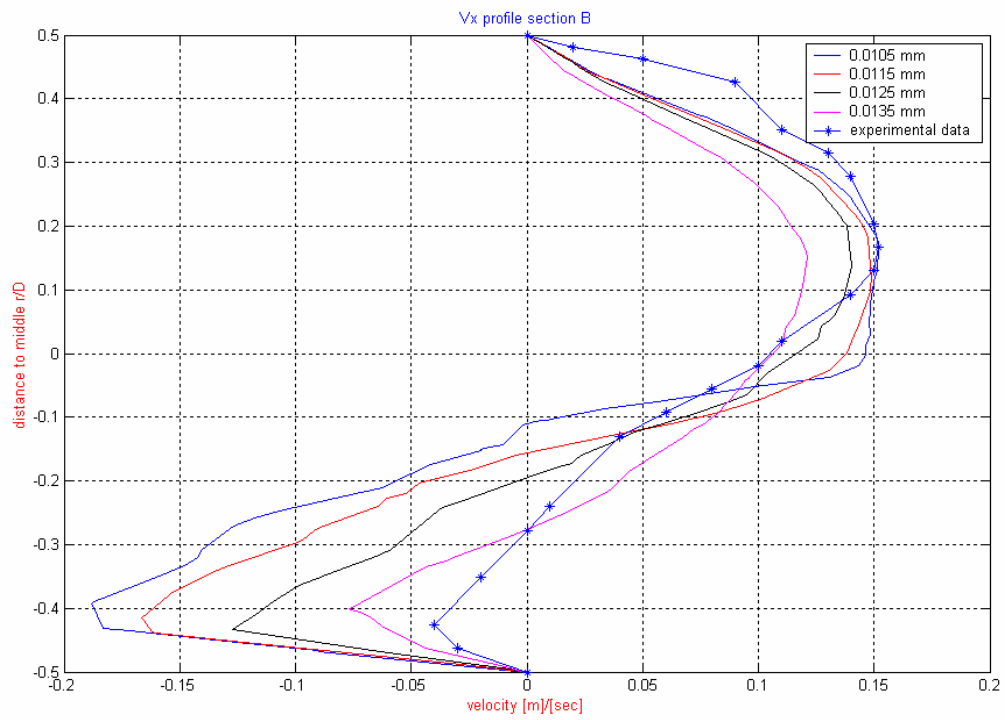
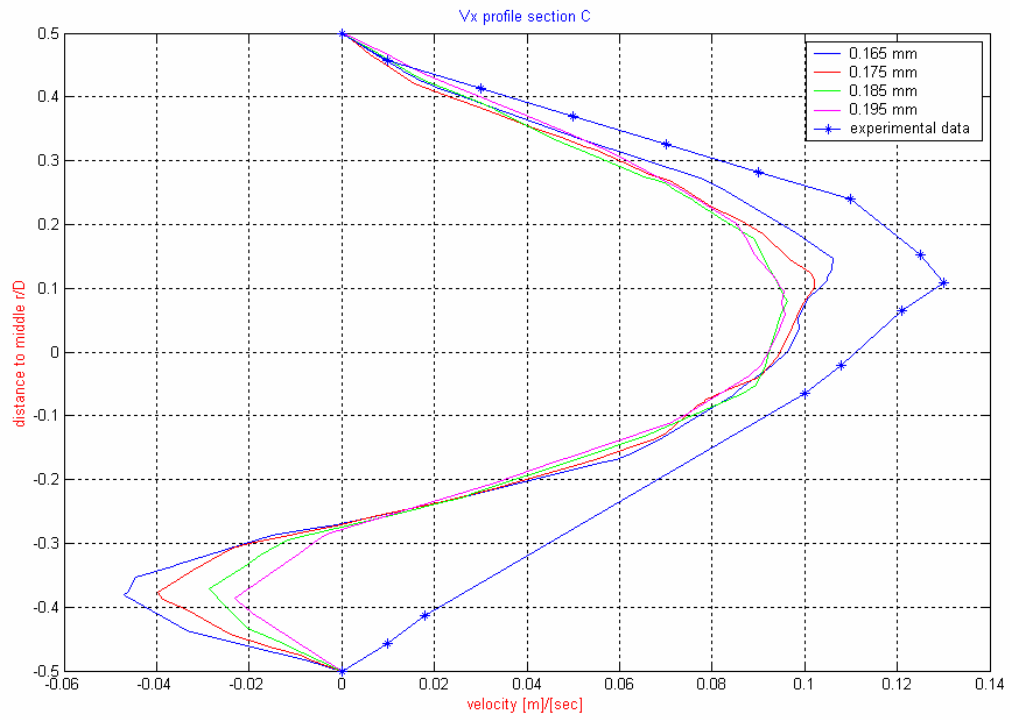
We compared the Taylor's experimental results with the ones obtained by our simulations. To have the Taylor's data we must take them with a measure and approximate

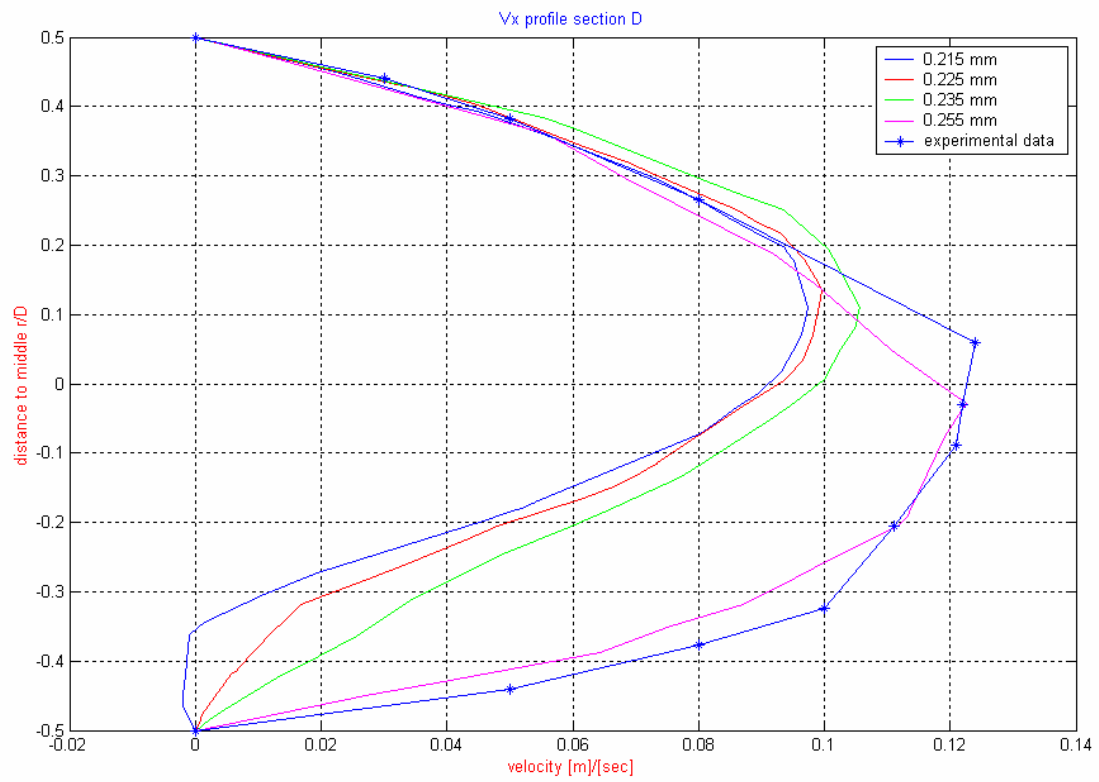
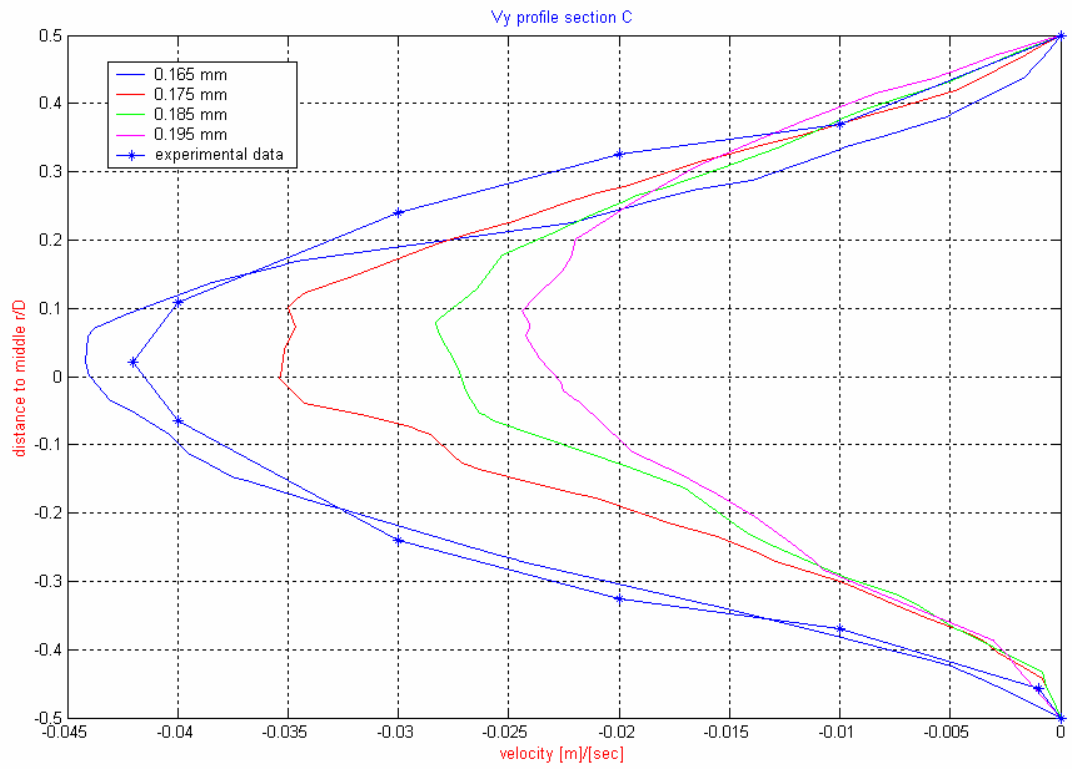
them; after we normalize them to have a simple and clear plot, showing the velocity variation along the diameter.

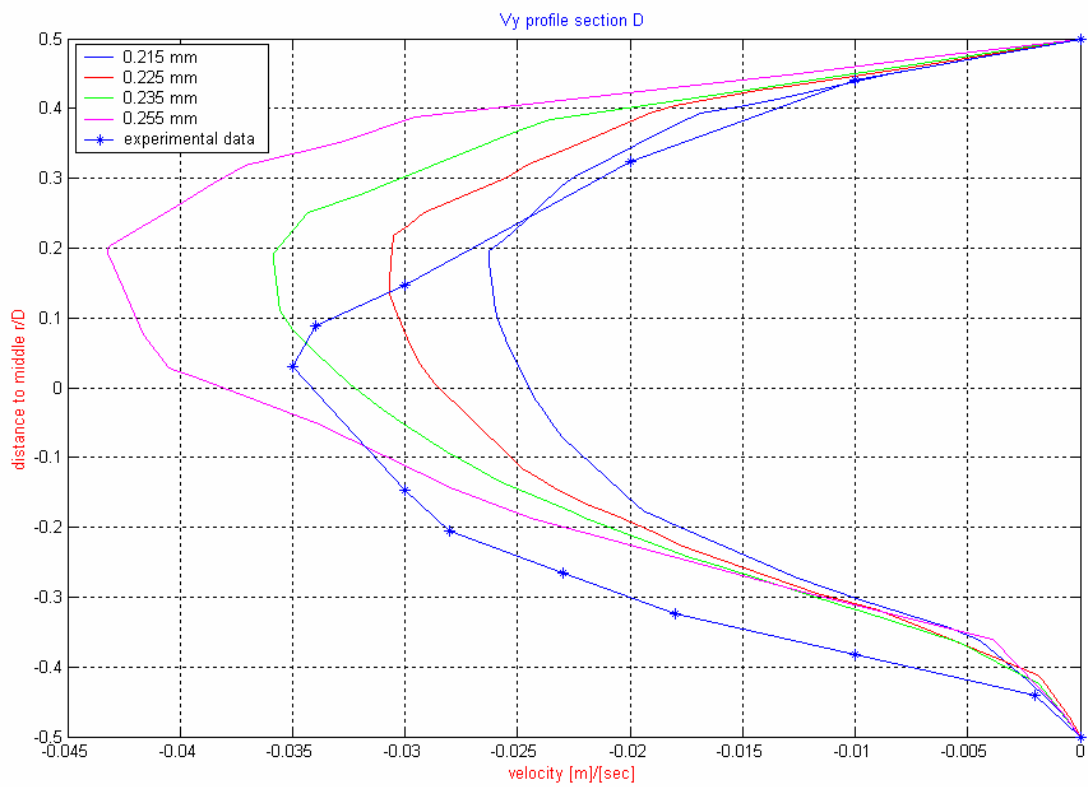
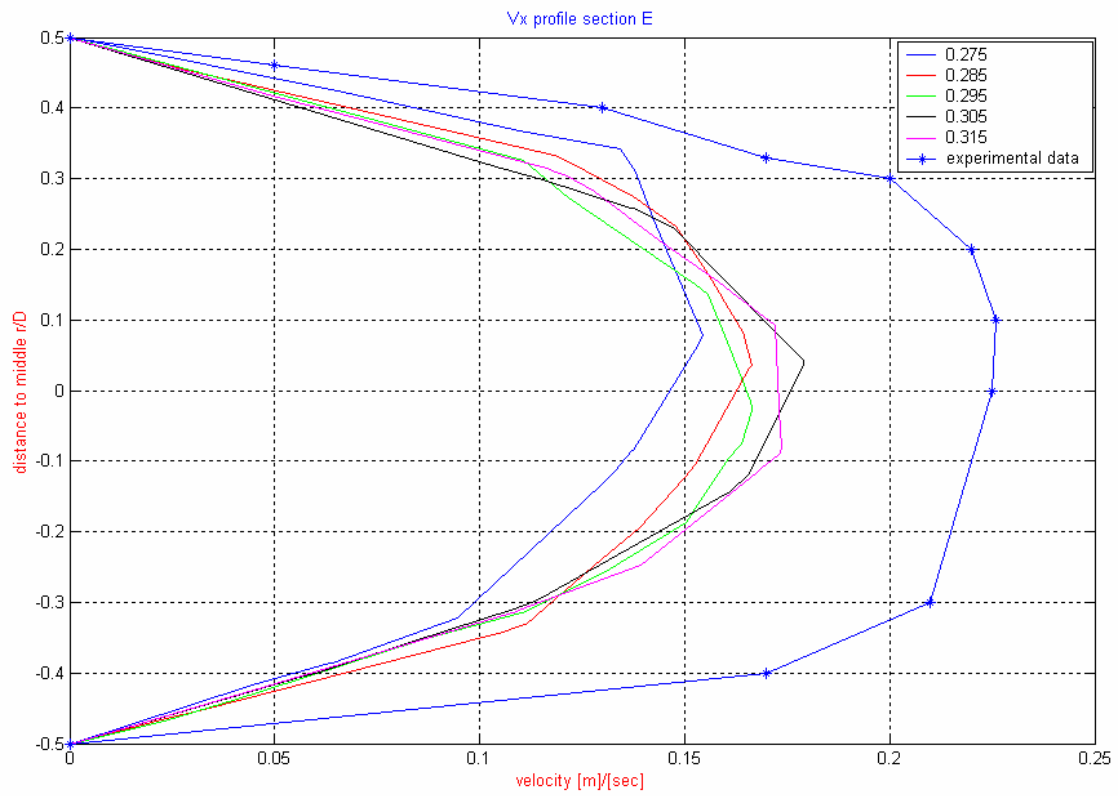
This method give us the possibility to compared all the results calculated in the same section, even if the meshing process creates different points in the generation of the finite element mesh

The first experiment was planed to change the position of the cut point, searching the most similar graphic to the Taylor's one. We obtain these results, showing that the Tdyn simulations give results comparable to the Taylor's ones.









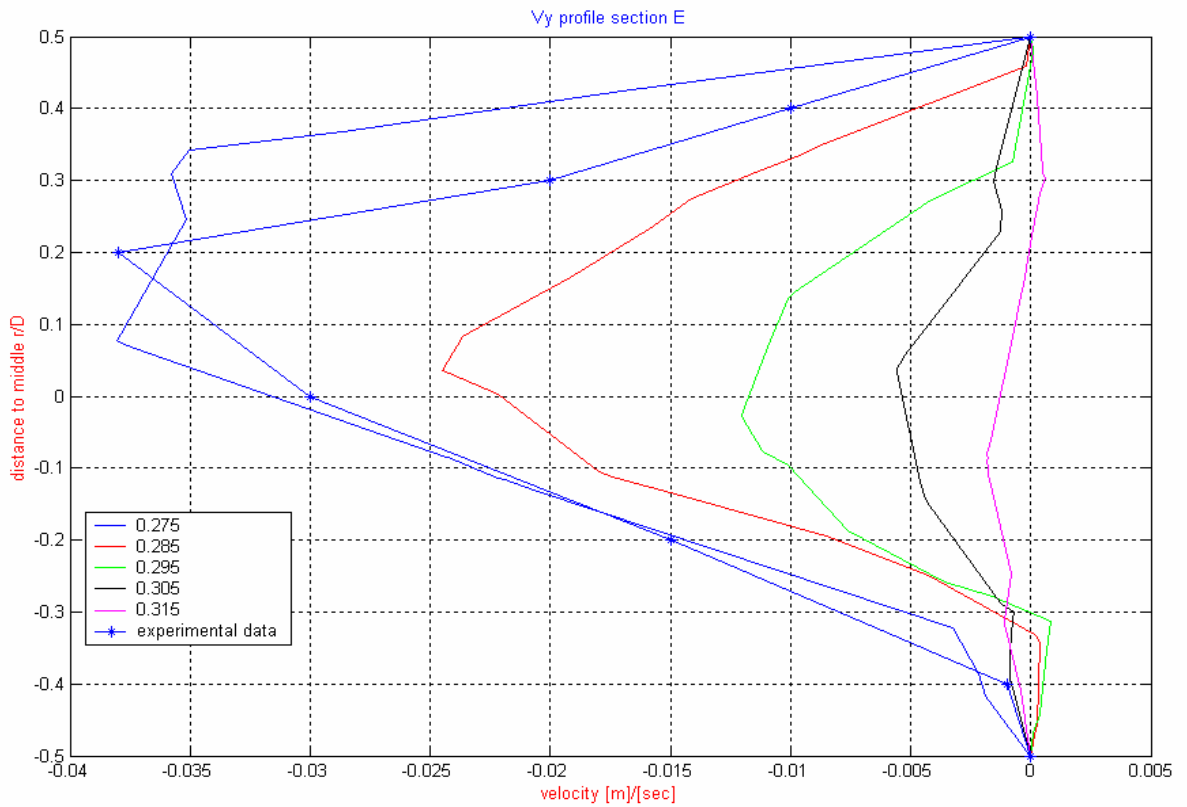


Figure 18 Series of the results of the velocity varying the point of cut.

From those plots we choose the more similar profile respect to the Taylor's ones, and select the positions of the cuts:

Section	<i>A</i>	<i>B</i>	<i>C</i>	<i>D</i>	<i>E</i>
Position	<i>0.0085</i>	<i>0.0135</i>	<i>0.0205</i>	<i>0.023</i>	<i>0.0275</i>

We encounter some discrepancies in the graphics and in this situation we choose with these rules: before the most similar in x-velocity profile, then in the y-velocity profile.

he difference can be determinate by an uncertainly pressure value, so the next step is determine the better one to make realistic modelization.

We take three different values for this parameter, and taking the value of the density of the blood, fixed as 1050 kg/m^3 we calculate the dynamic pressure as

$$DP = P/\rho$$

We obtain the sequent table of conversion for the chosen pressures:

Pressure [mmHg]	<i>60</i>	<i>120</i>	<i>140</i>
Dynamic Pressure $[\text{m}]^2[\text{s}]^{-2}$	<i>17776</i>	<i>15236</i>	<i>7618</i>

Was sufficient to change in the menu *initial data*, the *initial conditions*, and put these new values instead of the null one.

We have to make the meshing operation every time we change this condition, because only in this way we can recomputed correctly the solution of the fluid dynamic problem, and obtain right results.

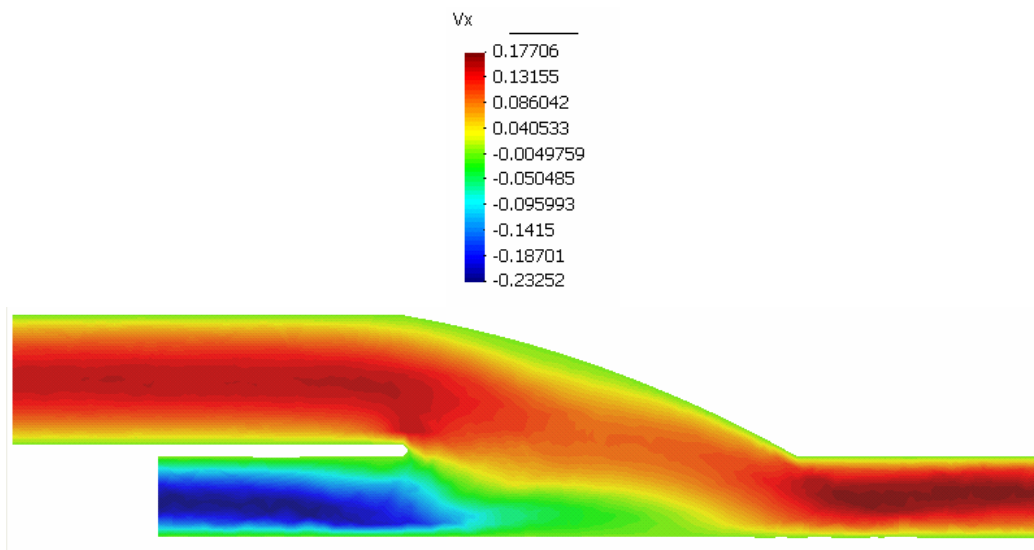


Figure 19 Velocity profile in X direction, this is the principal direction of the velocity

We now show the different profiles of the velocity in the middle section of the geometry. We can denote the difference between the two-value scales: the extreme value is substantially different.

Anyway also the distribution of the velocity show some difference like more regularity in the case of pressure put to 140 mmHg, like we can observe in the two next pictures

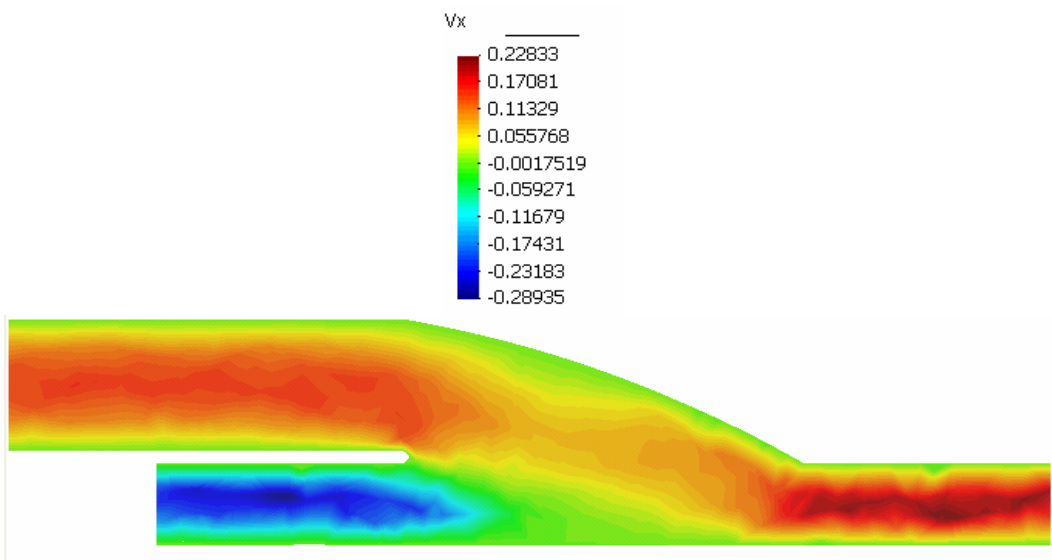
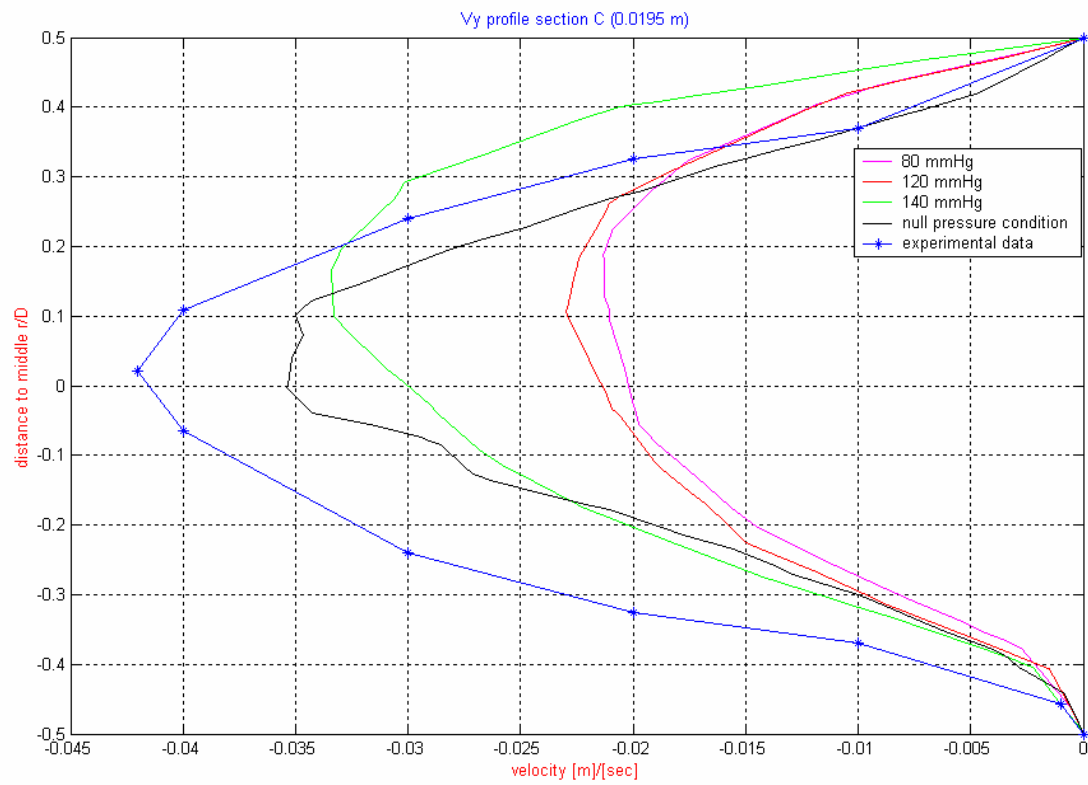
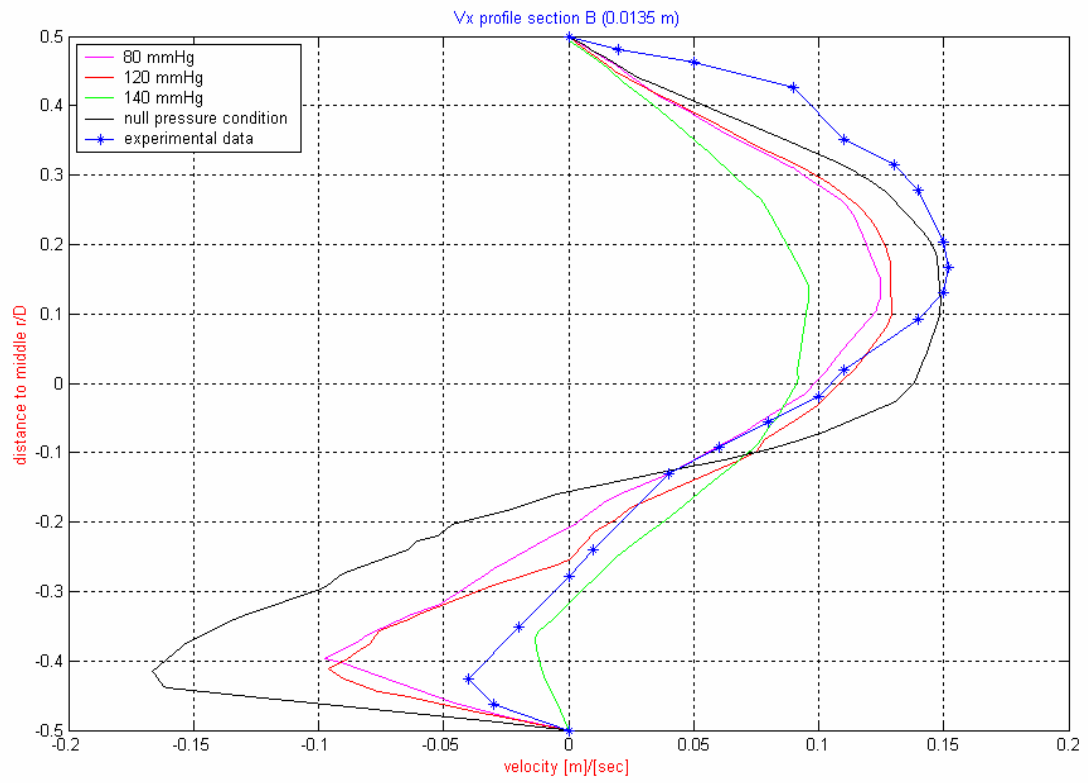
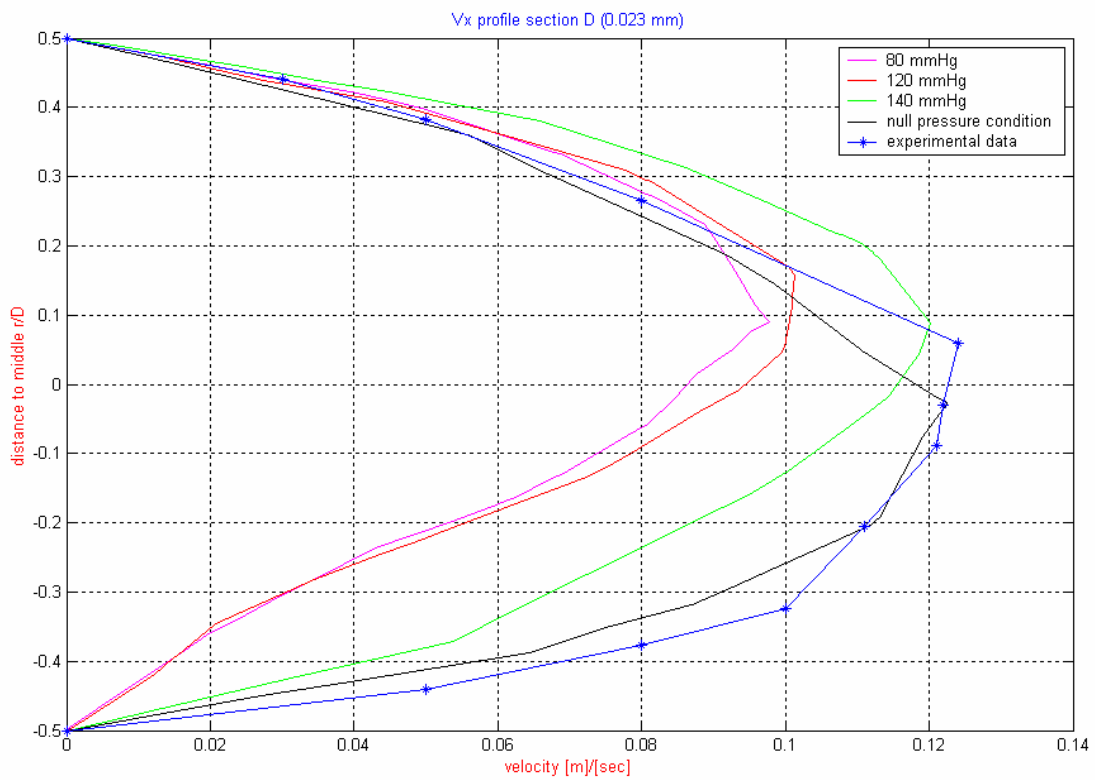
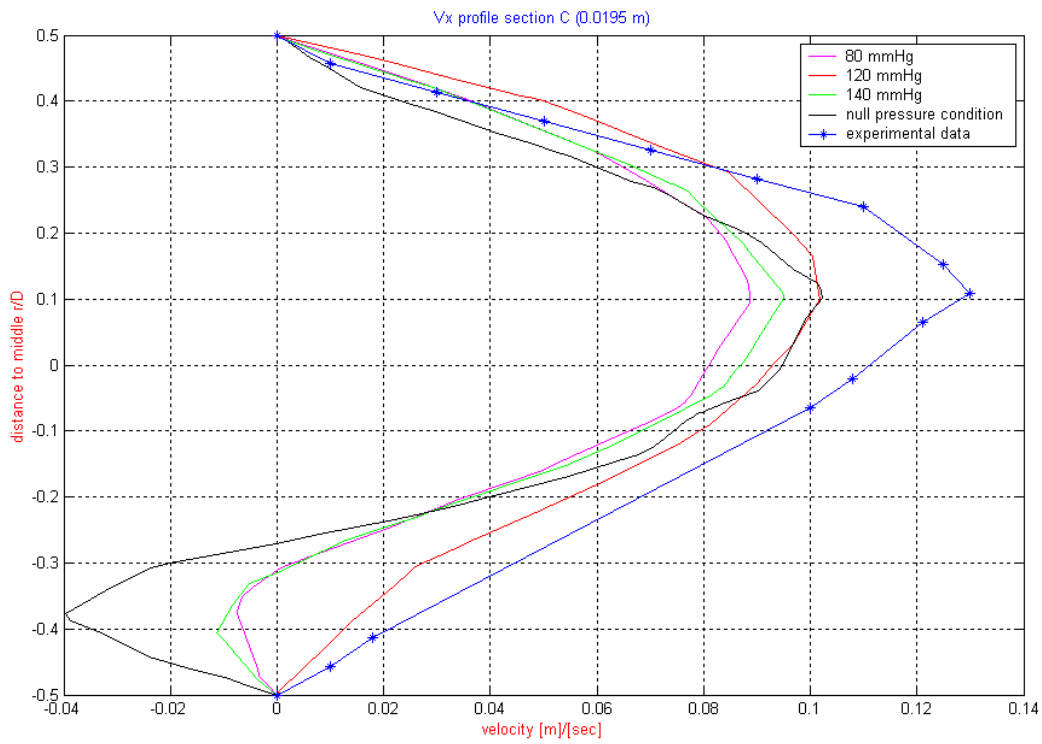
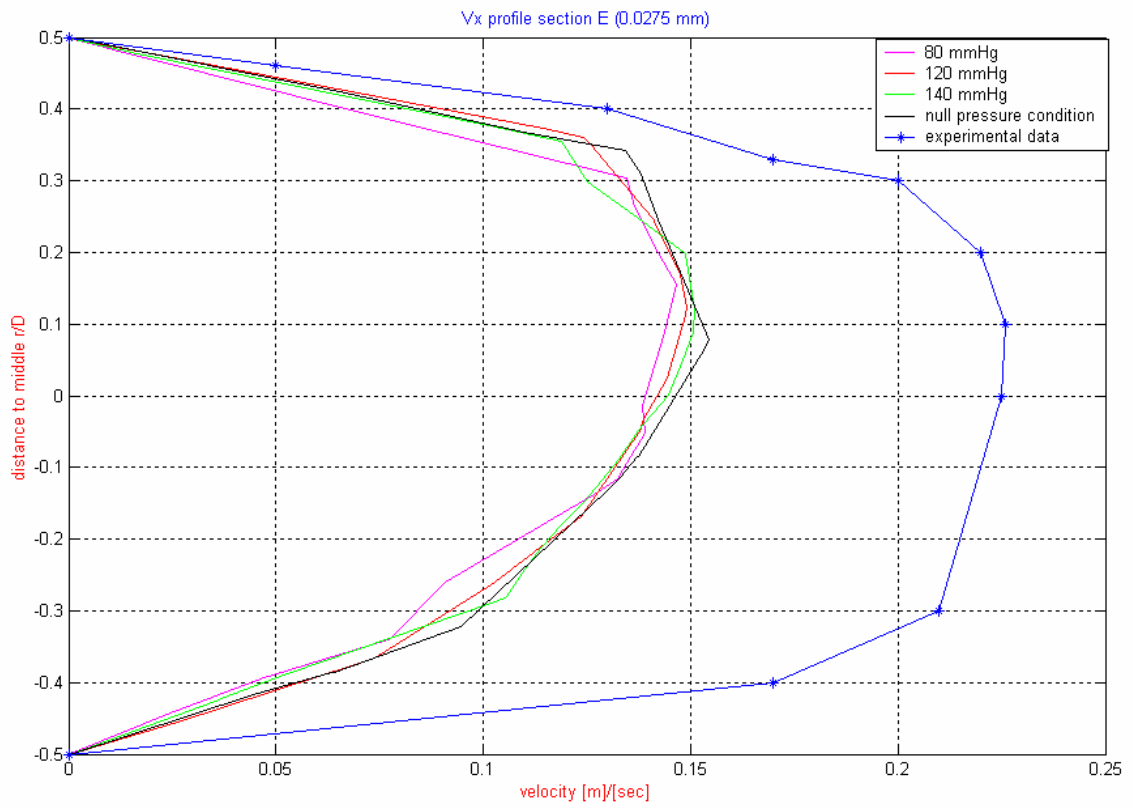
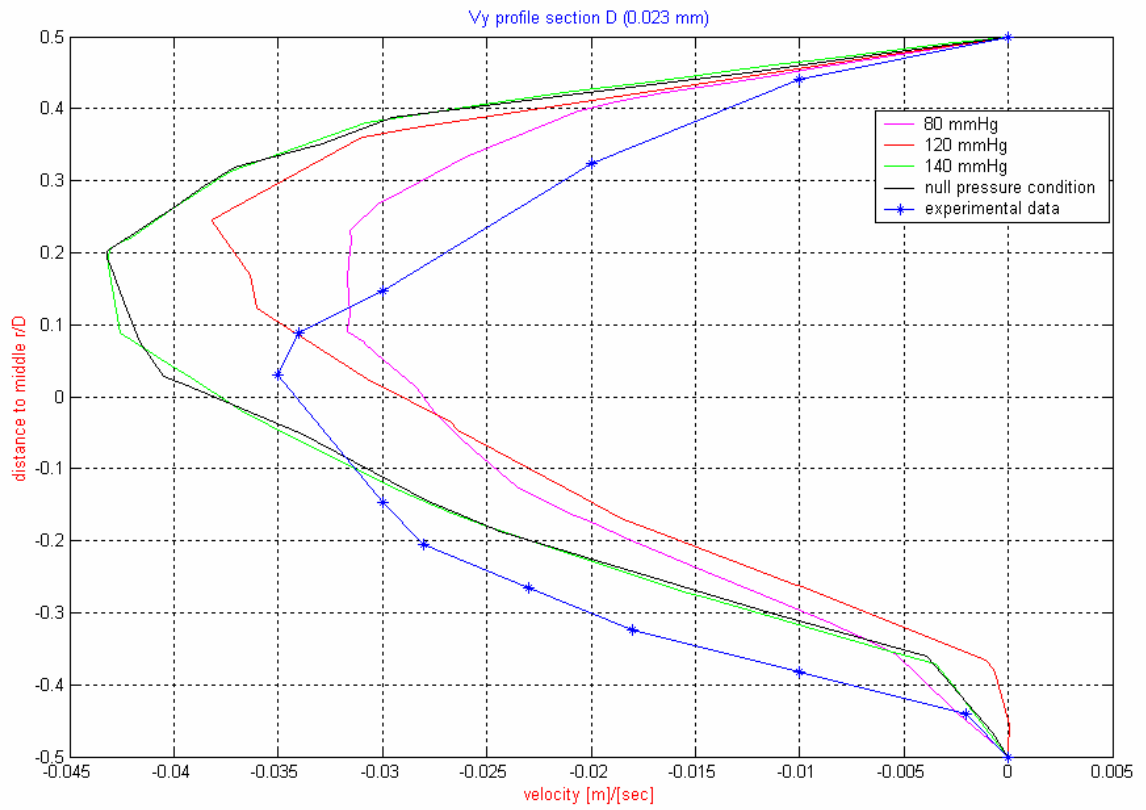


Figure 20 Velocity profile in Y direction, this is the vertical direction







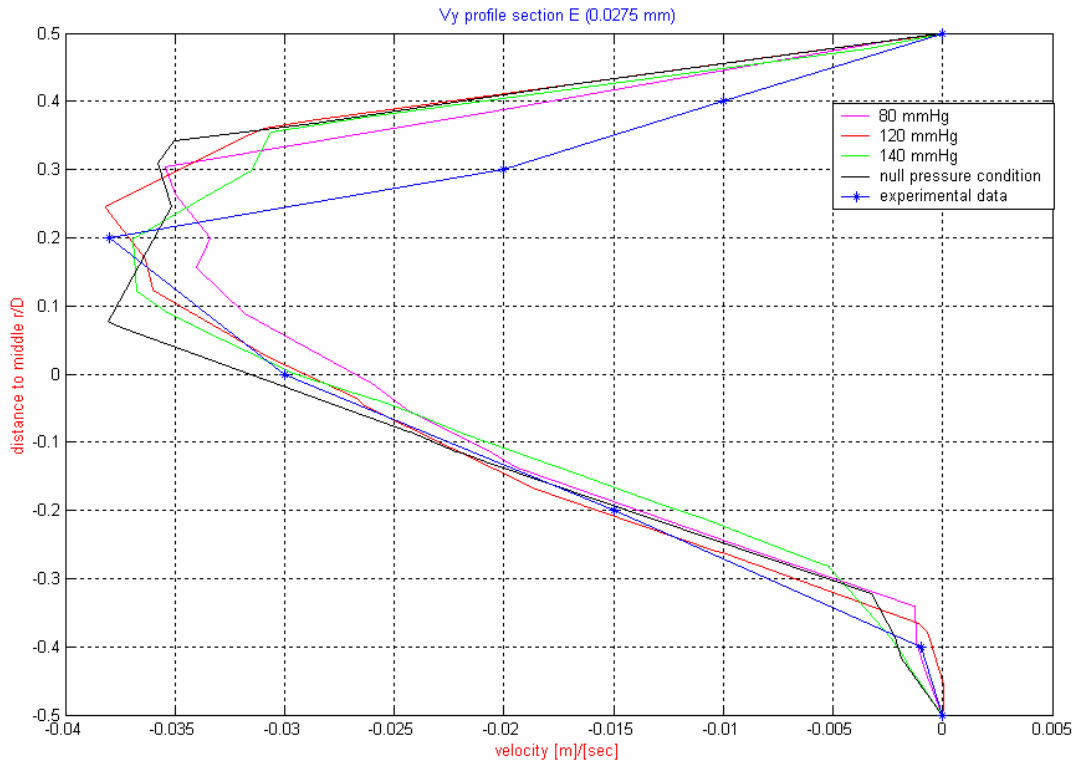


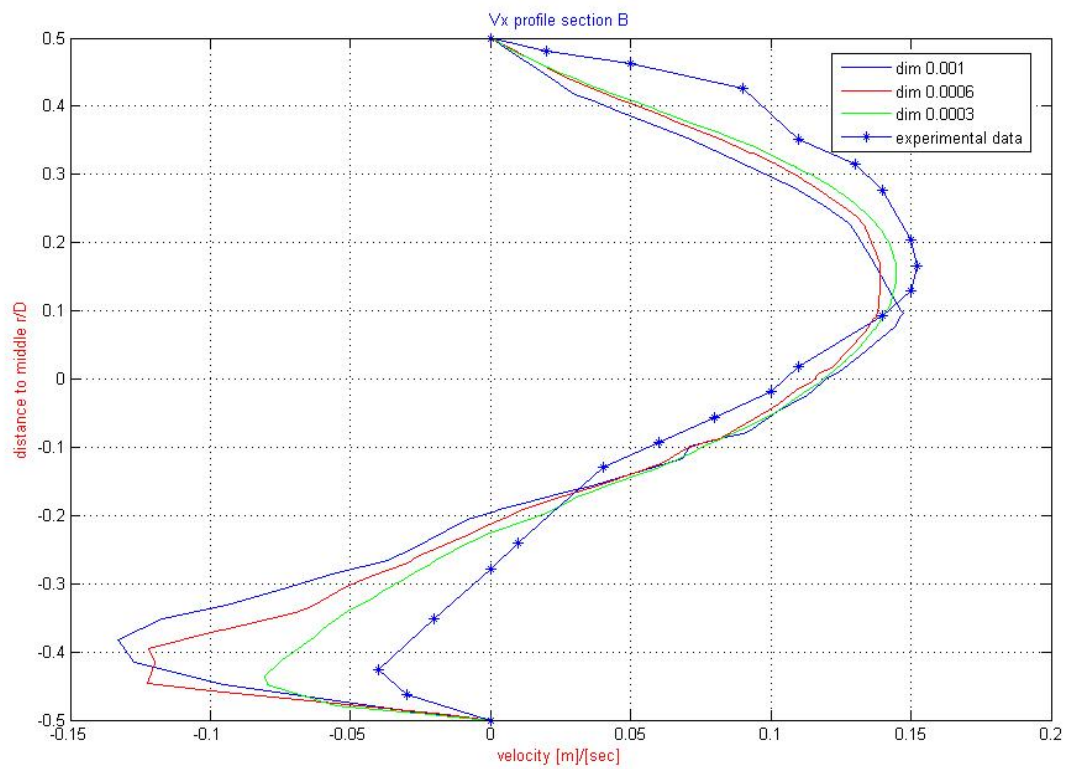
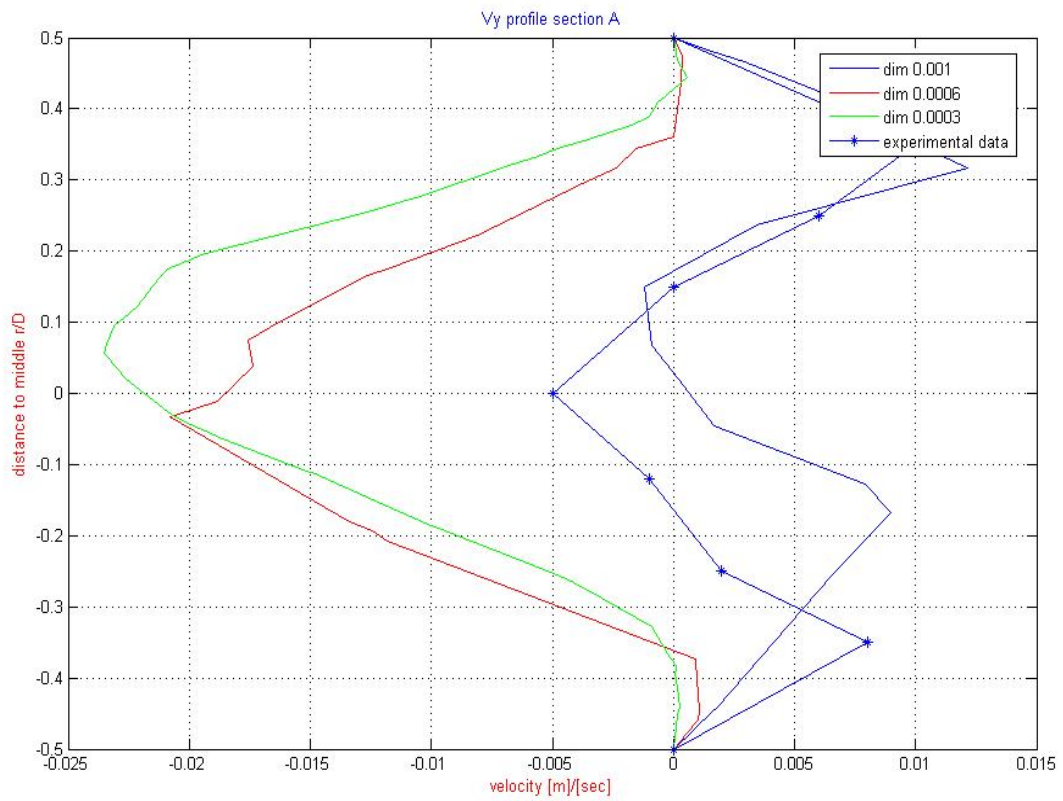
Figure 21 Series of results obtained changing the pressure imposed

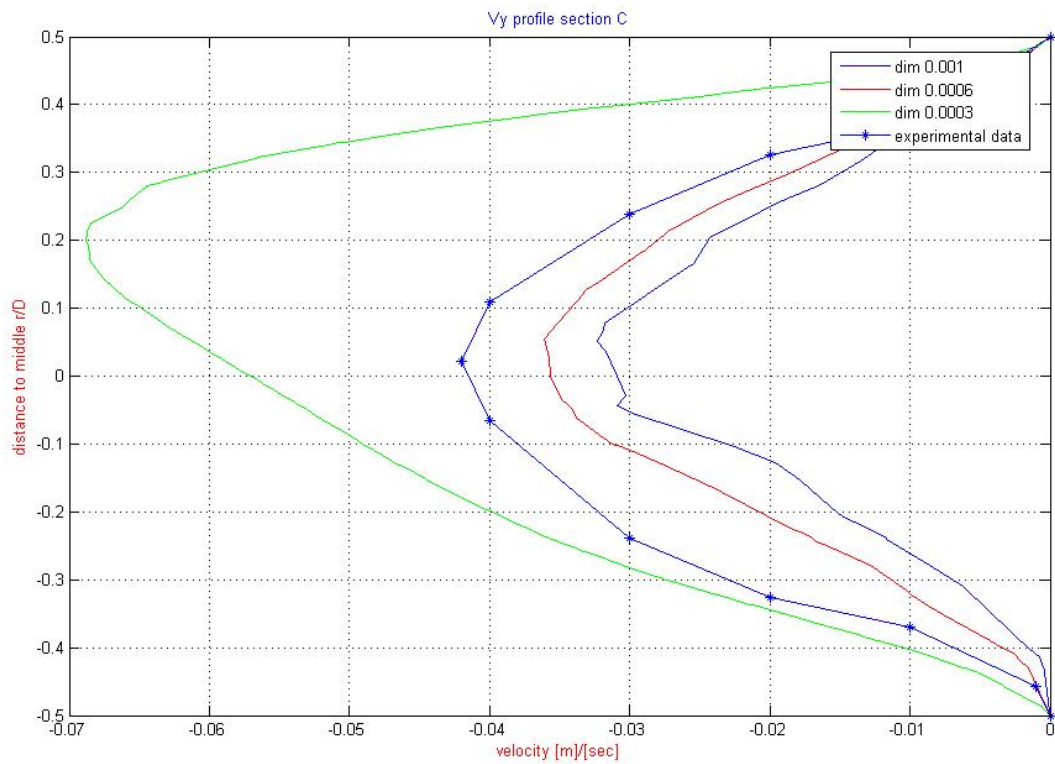
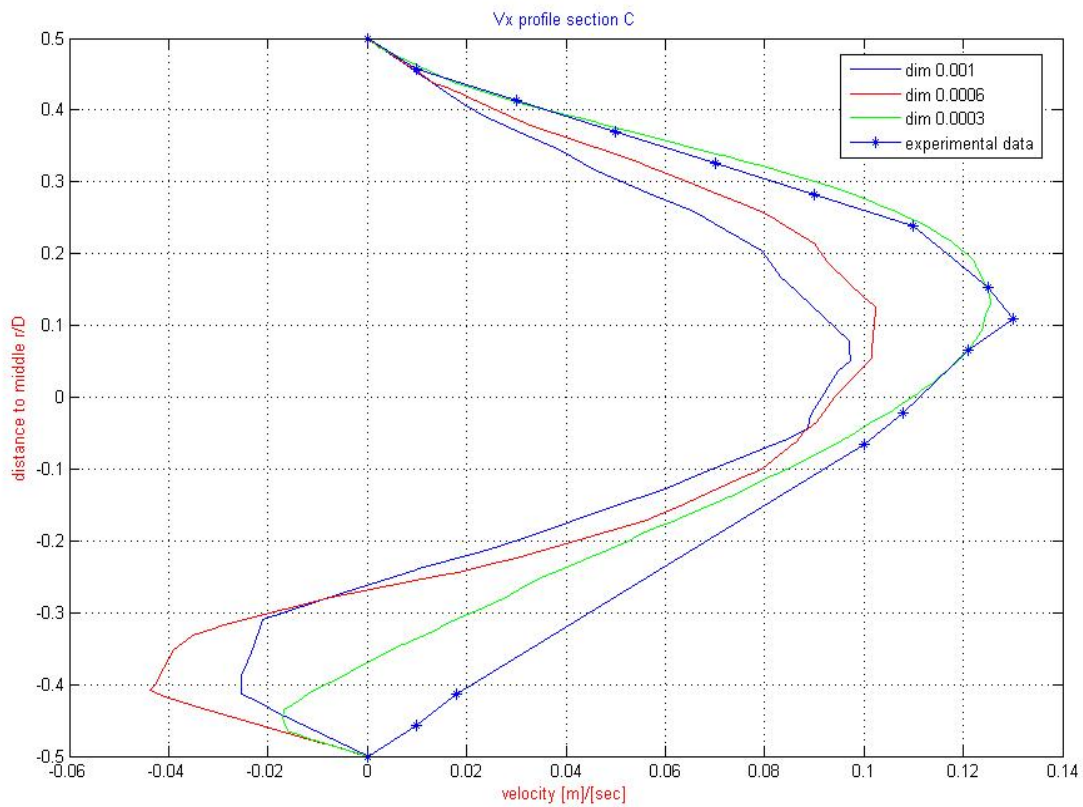
The variation of the pressure field doesn't give a unique direction to follow to come more near to the Taylor's solutions, as we can show here:

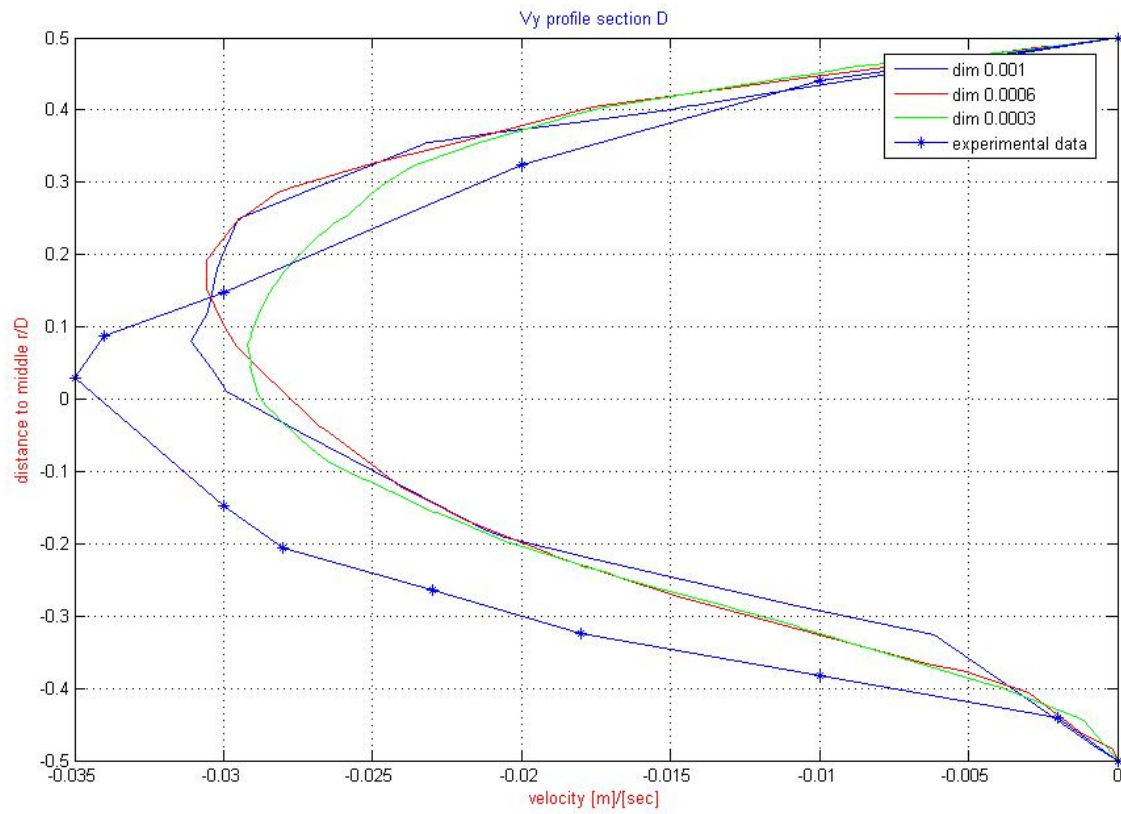
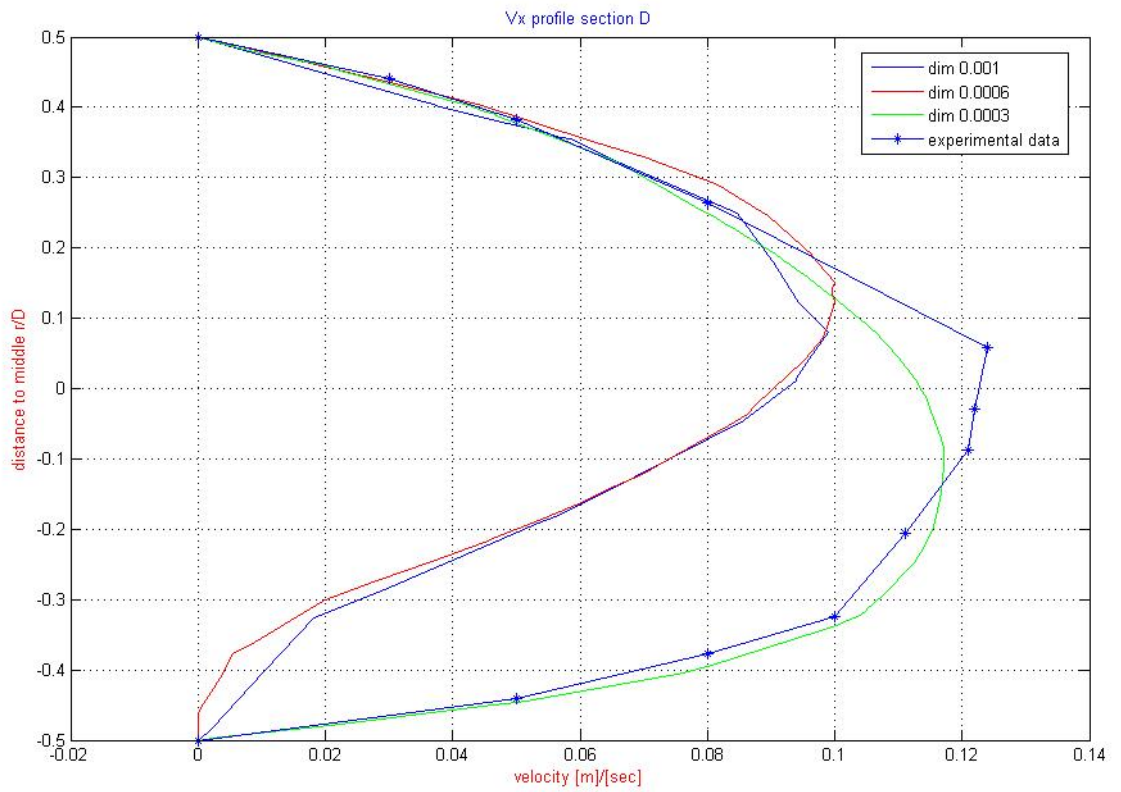
Section	<i>A</i>	<i>B</i>	<i>C</i>	<i>D</i>	<i>E</i>
Best in X direction [mmHg]	---	140	120	null	---
Best in Y direction [mmHg]	80	140	null	120	---

So is impossible to opt for a preferable pressure value that gives the same results to the Taylor's ones.

Last was made a refining of the meshes used to show how a fine mesh can improve the quality of the results.







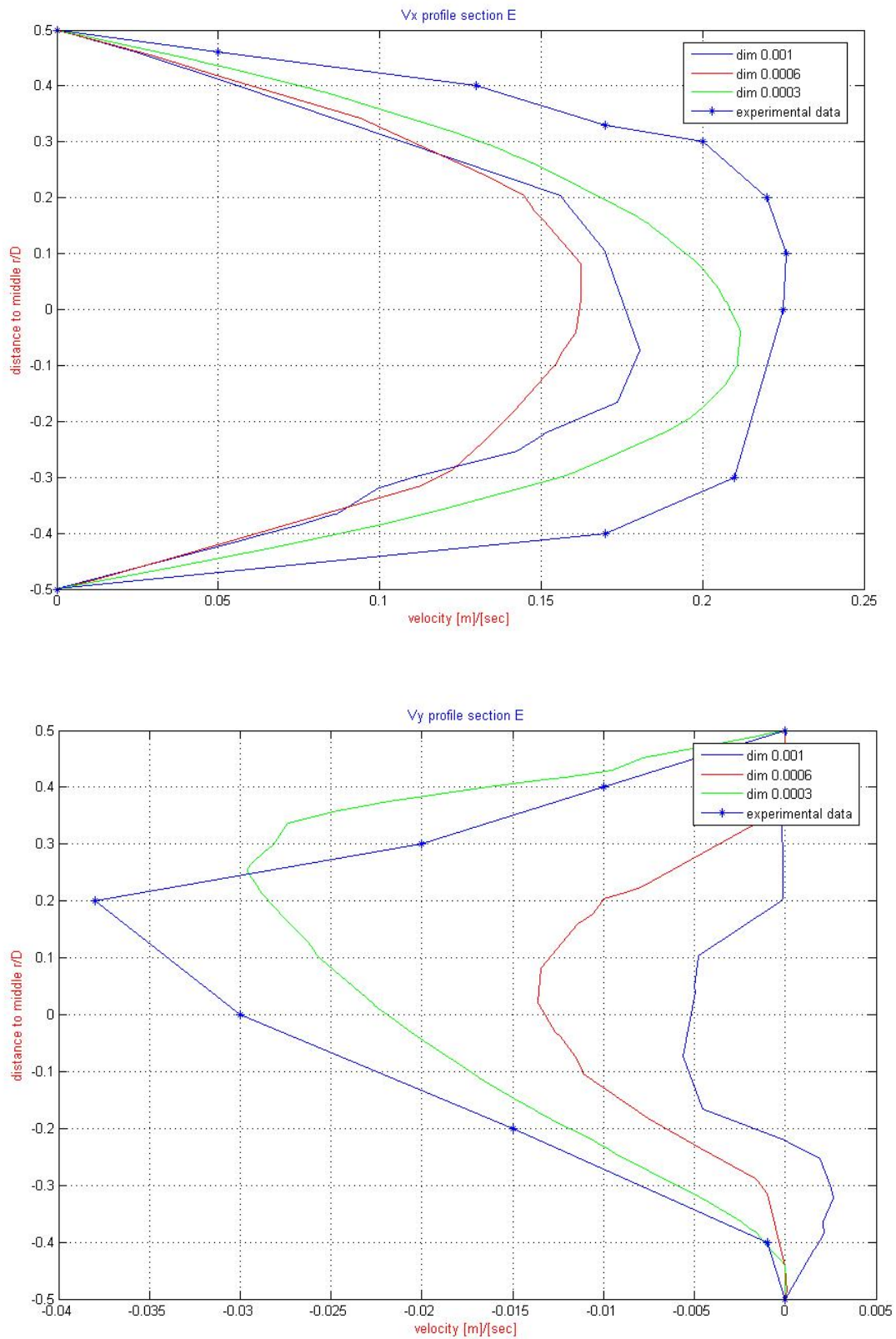


Figure 22 Series of results obtained changing the elements dimension

6. Pulsatile Flow in an End to Side Anastomosis (graft bifurcation)

This third test is a variation of the precedent one. The evolution of the test const in a variation of the flow profile. The test is set with a flow similar to a pulsatile period in a real human vessel. In this test only two sections will be studied just after the joint of the two channels and just before the single channel of exit.

The geometry, the construction of the mesh is the same of the precedent case. The variations imported are only visible in the change of the type

6.1. Data: the pulsatile blood flow

As a natural evolution of the precedent case, were changed some condition in the flow and in the boundary fixed condition.

The first change was the expression of the velocity in the section of entering blood.

The parabolic profile is present here too, but the flow now takes variation in the time. The function fixed so take this expression showed below.

The expression with the function “if()then()else()endif” was used to see how differences can occur, even if these differences are very little and not change the final results.

This expression produces a curve that well interpolates and simulates a cardiac wave pulsation.

We decide to make this using the software MatLab, so we can modify and modeling better all the plots.

In the incoming section, upside, we set that the velocity has a parabolic expression for all the duration of the cycle, with the higher velocity in the middle of the circle, and zeros value in the correspondence to the circumference the higher speed reach 0.644m/sec.

```

if(x<-0.004)then(2*(-(y^2+z^2)/(0.0028^2)+1)*
((-2.09011*(10^(-19))*(t/0.1)^9)+(4.21019*(10^(-16))*(t/0.1)^8)+
(-3.55119*(10^(-13))*(t/0.1)^7)+(1.62266*(10^(-10))*(t/0.1)^6)+
(-4.32593*(10^(-8))*(t/0.1)^5)+(6.70523*(10^(-6))*(t/0.1)^4)+
(-5.58040*(10^(-4))*(t/0.1)^3)+(1.946850*(10^(-2))*(t/0.1)^2)+
(-4.44535*(10^(-2))*(t/0.1))+0.68607)
*(10^(-6))/((0.0028^2)*pi)
else(-2*(-((y+0.00505)^2+z^2)/(0.00175^2)+1)*
((-2.98391*(10^(-21))*(t/0.1)^9)+(7.99312*(10^(-18))*(t/0.1)^8)
+(-9.04536*(10^(-15))*(t/0.1)^7)+(5.59343*(10^(-12))*(t/0.1)^6)
+(-2.03623*(10^(-9))*(t/0.1)^5)+(4.35424*(10^(-7))*(t/0.1)^4)
+(-5.07046*(10^(-5))*(t/0.1)^3)+(2.55189*(10^(-3))*(t/0.1)^2)
+(-1.41935*(10^(-2))*(t/0.1))+0.814879)
*(10^(-6))/((0.00175^2)*pi)endif

```


The blood data remain the same ones

Density	1050	Kg / m^3
Viscosity	0.0035	$Kg / m \cdot s$
Compressibility	0.0	s^2 / m^2

We also put a fixed field of pressure in the two section of exit for the blood, so to emulate the precise definition of pressure of Taylor.

Step number	Time increment	Max iteration	Output step
800	0.003	3	50

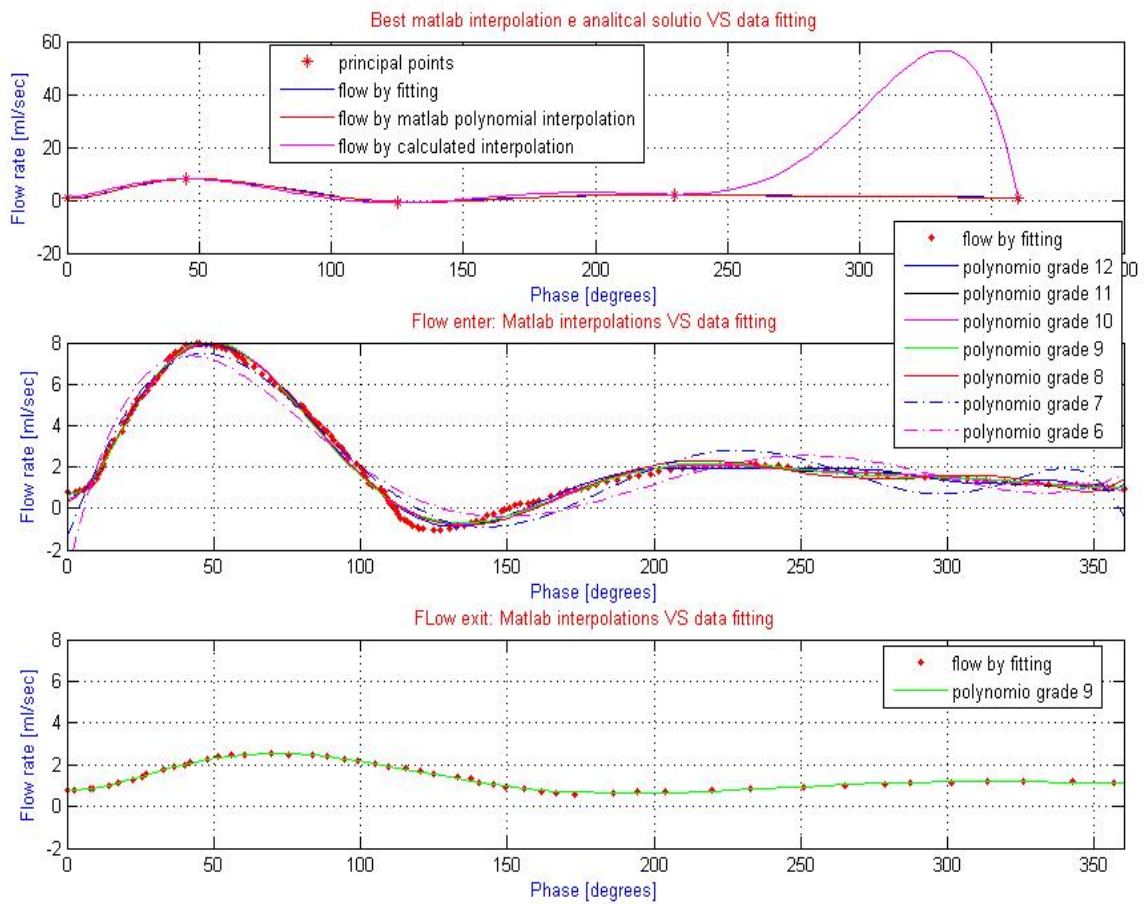
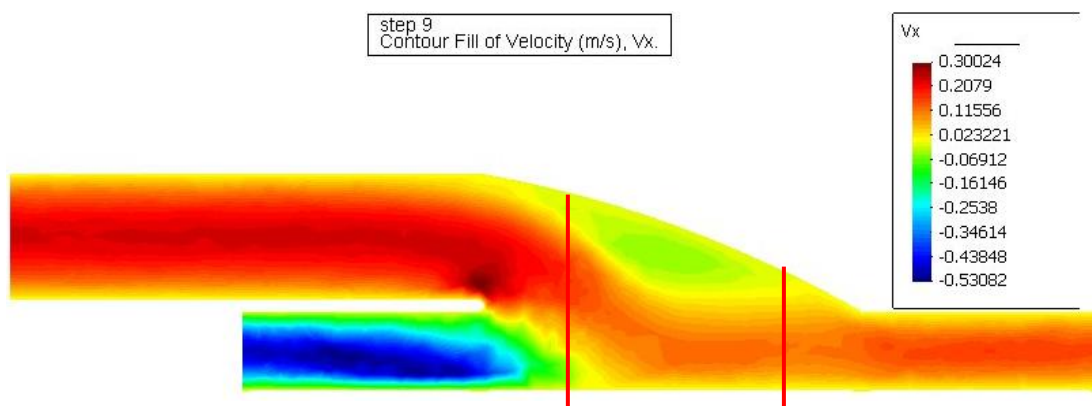
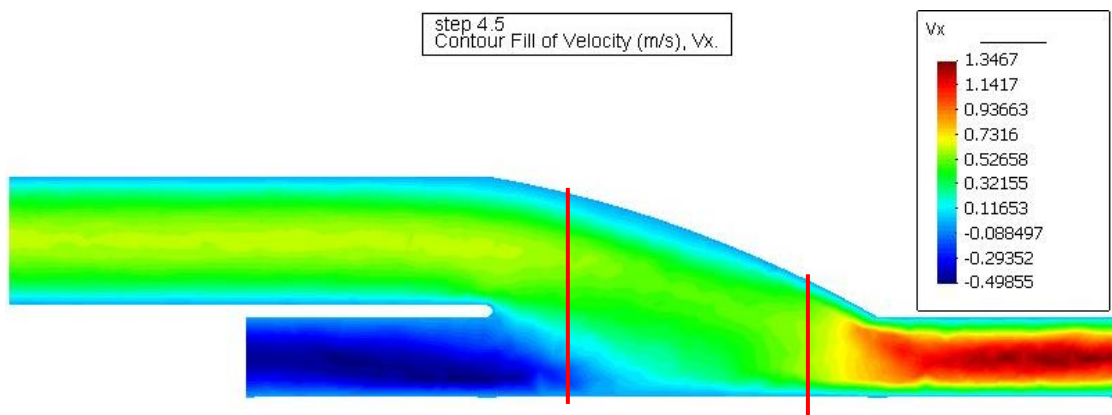


Figure 23 Polynomial interpolation: best polinomy choice

6.2. Results

We evaluate and compare the results of the simulation in two different sections: at 3mm 12mm to the graft.

These values was chosen because in the precedent study we encounter that values like the ones that give us the best results, because we don't have the precise data that Taylor used in his studies.



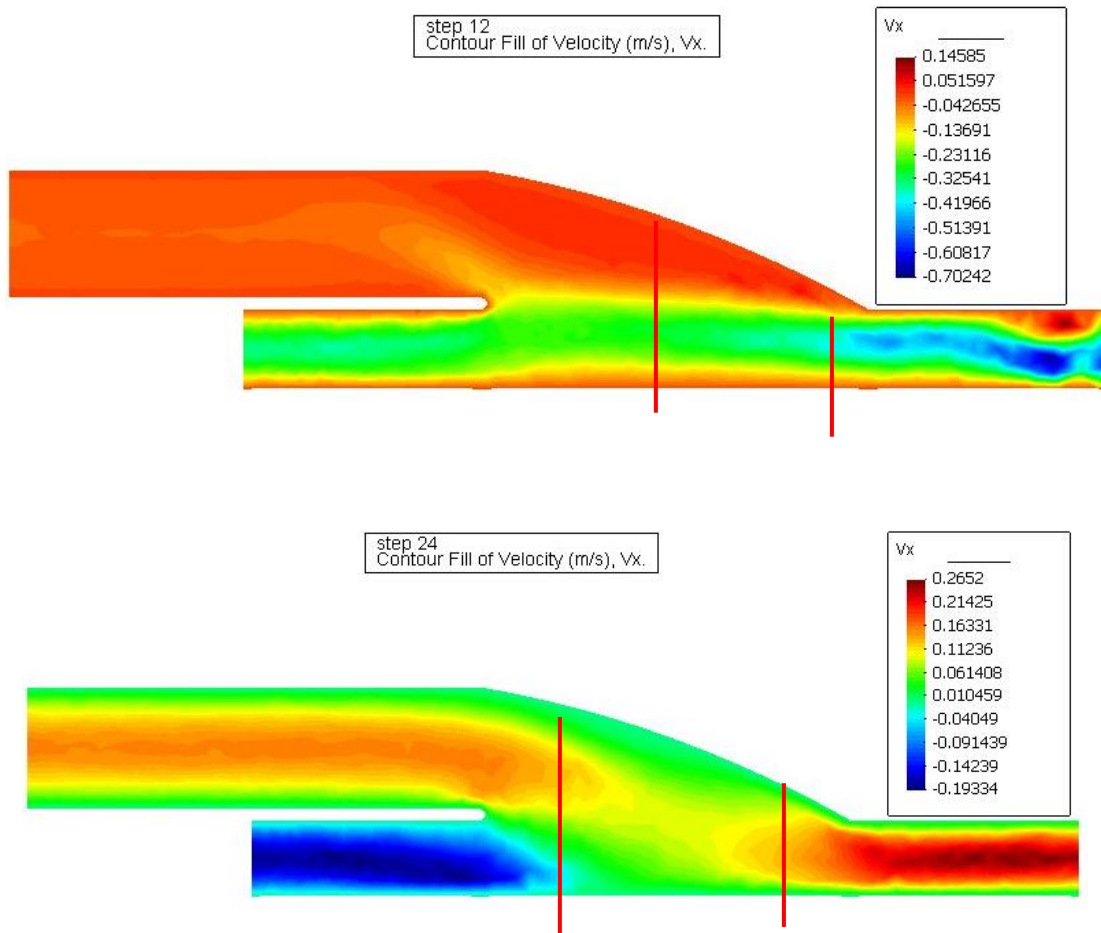
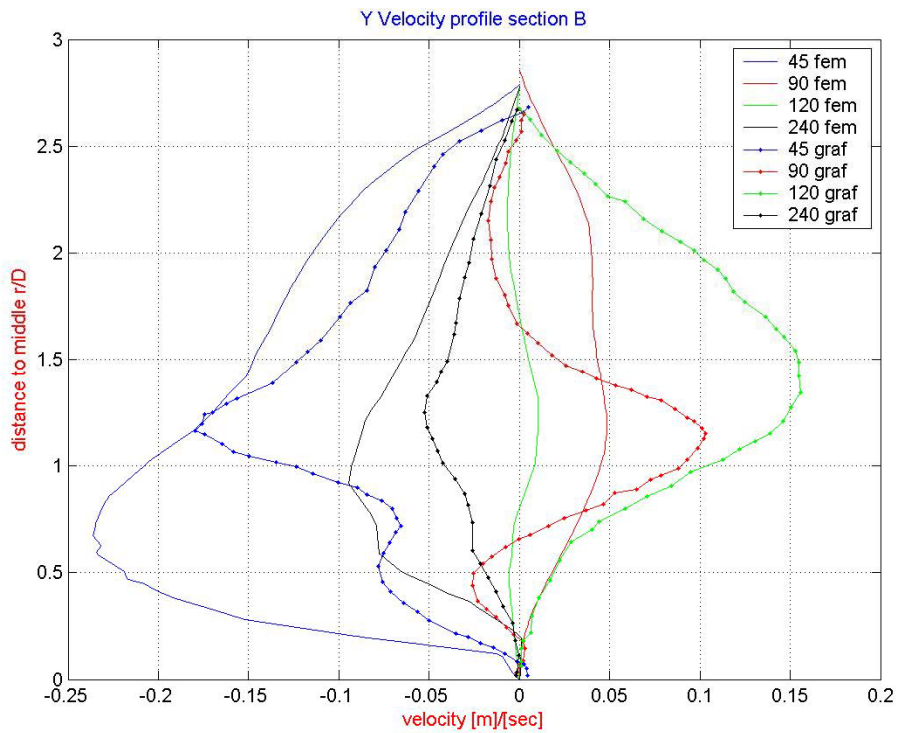
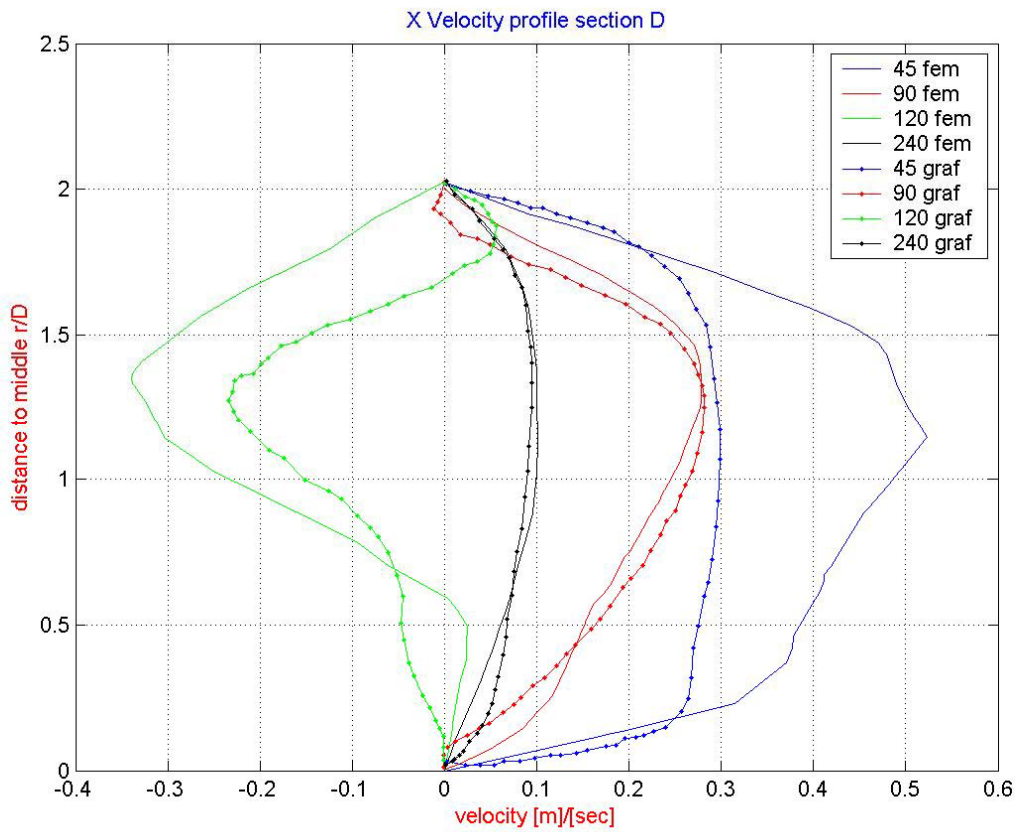
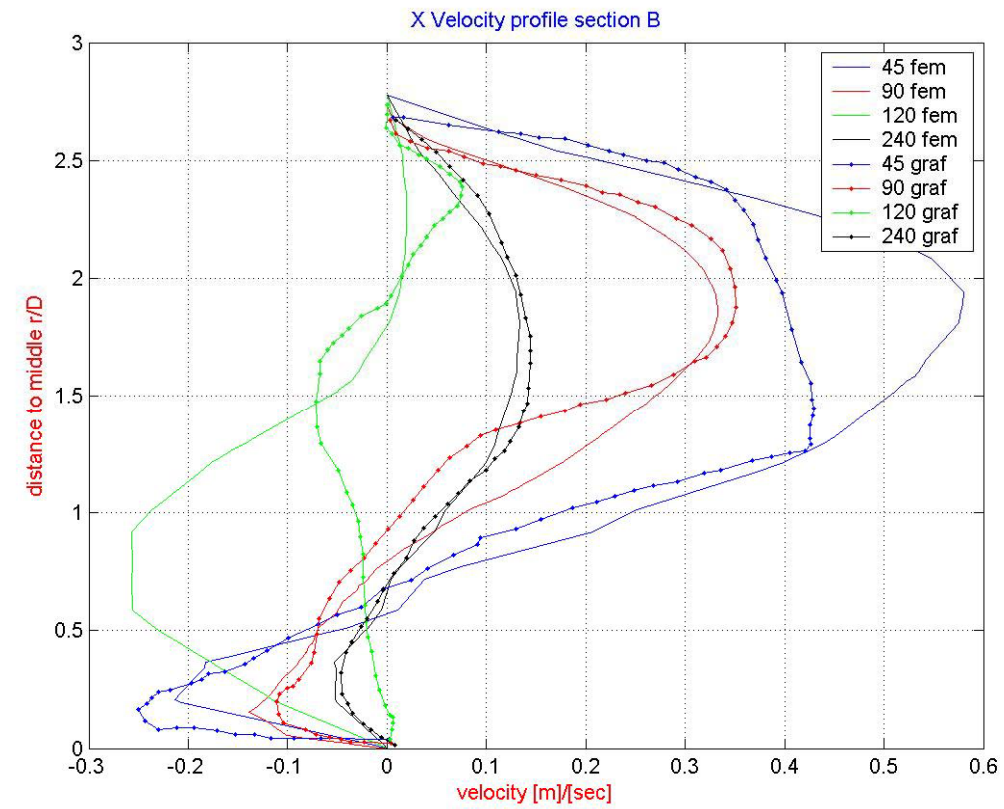


Figure 24 Evolution of the flow velocity profile at 45°, 90°, 120° and 240°





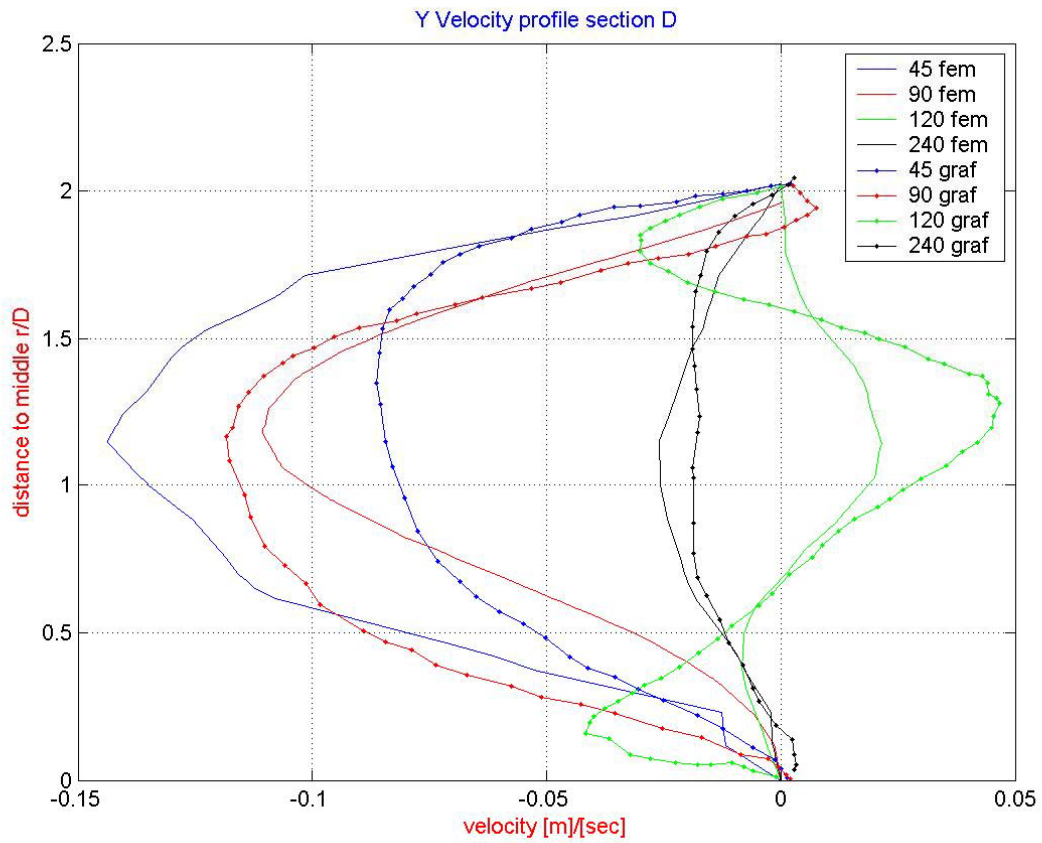


Figure 25 X and Y Velocity profile in the 2 section for the 4 time instants

The results give us also the possibility to calculate the flow that go out to the distal section and repurpose us the same data that we have toke to the Taylor's works.

Flow dos	Flow pos	Flow ent	Per cent error	Rate Pos/Dos
0.706570 ml/sec	2.220619 ml/sec	2.883889 ml/sec	0.014902 ml/sec	3.14

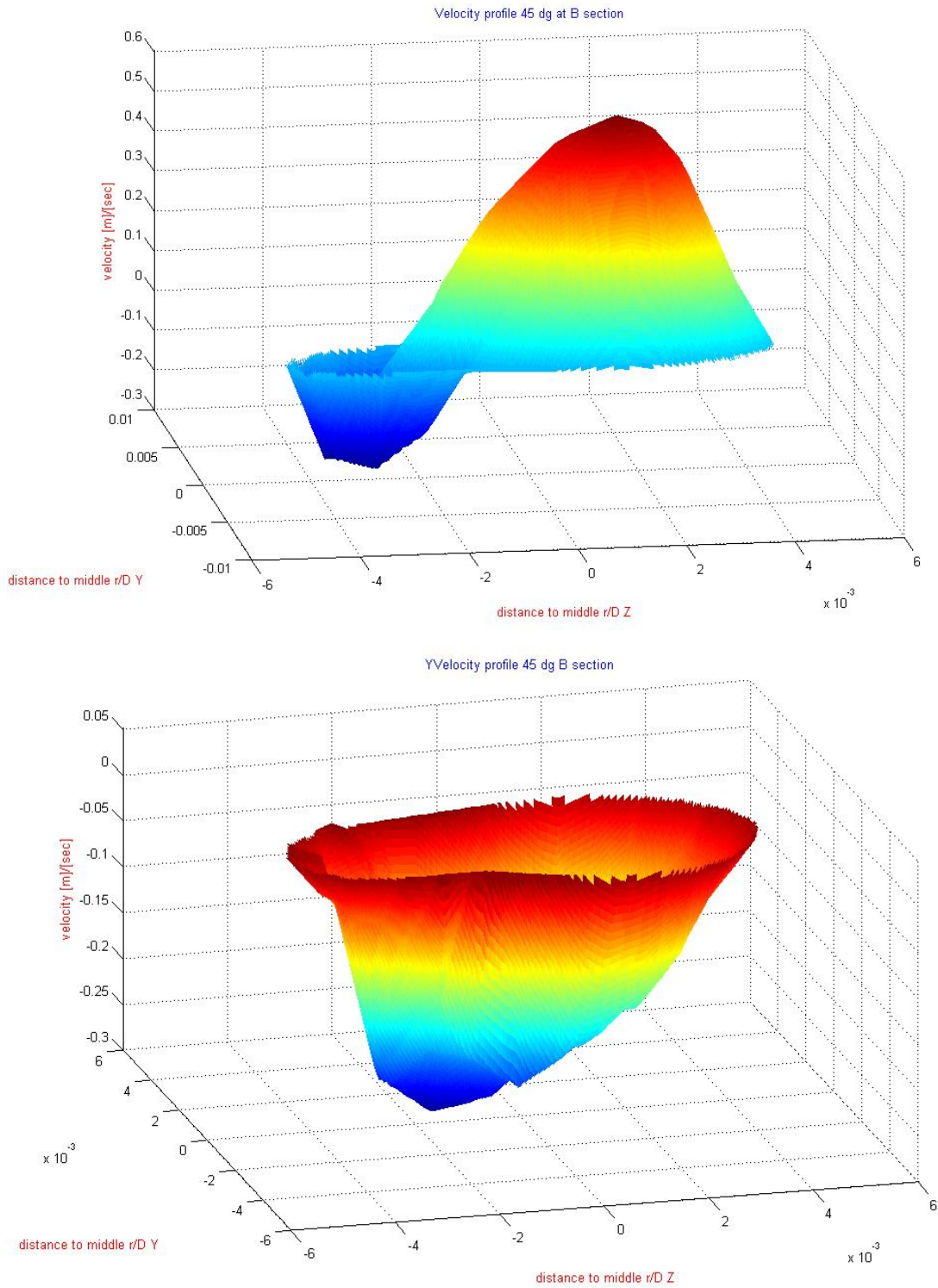


Figure 26 3D representations of velocity profiles

7. Carotid bifurcation (pulsatile flow)

This is the first test of a real simulation of a particular human vessel. The carotid is very important in the blood circulation direct to the head, and problems in this area can give very dangerous injury in cerebral area or more (Stroke, Oxygen insufficiency)

The enlargement that occurs in the zone of the bifurcation presents a possible risk of aneurysms or difficulty in the circulation if this enlargement grows. So is interesting to see the movement of the blood in a cycle similar to the pulsation of the heart.

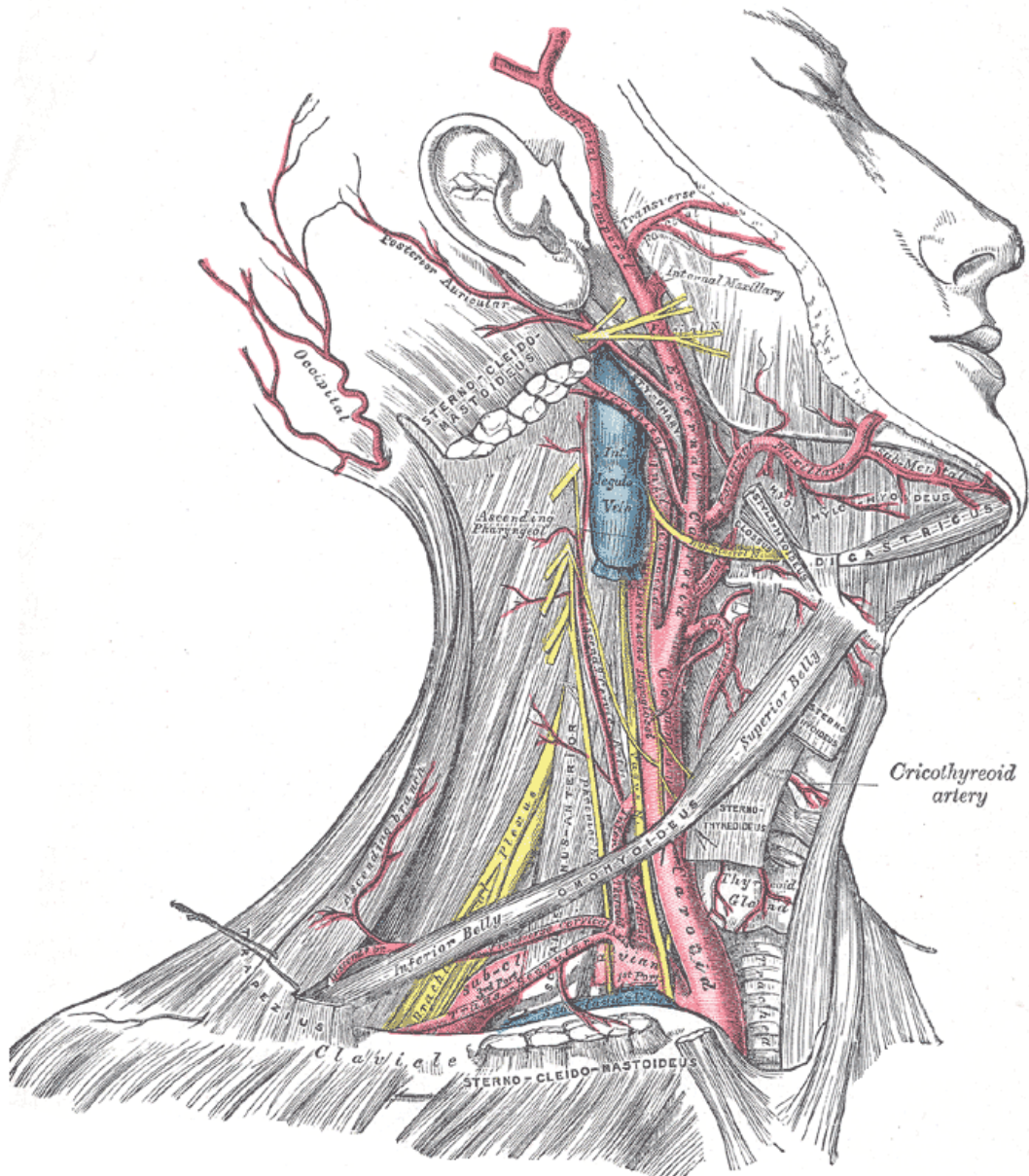


Figure 27 Carotid anatomy

7.1. Geometry, Mesh and Data

Using GID and Tdyn we reconstruct the geometry of a carotid bifurcation, when the carotid divide itself in the external and internal carotid, this one taking an enlargement at the proximal position of from the bifurcation, where the problems can occur.

We simplify the geometry like Taylor did.

We have to modify only a little bit the geometry when we design it with GID so we can construct a good mesh to calculate the problems.

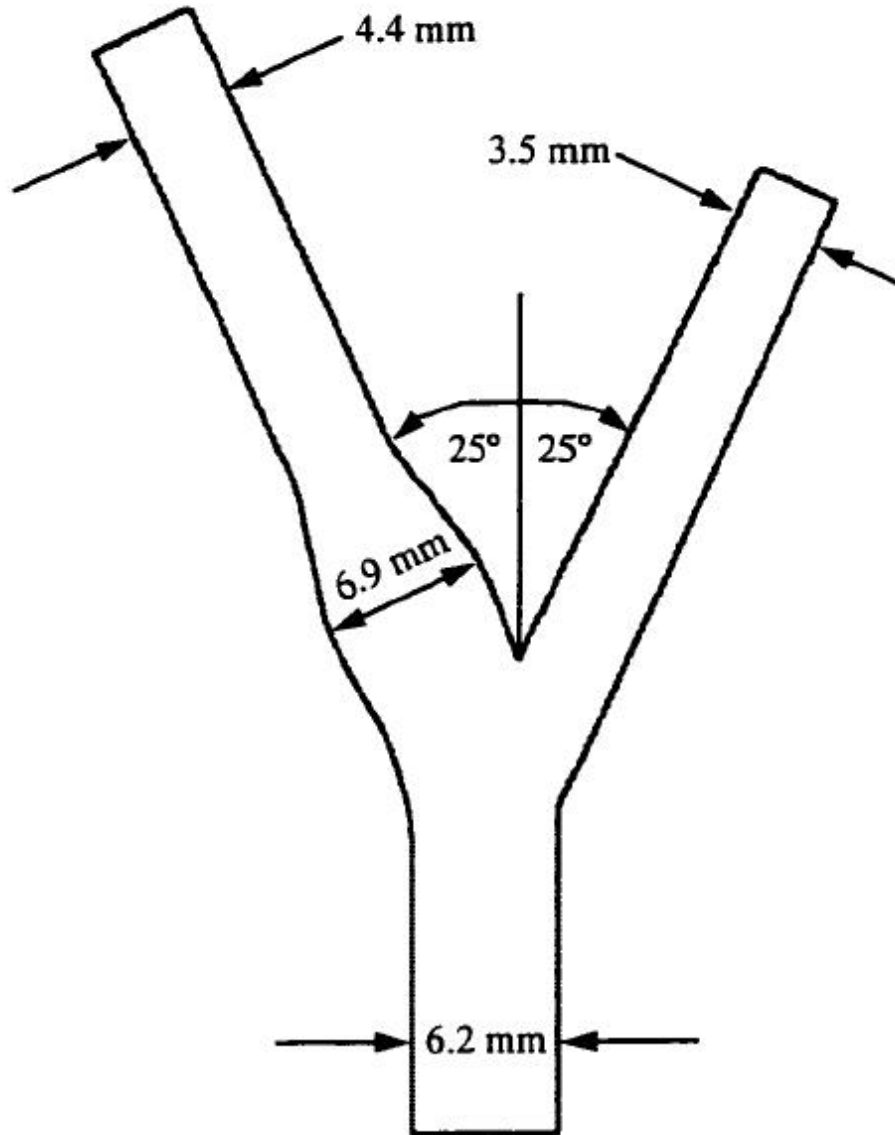


Figure 28 Geometry model of idealized carotid vessel

We construct the enlargement with many little surfaces, so we can produce a more regular volume.

Using more surfaces produces a problem that manifest himself in the creation of many lines, that the program use like base to construct the mesh. So is it important to construct a

geometry that have not angles with little degree, so that the tetrahedras constructed don't have too little volume.

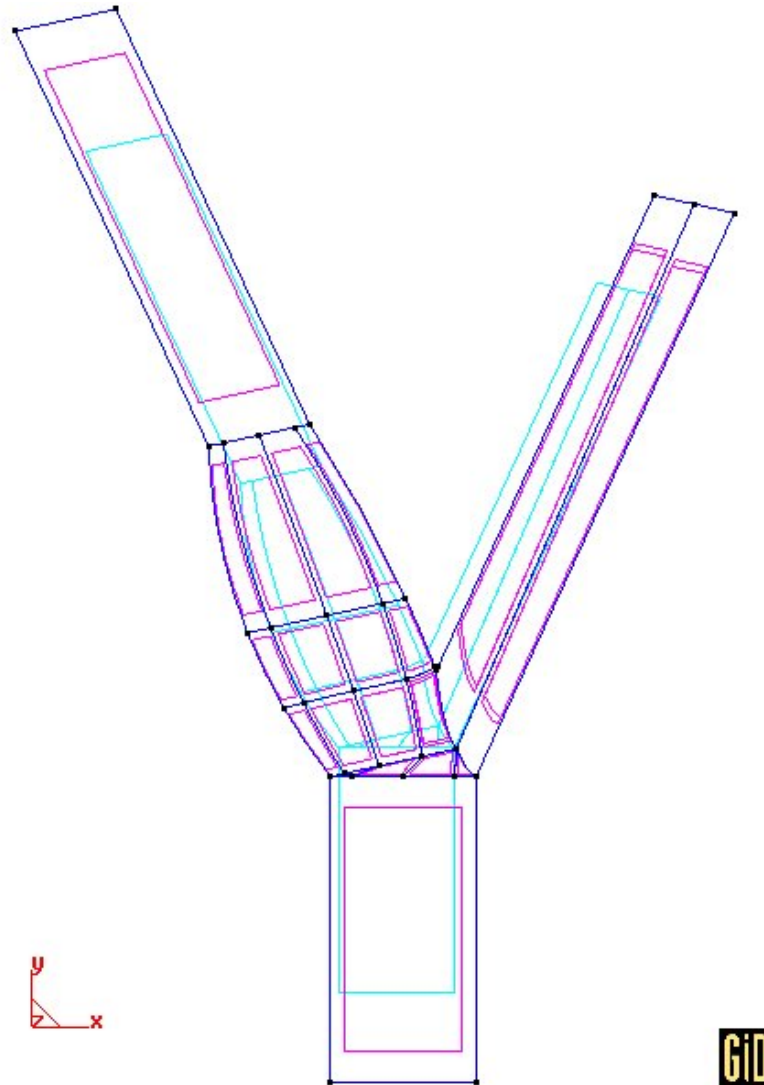


Figure 29 Geometry model realized for carotid test

We have a second comparing test to try to evaluate the changes in the flow when the quantity that goes out in the littler part of the division was fixed.

After we impose all the boundary conditions and the fluid conditions, we can construct the mesh, resulting so shown now:

Element size (m)	Triangles number	Tetrahedras number
0.0003	36672	477959

The first mesh constructed contains only 94567 tetrahedral elements, but to obtain more precise data the number of these ones was increased until they come to 477959.

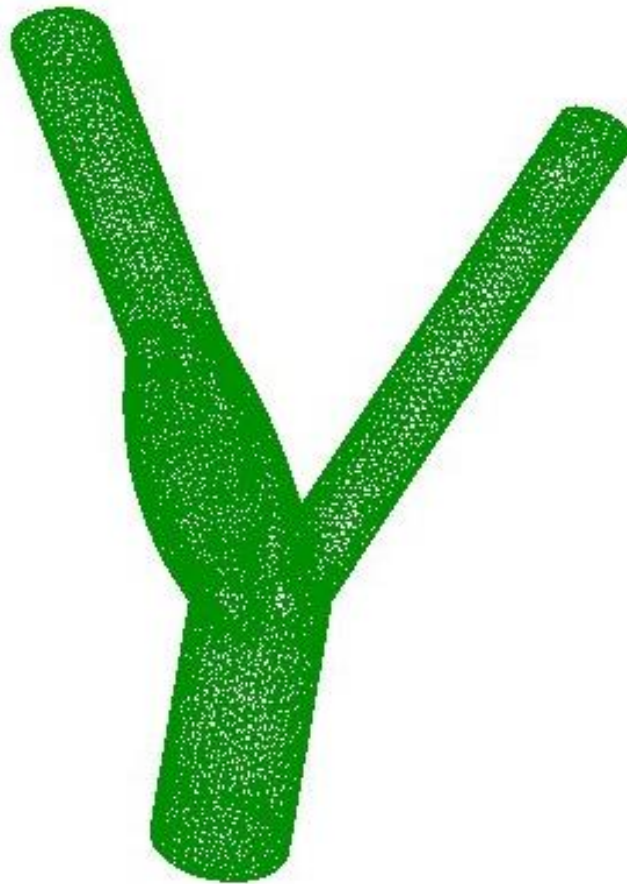


Figure 30 3D mesh representation of carotid model

The data used for setting the fluid body were the same of the studies run before; equally we use the VfixWall condition to fix a no slip boundary condition in the vessel lateral walls.

Density	1050	Kg / m^3
Viscosity	0.0035	$Kg / m \cdot s$

Compressibility	<i>0.0</i>	s^2 / m^2
------------------------	------------	-------------

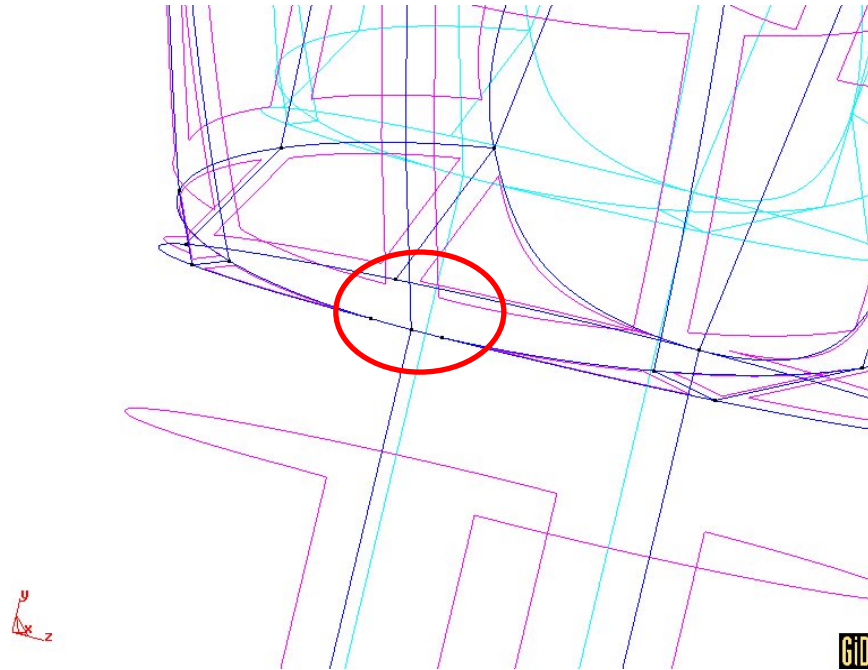


Figure 31 Angles changed to obtain larger ones

7.2. The pulsatile blood flow

After we set the condition of the flow and impose that the lower surfaces is the one trough that the flow enters. We extrapolate the expression of a polinomy that can best emulate the flow imposed by Taylor with MatLab software into 5 different level of complexity. We chose a polinomy of 12' degree and it have this profile and after using a mesh finer was used a polynomial expression of 8' degree. This change was operated because the computation could become too expensive and the time of the simulation could reach many weeks of work. With an expression less complex was possible to use a limited number of steps. The polynomial expression can interpolate the flow in the most important points and with the same variation

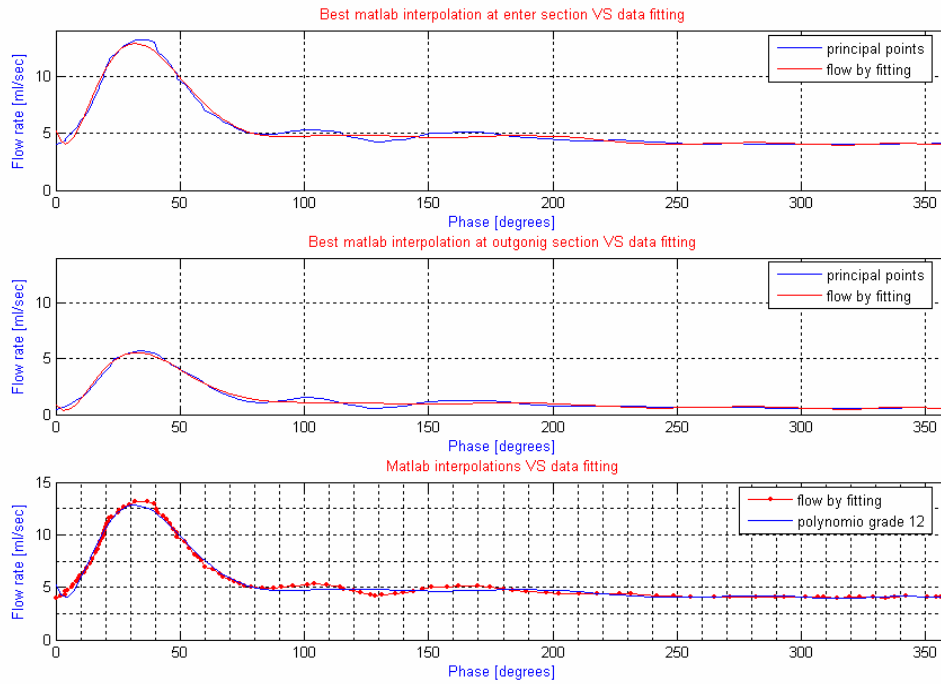


Figure 32 Test results for best polinomy choice

The polinomy expression, in the surface takes this shape.

$$\begin{aligned}
 & 2*(1-(z^2+x^2)/(0.0031^2))*((5.244621727567987*(10^{(-25)})*(t/0.1)^{12})+ \\
 & (-1.221983541909621*(10^{(-21)})*(t/0.1)^{11})+ \\
 & (1.256453799398373*(10^{(-18)})*(t/0.1)^{10})+ \\
 & (-7.497964893663985*(10^{(-16)})*(t/0.1)^9)+ \\
 & (2.872461096163208*(10^{(-13)})*(t/0.1)^8)+ \\
 & (-7.375019313081318*(10^{(-11)})*(t/0.1)^7)+ \\
 & (1.284900902261524*(10^{(-8)})*(t/0.1)^6)+ \\
 & (-1.501980894565149*(10^{(-6)})*(t/0.1)^5)+ \\
 & (1.133431264749728*(10^{(-4)})*(t/0.1)^4)+ \\
 & (-5.077333737038586*(10^{(-3)})*(t/0.1)^3)+ \\
 & (1.114128658713102*(10^{(-1)})*(t/0.1)^2)+ \\
 & (-6.22482280376416*(10^{(-1)})*(t/0.1)^1)+ \\
 & (5.077670969168930))*(10^{(-6)})/((0.0031^2)*\pi)
 \end{aligned}$$

$$\begin{aligned}
 & 2*(1-(((x-0.01239)*(0.955)-(y-0.037372)*(0.207))^2 \\
 & +((y-0.037372)*(0.046)-(x-0.01239)*(0.207))^2+(z)^2)/(0.00175^2))* \\
 & ((3.408876497926587*(10^{(-25)})*(t/0.1)^{12})+ \\
 & (-7.831421390246382*(10^{(-22)})*(t/0.1)^{11})+ \\
 & (7.934060093717072*(10^{(-19)})*(t/0.1)^{10})+ \\
 & (-4.662284342931503*(10^{(-16)})*(t/0.1)^9)+ \\
 & (1.757991718378535*(10^{(-13)})*(t/0.1)^8)+ \\
 & (-4.441698707136652*(10^{(-11)})*(t/0.1)^7)+ \\
 & (7.616897115308278*(10^{(-9)})*(t/0.1)^6)+ \\
 & (-8.771472994508260*(10^{(-7)})*(t/0.1)^5)+ \\
 & (6.532389778050600*(10^{(-5)})*(t/0.1)^4)+ \\
 & (-2.896028274269553*(10^{(-3)})*(t/0.1)^3)+ \\
 & (6.304805543217139*(10^{(-2)})*(t/0.1)^2)+ \\
 & (-3.393922678185155*(10^{(-1)})*(t/0.1)^1)+ \\
 & (0.8476051833550092))*(10^{(-6)})/((0.00175^2)*\pi)
 \end{aligned}$$

The polinomy in the other out going section is quite different, because we have to separate the flow contribution in the different components of the normal to the section studied.

We have a second comparing test to try to evaluate the changes in the flow when the quantity that goes out in the littler part of the division was fixed. So the second polinomy in the figure corresponds to the out going flow.

After we impose all the boundary conditions and the fluid conditions, we can construct the mesh, resulting so shown now:

Increasing the number of element, the problems to find a good step time to permit a stability of the problem, with a limited number of steps, become hard.

It was necessary to change the polynomial expression, using one of order 9.

$$\begin{aligned}
 & 2*(1-(z^2+x^2)/(0.0031^2))* \\
 & ((-1.012*(10^{-18})*(t/0.01)^9)+ \\
 & (1.63*(10^{-15})*(t/0.01)^8)+ \\
 & (-1.09*(10^{-12})*(t/0.01)^7)+ \\
 & (3.88*(10^{-10})*(t/0.01)^6)+ \\
 & (-7.80*(10^{-8})*(t/0.01)^5)+ \\
 & (8.51*(10^{-6})*(t/0.01)^4)+ \\
 & (-4.07*(10^{-4})*(t/0.01)^3)+ \\
 & (-1.67*(10^{-3})*(t/0.01)^2)+ \\
 & (5.97*(10^{-1})*(t/0.01))+ \\
 & (2.45)*(10^{-6})/((0.0031^2)*\pi)
 \end{aligned}$$

This change can permit a quicker resolution of the problem, and leave a good approximation of the flow used in the testes run by the other researchers.

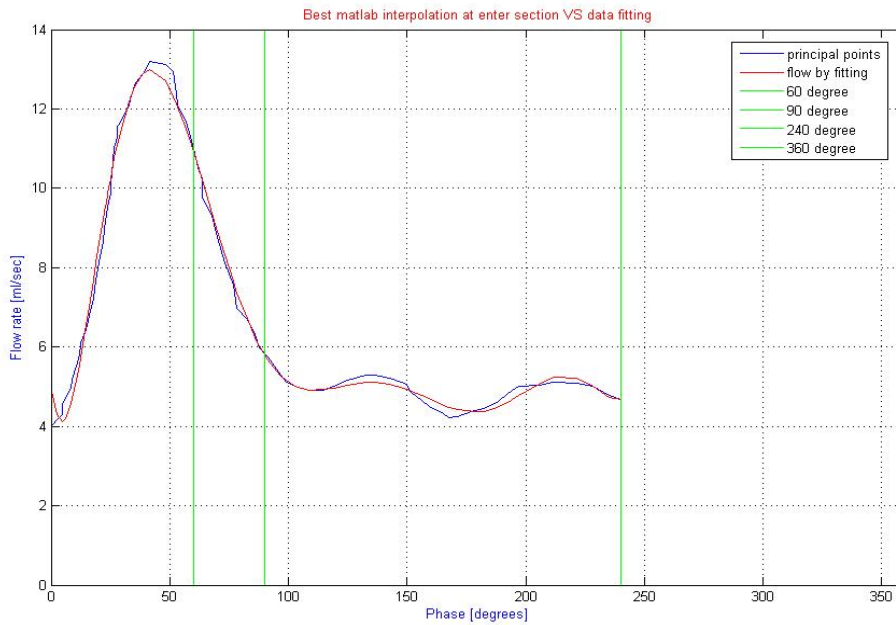


Figure 33 Interpolation of the first part of the flow

The final part of the flow was reproduced with a right line that goes down till the value of rest of the flow. This change doesn't modify meaningfully the final result of interpolation.

The tale of the flow was replaced by another function that follows only the last points of the graphic. This change of function permits to have a good quality flow.

Element size (m)	Triangles number	Tetrahedras number	Nodes number
0.0045 m	20500	177566	32248

The blood characteristic doesn't register variations.

Density	1050	Kg / m^3
Viscosity	0.0035	$Kg / m \cdot s$
Compressibility	0.0	s^2 / m^2
Thermal conductivity	1.0	$W / m \cdot ^\circ C$

The quality of the mesh using are resumed in the follow table

Step number	Time increment	Max iteration	Output step
6000	0.00006	5	100

7.3. Results

In this experiment the goal was to evaluate the entity of the reflux in the zone if the aneurysm. The enlargement that we encounter just upside the bifurcation is considerable like an aneurysm; this is a typical problem that can prejudice the health of a patient, because a rupture of a vessel in this location can interrupt the flux of blood and so of the oxygen to the brain. The studies were effectuated in four different instant of the cycle. The first at 0.6 seconds (60°) the second one at 0.9 seconds (90°), the lasts ones at 2.4 and 3.6 seconds (240° and 360°). The profile of velocity was the principal one: in Y direction (up-down) and the place of the cut is shown in the last picture by a white line.

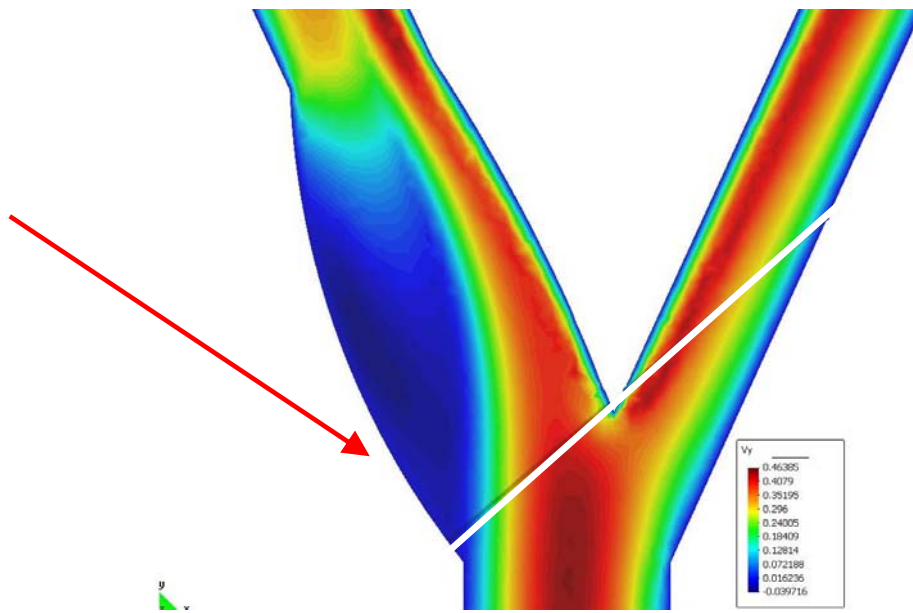
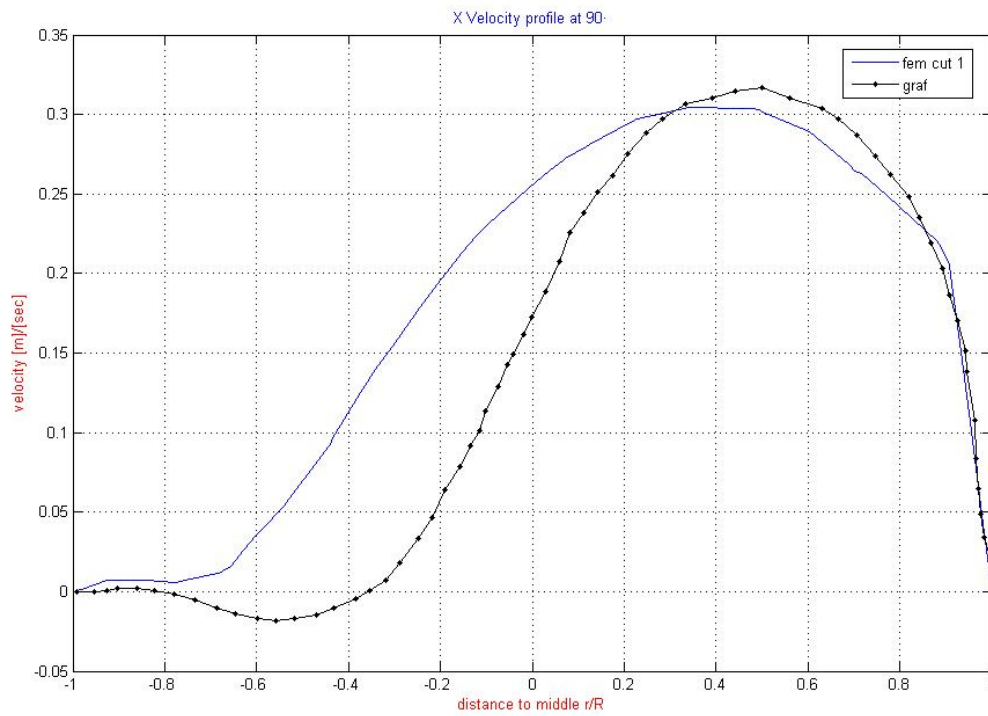
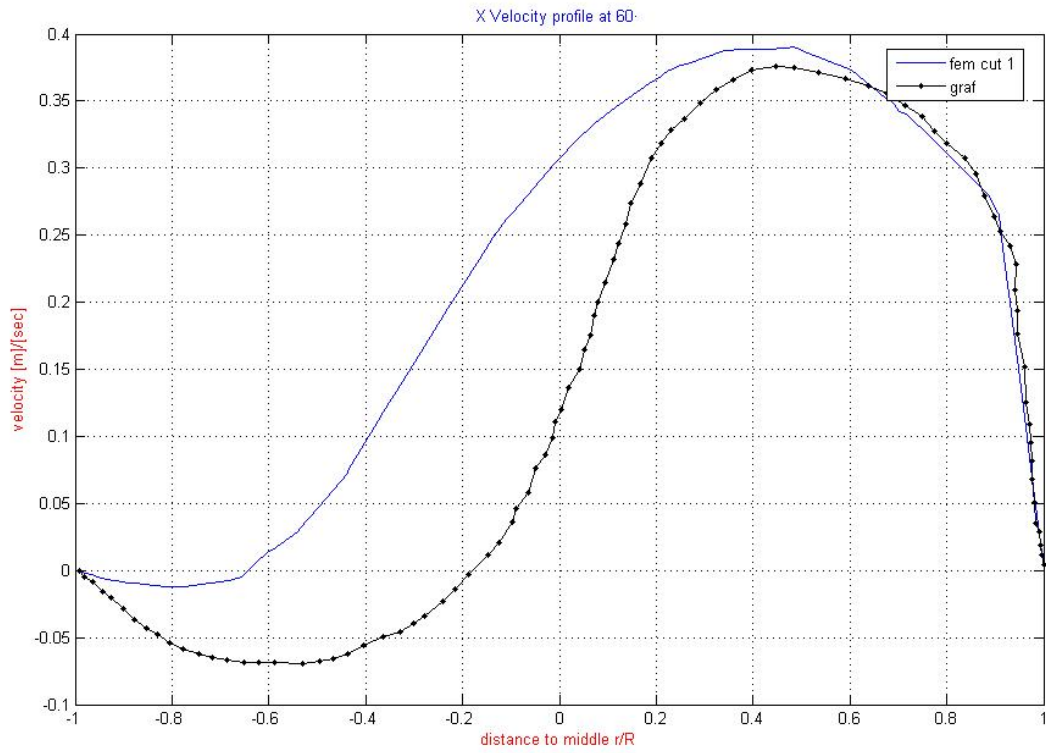


Figure 34 The arrow shows the negative velocity and blood reflux. The white line shows the cut effectuated

All the results that we obtain follow the Taylor's experimental data they have the same profiles and very similar domain of velocity. The differences that it is possible to meet are due to the possible discrepancy of the geometry of the polynomial expression that we use.

The negative flow encountered might be the cause of injuries or problem; cause can occur that the blood plays an important rule in the rupture of the vessel in the zone where the aneurysm formed. The aneurisms are usually more fragile than a normal and sane vessel and so the possibilities of the injuries can increase.



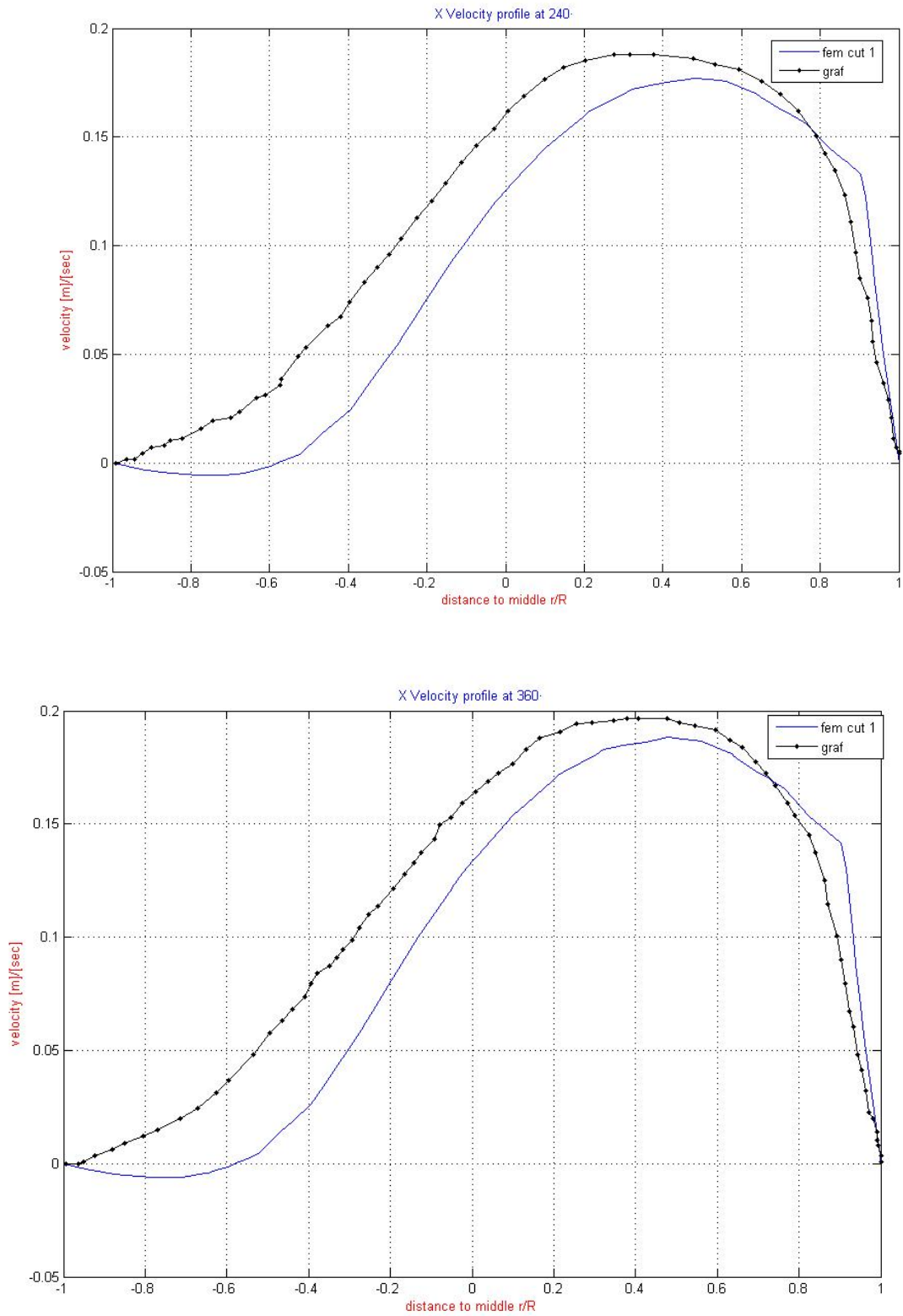
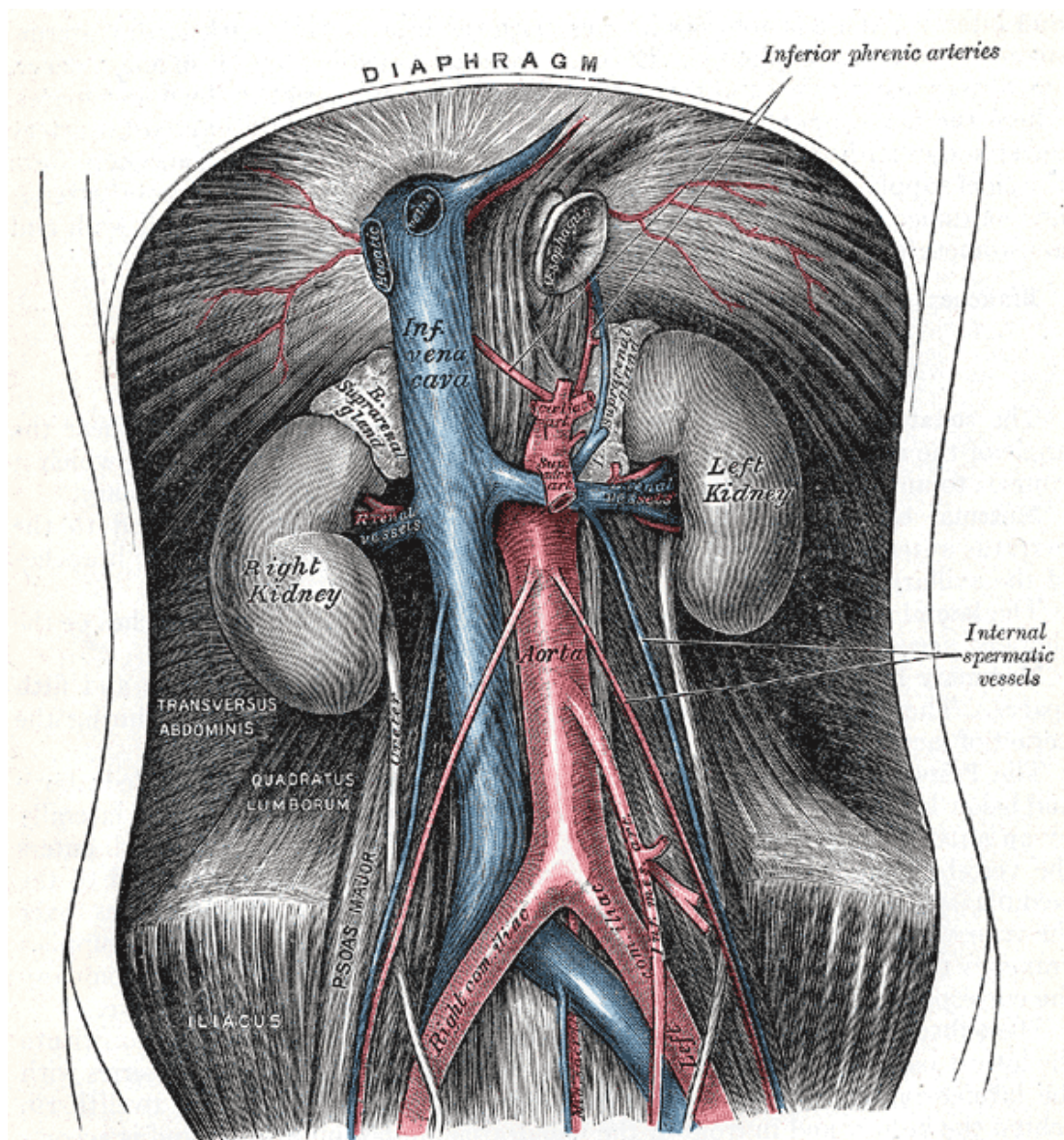


Figure 35 Representation of the Y velocity profile (principal direction) in the cut zone

8. Idealized abdominal Aorta

The last example that was run is idealized aorta geometry. We set the velocity profiles in the upper section and the results were taken in some surfaces where the flow can go out. The three profiles had different levels of intensity and different maximum velocities.

The substantial difference in this test, respect to the precedents is the complexity of the velocity and that were taken the flow rate evolutions in the time, instead of the velocities at fixed time instants in a section that correspond to the diameter of an exit surface.



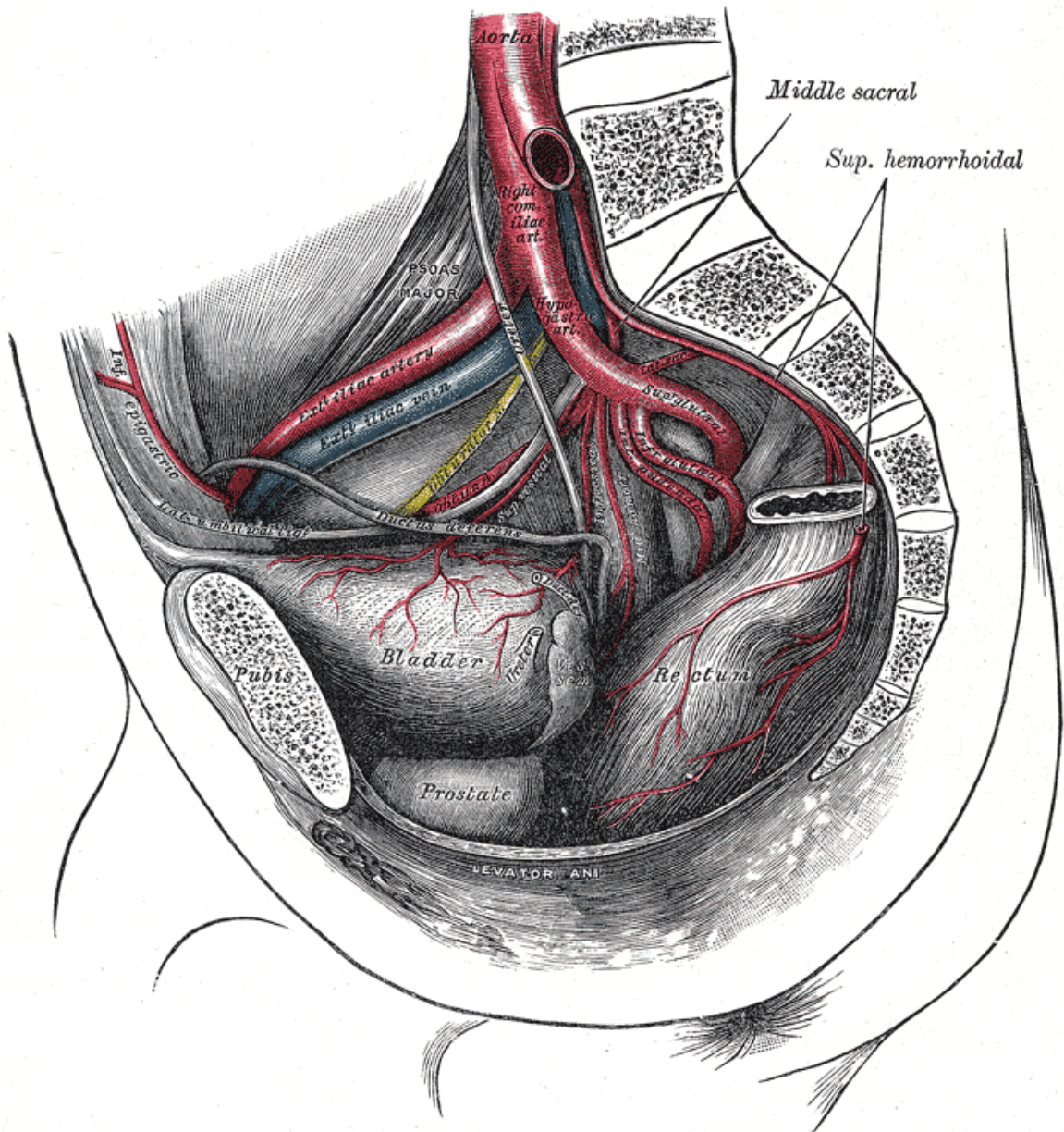


Figure 36 Abdominal Aorta anatomy

8.1. Geometry, Mesh and Data

This is the most complicated work, because the geometry has a lot of variation and change of direction.

The geometry follow the design of the abdominal aorta, when it divides itself in the two vessels directed to the legs, it is also possible to see the bifurcation to the rein and the starting vessels like the mesenteric ones.

Construct the geometry with similar dimension was possible searching in the documentation all the data that show the anatomical shape of this artery.

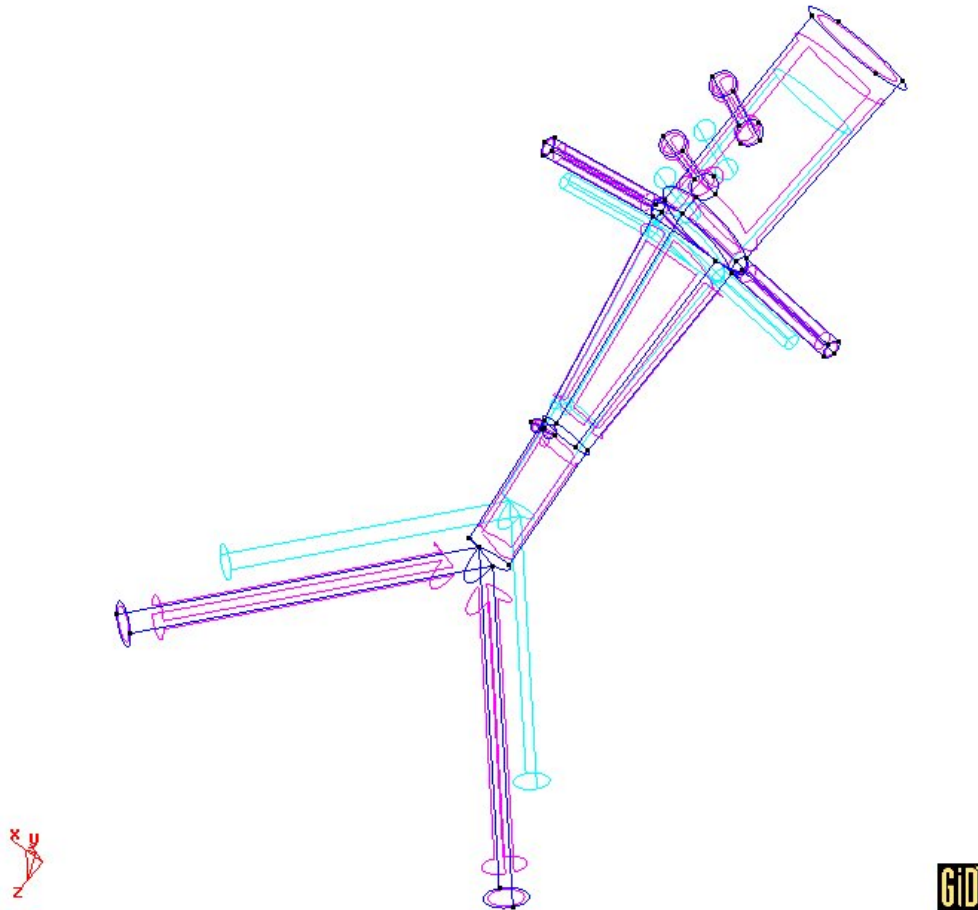


Figure 37 Geometry visualization of the Idealized Aorta Model

The particular conformation of the aorta, the variations of inclination and the numerous bifurcations need a refinement in the places where the surfaces had a little angle of junction.

The technique used for this improvement was to join and collapse the lines and the points that create geometries with very fine angle, in the way to form angles larger and so

the mesh constructed can use very little elements and can not generate elements with a value of volume too little that the tolerance of the program can read like null volume.

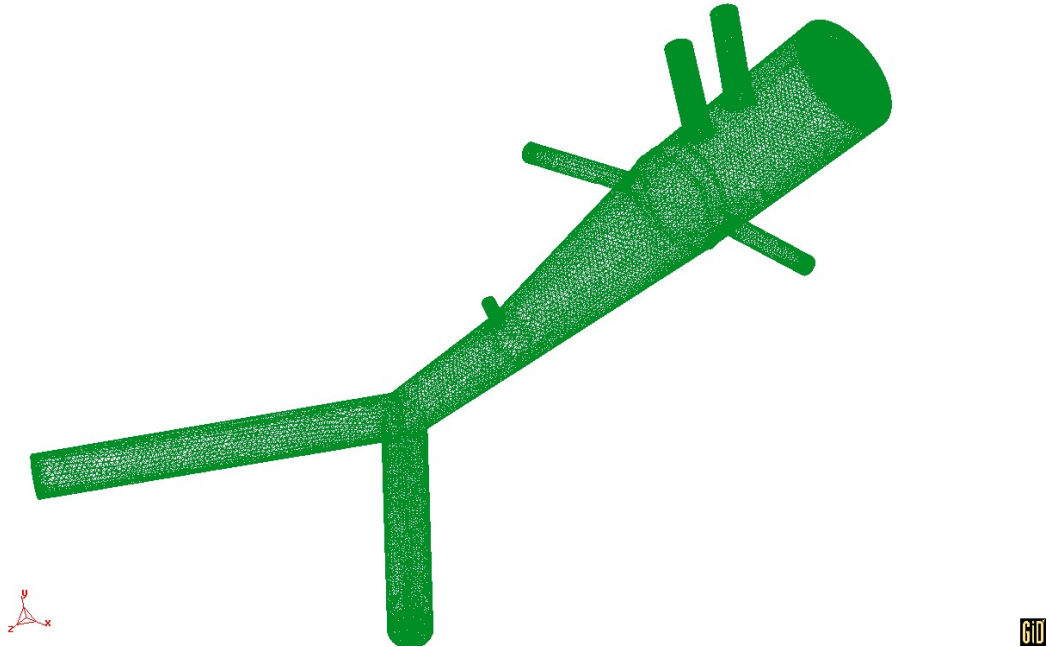


Figure 38 Mesh visualization of the Idealized Aorta model

Element size (m)	Triangles number	Tetrahedras number
0.0003	60552	472252

This is the last model used. Here were prescribed three different testes: maintaining the same geometry, the same blood characteristics and the same mesh dimensions; we studied three different cases of blood flows. The blood characteristic doesn't register variations. And are the same of the other testes

Density	1050	Kg / m^3
Viscosity	0.0035	$Kg / m \cdot s$
Compressibility	0.0	s^2 / m^2

8.2. Weak blood flow

In the precedent picture compare like a black line, was the most easy to run, because don't have many variations and the acceleration are smooth.

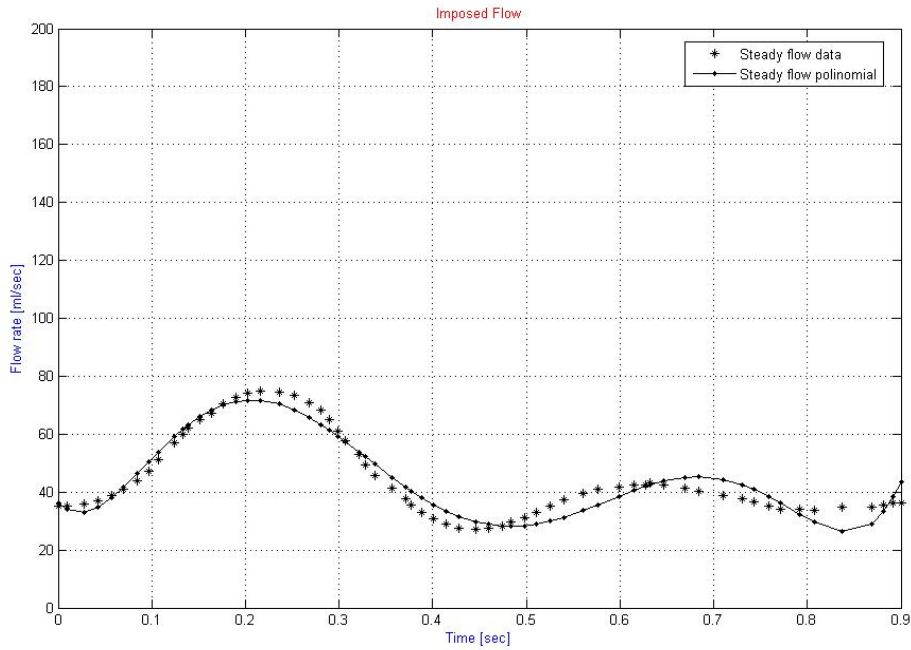


Figure 39 Blood flow rate profile in aorta test

So we can use a littler number of steps, because it is possible to use a step time bigger.

$$\frac{2*(1-(y^2+x^2)/(0.0179^2))*((3.95*(10^4))*(100*t)^6)+(-1.06*(10^5))*(100*t)^5+(1.055*(10^5))*(100*t)^4+(-4.655*(10^4))*(100*t)^3+(8.287*(10^3))*(100*t)^2+(-3.041*(10^3))*(100*t)^1+(3.612)*(10^{-6})}{((0.0179^2)*\pi)}$$

For this case was possible to interpolate easily with a 6 order polynomial expression. This is the minor order expression that was used in these studies. This easy expression, of the flow, simplifies enormously the solution of the problem, because the time of resolution can decrease.

The quality of the mesh using are resumed in the follow table

Blood flow	Step number	Time increment	Output start	Output step
Weak	3600	0.0000025	25	25

8.3. The flow rate

The last test requires a different study to the first four. The object of the simulation now is the flow rate that exits to the surfaces which closing the arteries that leave the principal body of the aorta.

To read these results we program a script with the language TCL that permits us to calculate, in all the instant of time that we want to consider, the flow rate.

This script reads the velocity in the nodes that makes up the triangles of the superficial mesh. Knowing the velocity is possible integrate the data and obtain the value of the flow rate.

The shapes form used by Tdyn are linear, so is possible calculating the mean value of the velocity in a generic triangle, and do a multiplication between the area of the triangle and its mean velocity value so was obtained the single value of flow. Adding the flow values of every single triangle finally we obtain the full value of the flow rate.

8.4. Results

The case of the aorta modelization requires some changes in the way to read the results. Now we take the output data of the flow rate that exits to the principal bifurcations of the vessel aorta.

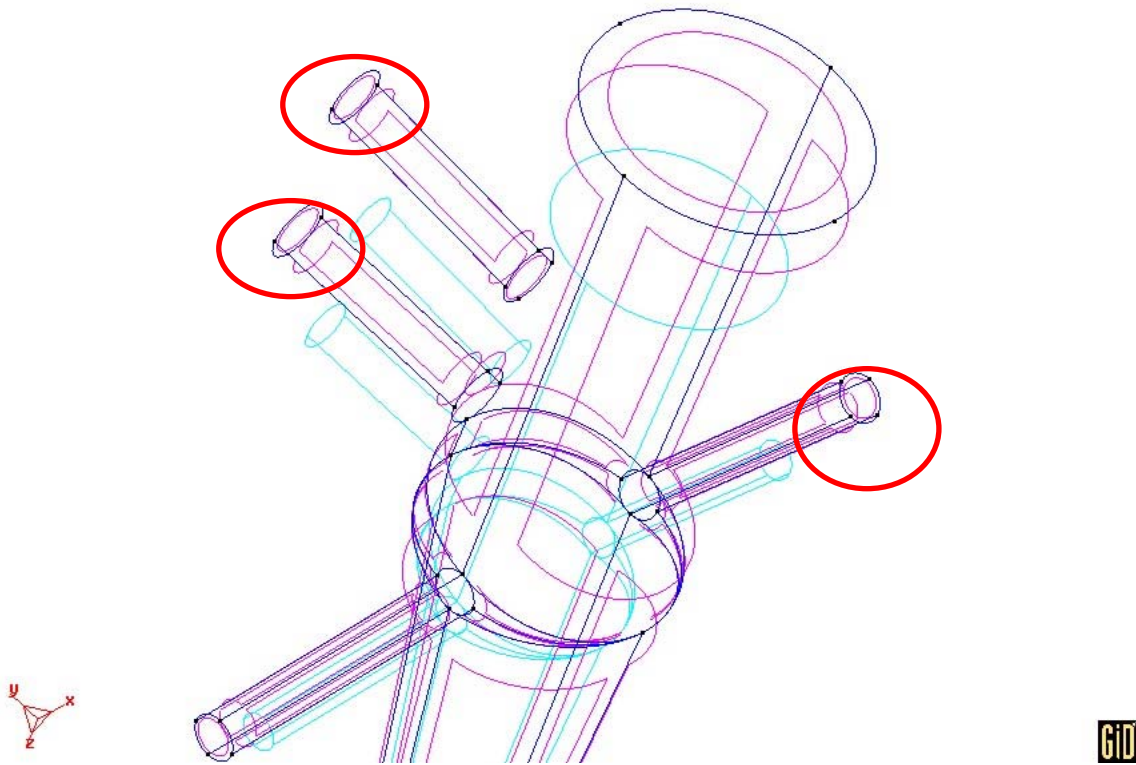


Figure 40 Studied exit surfaces

We take and compare the flows that exit to the vessel renal, to the celiac one and to the superior mesenteric one. The flow imposed was considerate weak, because does not have big accelerations or big velocities, and the profile is quite regular. This flow has a profile that can be compared to a real profile, even if the variation and the amplitude can be different to a real one.

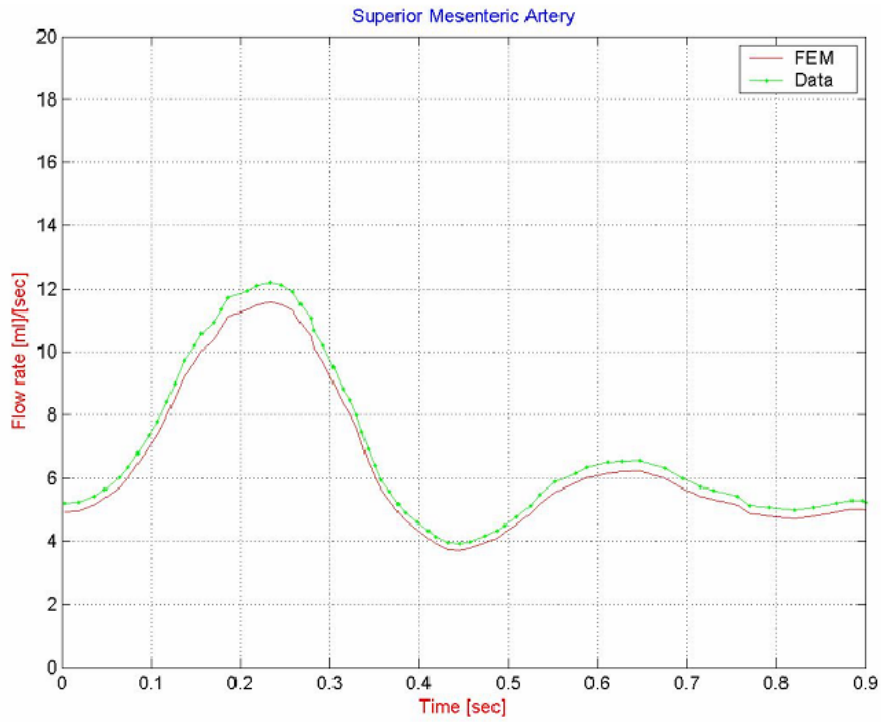


Figure 41 Superior Mesenteric Caudal

The results can show that our simulations produce very similar profile of flow, even if the geometry can have little differences. The outgoing flows reproduce also the profiles of the entering flow, with a high value of velocity in the first 0.2 – 0.3 seconds.

The little dimensions of the mesh now cannot play a relevant rule in the quality of the plots, the discretization of the graphic now depend by the step of the time with that we record the results. So we calculate the flow in 3600 points, and the program could give us a very high definition plots.

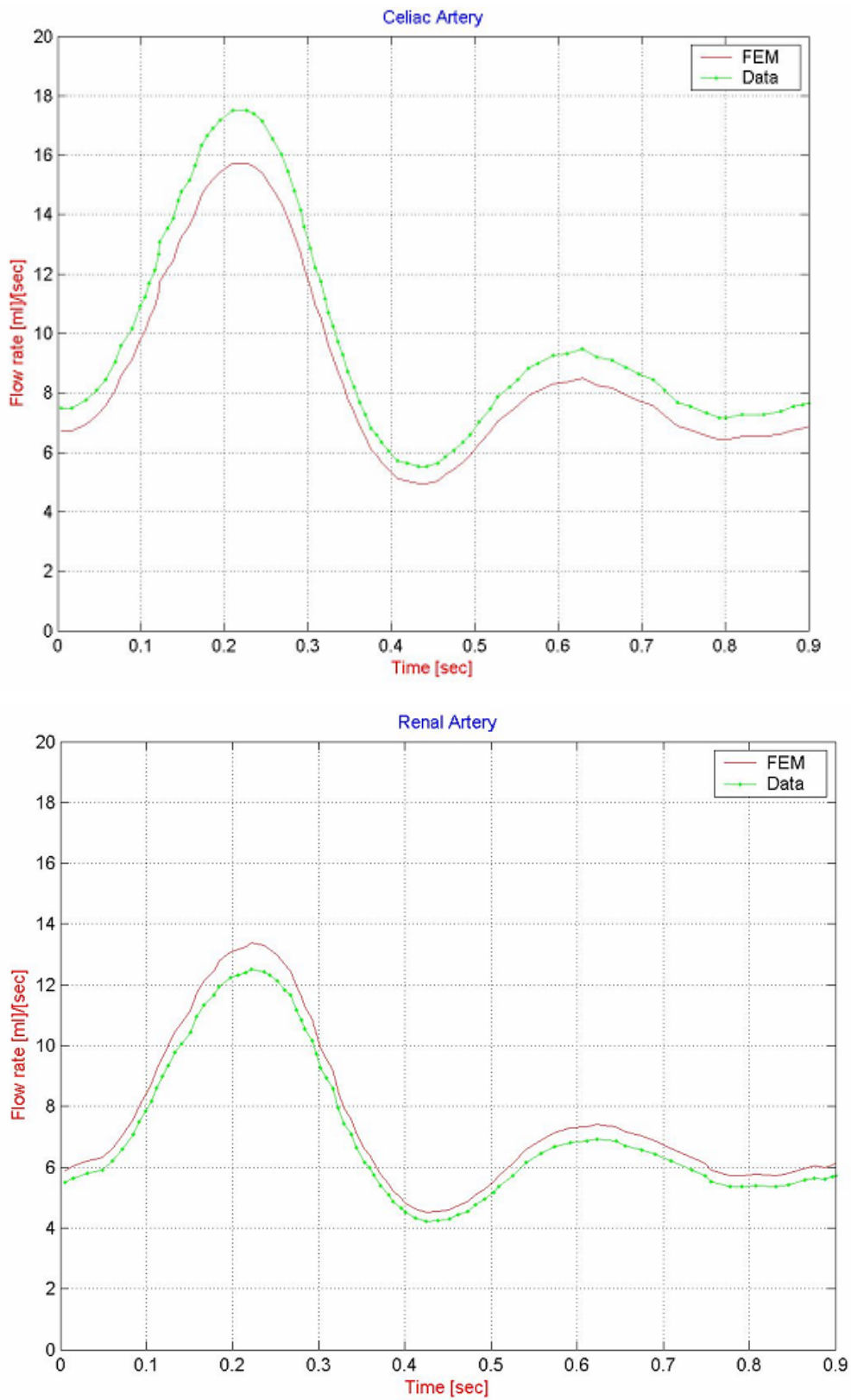


Figure 42 Representation of the 3 flow rate registered at the exit surfaces

9. Real Carotid

The results and the experiences taken until this moment, permit us to construct and to work with real cases. The first step that we can realize was to work with a real carotid and try to run a simple case, with a pulsatile flow, so we have the prove that is possible to take and use real geometries directly from medical imagines.

The technique is named Voxelization and is made up by three steps:

- Imagine acquisition
- Imagine segmentation
- Reconstruction of the surface and its volume

There are a lot of devices that can take the imagine from a subject, so the data are very different and the formats of the imagine can be very singular or diverse. At the end is possible to convert the data in a scalar or vectorial value, representing a union of points that normally make up a regular and orthogonal mesh. Our team works with a format of the medical imagine called DICOM.

The image must be cleaned by the noise and the data that don't are in the field of interest, only so is possible to make visible the zones utile for the test, that the doctor also can use like a normal bio-image of high quality level. To select a single vessel we have to segment the zone of interest, and so to discriminate the shape values that make possible to assign a unique value to the surface of the vessel. Finished this step the medical image is saved en format .VTK of structured meshes STRUCTURED_POINTS. This values joint to the points distribution in this uniform and orthogonal mesh are utilized by an algorithm that reconstruct the surface (marching cube or marching tetrahedras); after we can reconstruct the 3D mesh of the volume with traditional techniques of meshing.

The result of this work is showed below

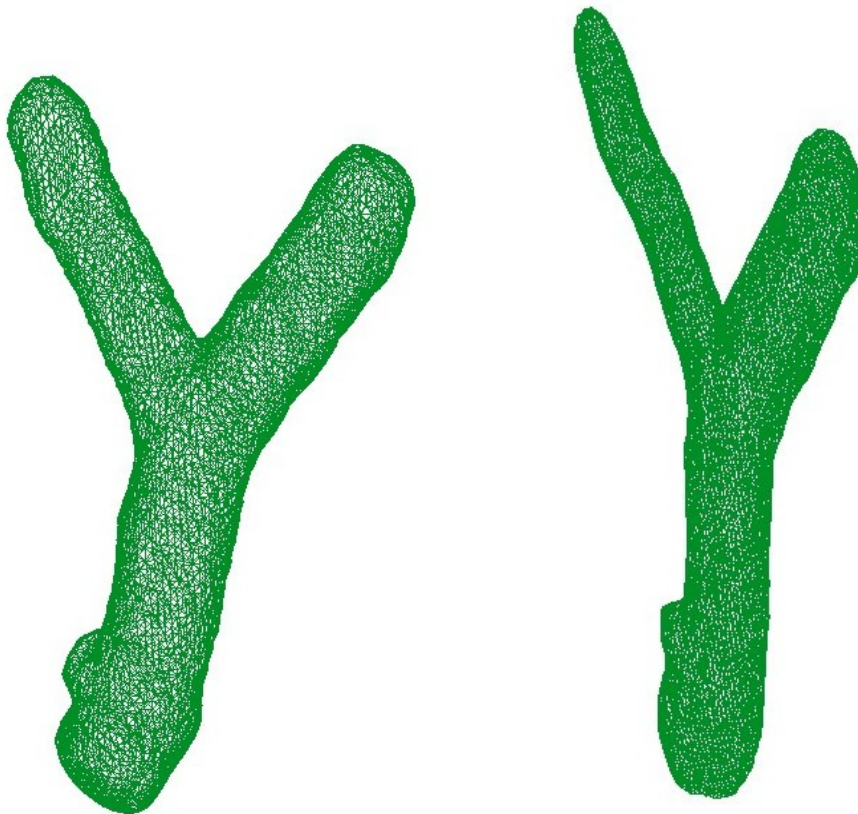


Figure 43 3D visualization of the geometry obtained by the Voxelization

The imagine results a little bit pressed because the position of the carotid is subject of big displacements and modification, even if the mesh obtained is very similar in form and dimensions to the one that we previously design and construct.

9.1. Data and conditions

The data utilized in this test are very similar to the ones used before. The mesh was modified so that was created a boundary mesh and the layers that could represent the zone where the blood can flow in or out. In the two upside section were imposed the property of null pressure, and these ones will be used like outgoing sections. The inferior part is the one that takes blood directly to the aorta, so it receives the blood flow, for this motivation was imposed a ix field of velocity value that describes a sinusoidal profile with this expression (in meter per second):

$$“ 0.1*(1+\sin(\square *t))”$$

A difference to the last testes is findable in the fact that the profile of the velocity is uniform in all the ingoing section. The paraboloid profile wasn't applicable because the entering section is not regular and has not a simple geometry where was possible to calculate a function with that characteristics. So the flow is similar to the one used in the first experiment. The mesh data are resumed like showed:

Element size (m)	Triangles number	Tetrahedras number
0.0014	10486	51012

And the fluid characteristic, imposed to all the fluid body are the same of the other testes and are showed below:

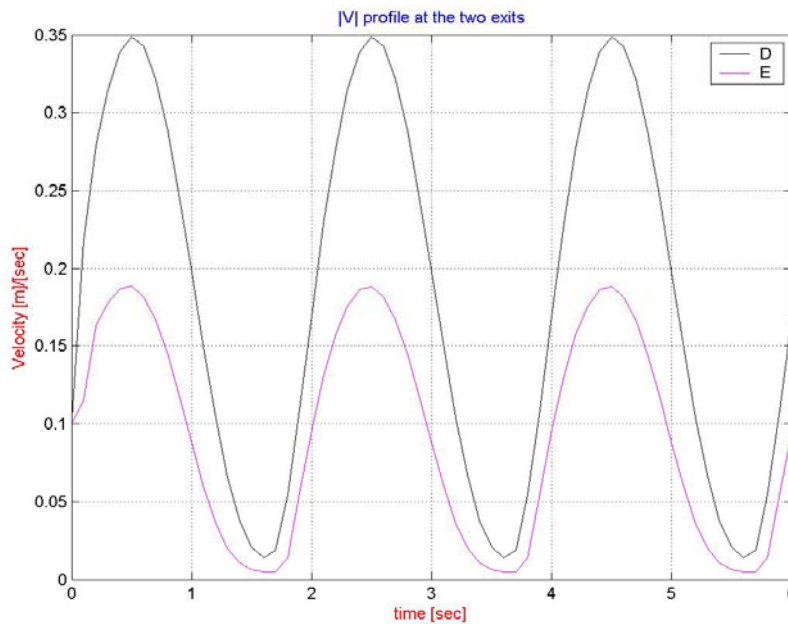
Density	1050	Kg / m^3
Viscosity	0.0035	$Kg / m \cdot s$
Compressibility	0.0	s^2 / m^2

Another property that we can use, is the possibility to create a boundary mesh and utilize it like external wall, we so impose in this place the no slip boundary condition and we also can isolate the extremities and use them like exit surface or entering surface. Is also possible to rotate and translate the geometry to find a correct direction of the imposed flow.

9.2. Results

The imposed sinusoidal profile respond well to the test effectuated. The profile imposed resolves in few steps the transitory moments and considering the space domain few millimeters are sufficient to the blood take a paraboloid profile, having null velocity values in the lateral sides, progressively increasing till the center of the vessel. The results also confirm the tendency of the flow to prefer as exit way the mayor branch that represents the external bifurcation of the internal carotid, as the precedent test made with an idealized carotid.

The pulsatile flow is transmitted well in all the length of the body, like the plots can easily show; the data are taken following the flow way from the lower zone till the two exit upper points.



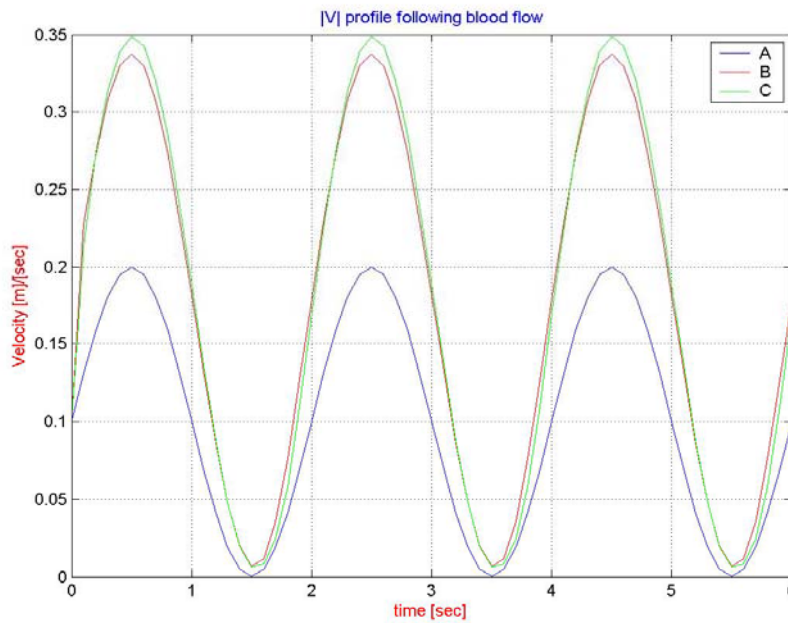


Figure 44 Velocity registered in different places of the model

All the flows are taken in the middle of the section selected, the letters used instead, indicate the position following the blood flow:

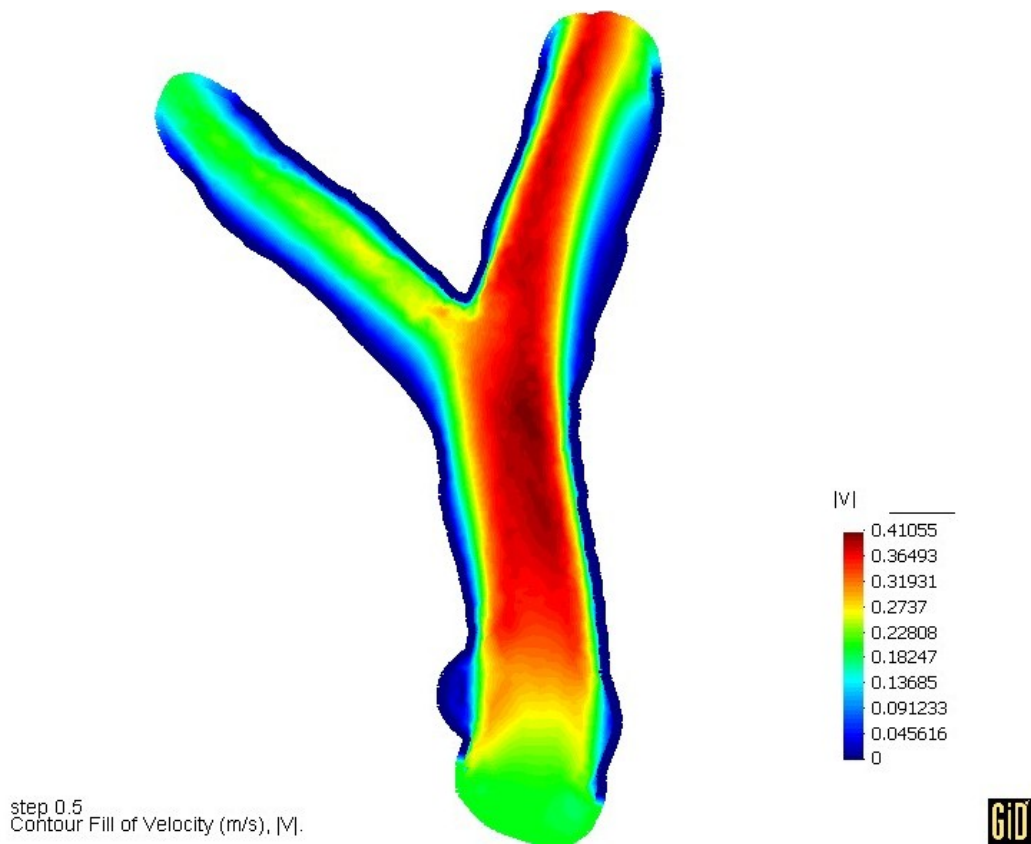
- A is the proximal entering position
- B is situated in the middle of the single branch of the carotid
- C is just below the bifurcation
- D is the exit point of the internal carotid (right branch)
- C is the exit point of the external carotid (left branch)

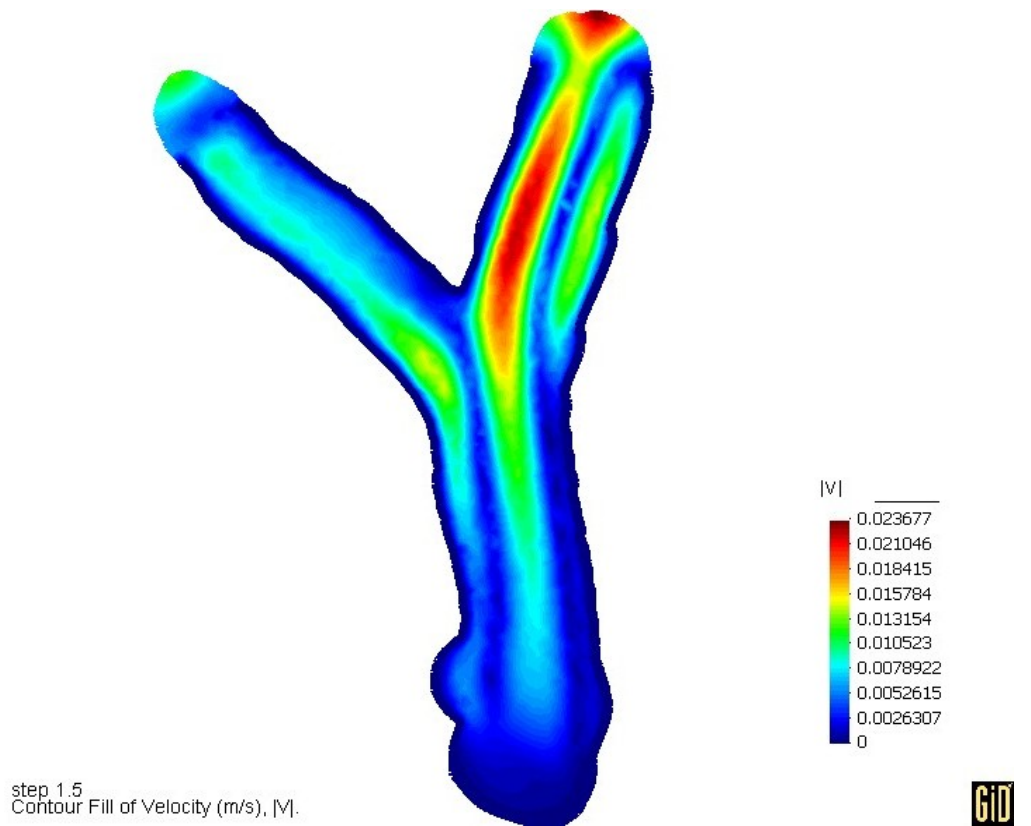
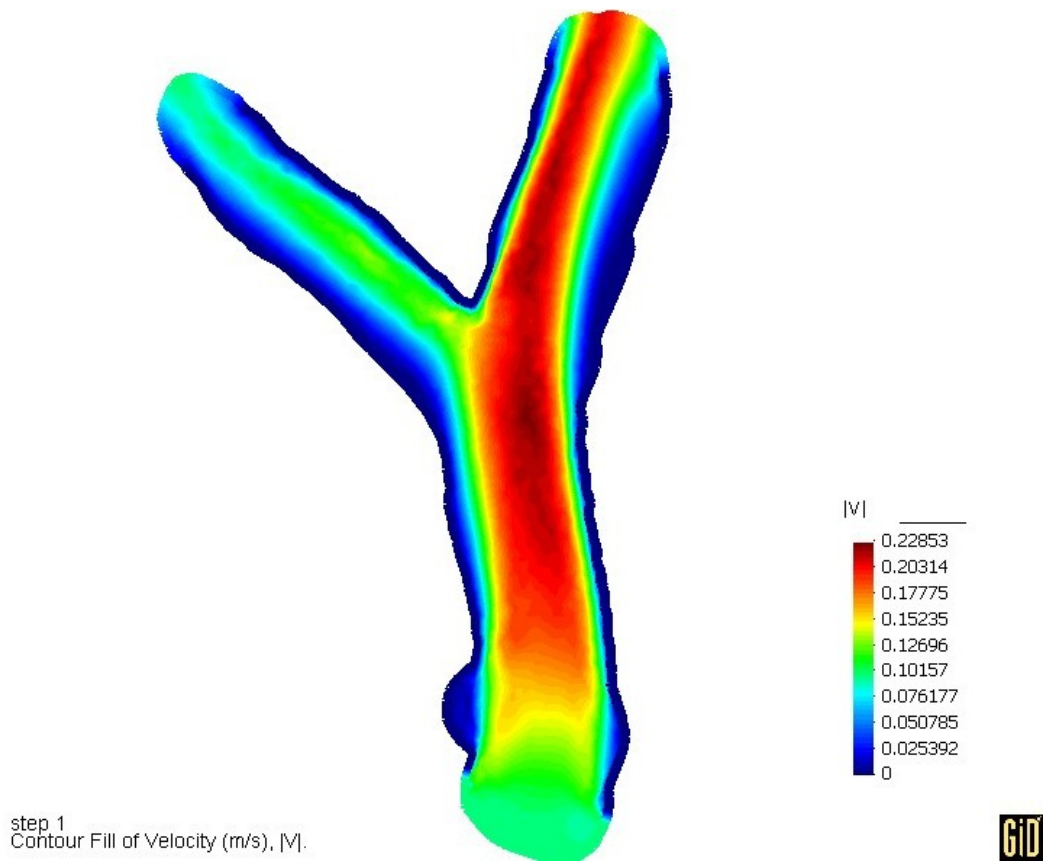
As is possible to see the velocity always have his sinusoidal profile, the velocity variations are modify by the changing of diameter section, but the velocity and the behaviour of the blood are comparable to the results obtained with the model with aneurism.

This fact is very important, because open the possibility to development in this field, acquiring imagine to real bio-imagine and translate it in data that can be used in a numerical simulation.

The changes portable to this solution are for example a modification of the surface where the blood cross like the entering and exit zone: a regular surface ideally cut by a bistuory have profiles more right, and so the velocity imposed can be studied better.

Other step will be the study with different imagines, so will be possible to confront the real deep of the body and work with the certain of right dimension.





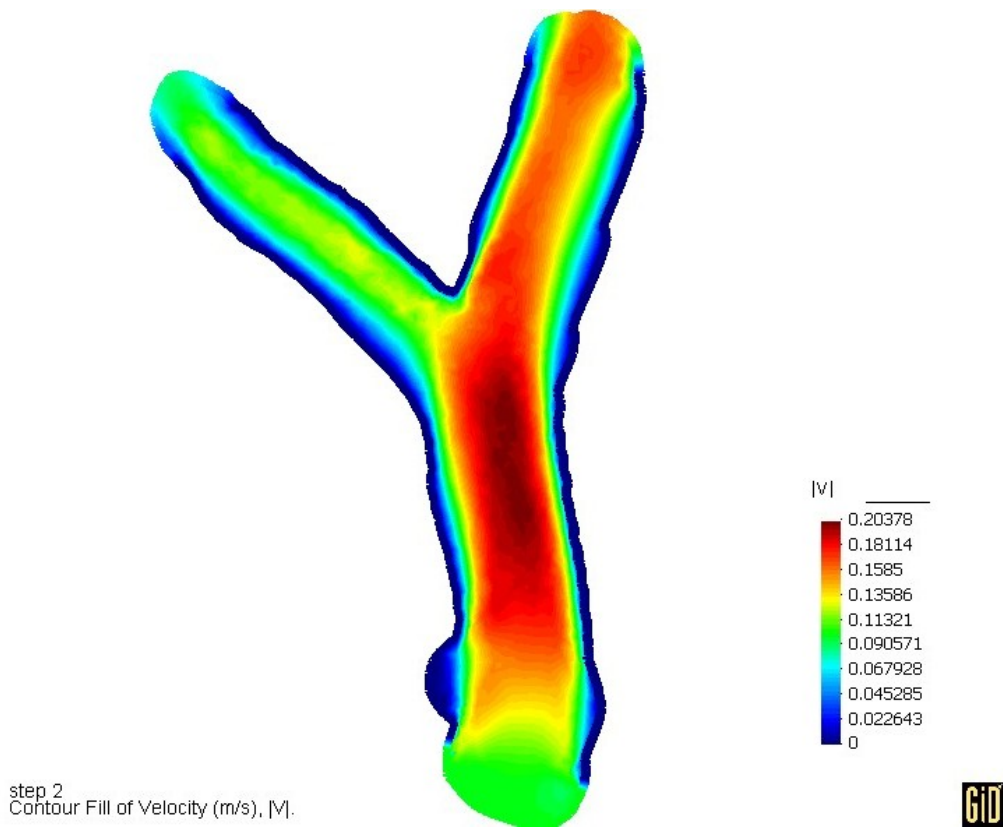


Figure 45 Velocity profile at 90°, 180°, 270° and 360°

10. Real Aorta reconstruction

The last experiment proposed was a reconstruction with real data of an aorta real. The subject has 27 years old and in wellness, he was subjected to an exam of magnetic resonance, and with this were registered the flow and the velocity of the blood flow and the geometry of the artery. So we reconstruct the conditions applicable to the vessel and design a geometry that correspond to the one registered during the exam.

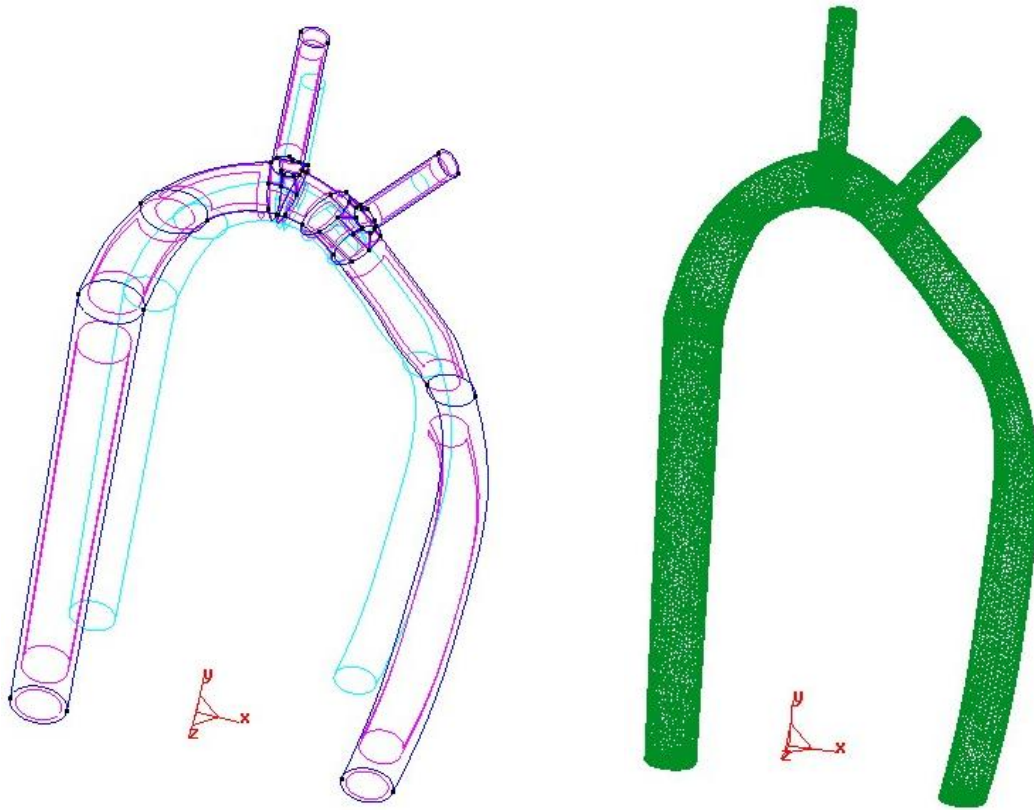


Figure 46 Geometry of the reconstructed aorta, geometry and mesh visualization

The goal of this last experiment is to confront the behaviour of the blood flow with the real one registered by the clinical exam effectuated. The idea is to compare the velocity profiles following the blood way, starting from the ascendant Aorta, that go out to the heart, until the descendent aorta, where the aorta go down to the abdominal aorta.

10.1. Data and Geometry

The geometry was reconstructed basing the design on the data of the magnetic resonance, we know the diameter in different altitudes of the vessel, so we put some circles with prefixed distance and after were constructed the cylinders and trying o follow the inclination and the degree of the aortic arc. The mesh data are so showed.

Element size (m)	Triangles number	Tetrahedras number
0.0022	22450	148095

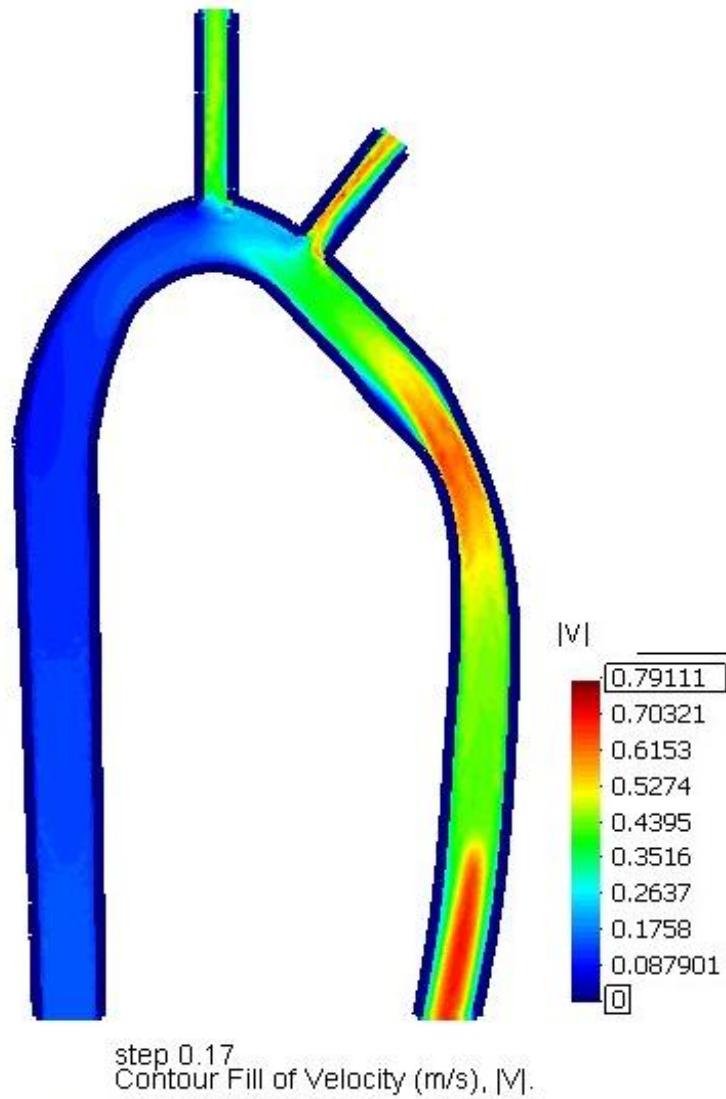


Figure 47 Representation of the absolute value of velocities

The principal dimensions are:

- Diameter of entering section 0.01705 m
- Diameter of exit section 0.0186 m
- Length of ascendant aorta 0.27 m
- Length of descendent aorta 0.25 m
- Diameters of outgoing superior sections 0.01 m

10.2. Results

Finding the goal to compare the real data with the simulations we construct the plots, joining the two kinds of graphics.

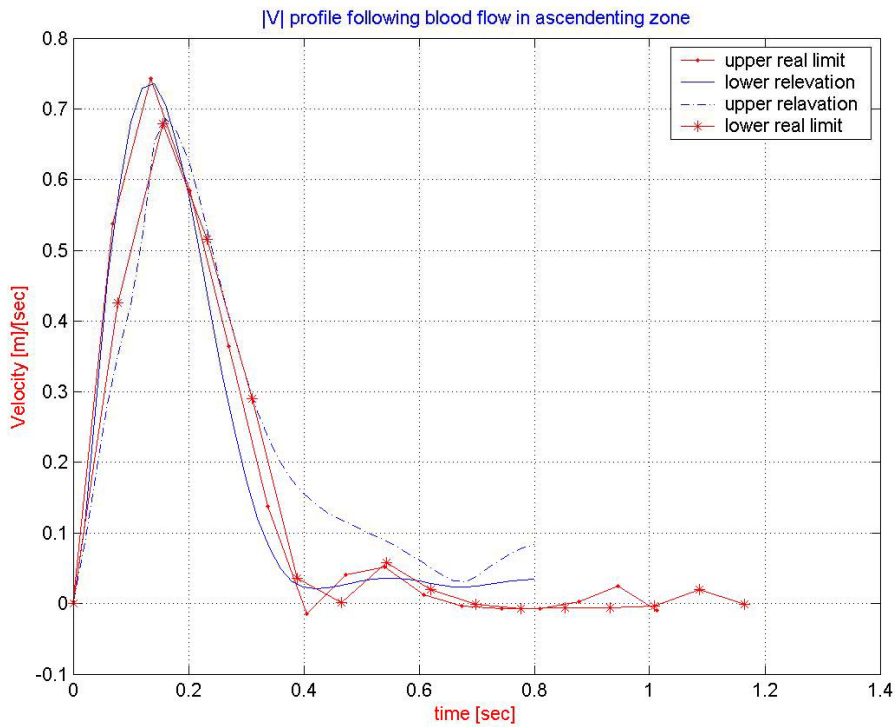


Figure 48 Representation of the velocity profiles in the ascending zone

So was possible to see how the simulation follows the test and which points go away too much to the real data. The points analyzed were taken in the middle of the hypothetical circular sections chosen. With this position we follow the verse of blood flow and go up until the bifurcations and after down till the final section where ideally finish the vessel.

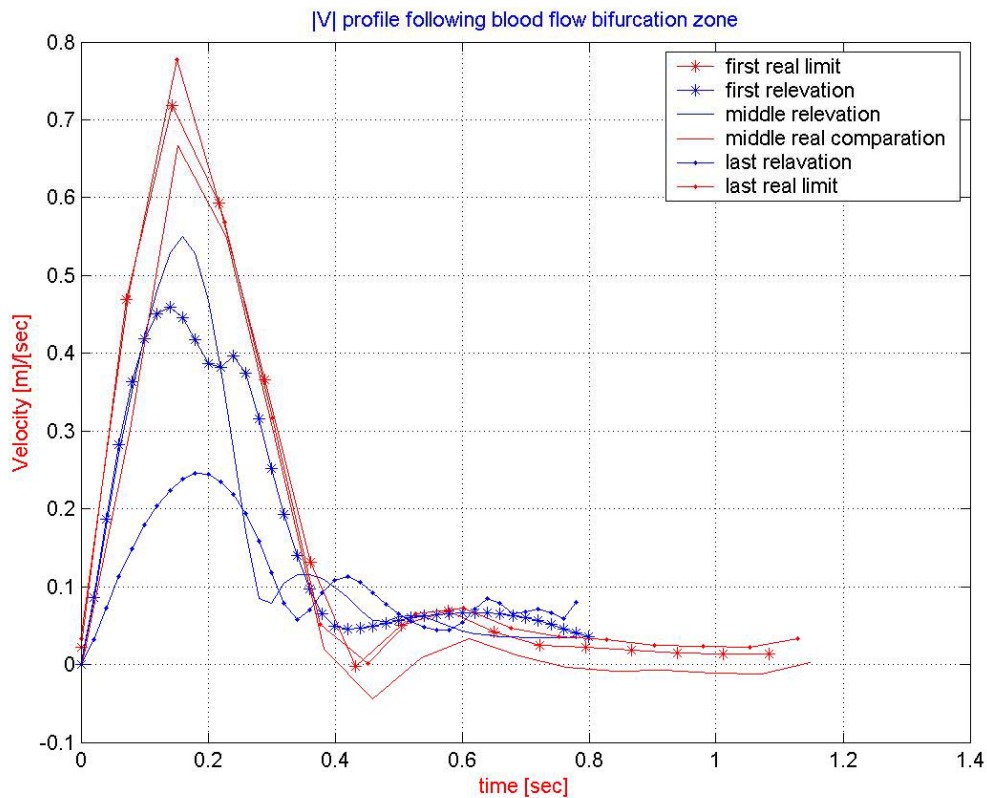


Figure 49 Representation of the velocity profiles in the aortic arc

Like is easy to see, the best results are the ones that belong to the first zone, the rising zone, the ascendant aorta, here the velocity, follows all the profile and takes similar values of magnitude, the pick zone is situated in the right place and the oscillations can be well recognized.

The second zone of study, the aortic arc, shows more difficult and troubles. In this place we find the bifurcations directed to the subclavia artery and the carotid, we only dispose of the initial section diameters, so we don't really know the behaviour of the vessels after this place, a possible restrict of the artery, the inclinations that the vessel can propose, are not represented, so the results are that in the simulation more blood go out confront to the experimental data.

This fact is visible by the big variation of velocity that we encounter and by the results in the lower part of the aorta, the descendent tract. Here the value are very different to the ones taken by the bio-image, because the values are near ten times littler than the values

of the waited ones, but we can denote that the pulsatile profile is equally conserved and a little shading is present, like in the real results.

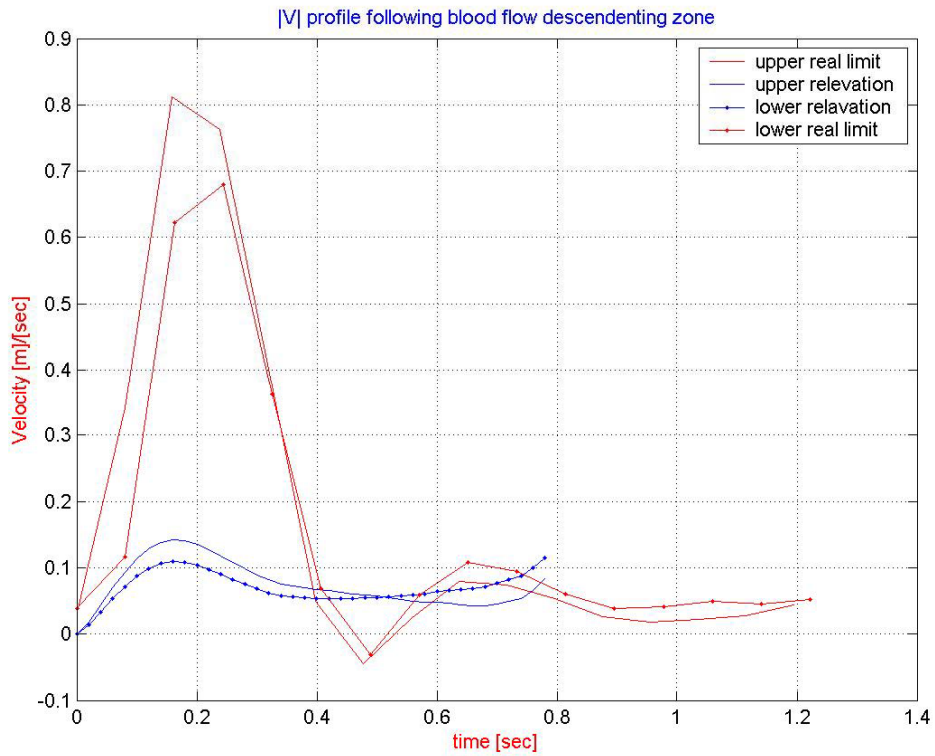


Figure 50 Representation of the velocity profiles in the descendent zone

11. 1D-3D Coupling in Carotid Modelization

11.1. Geometry and mesh

The geometry that we use was designed basing on the one-dimensional model, using three right tubes with no variable sections. This simplification was necessary to impose correctly the boundary conditions that one-dimensional program calculates before.

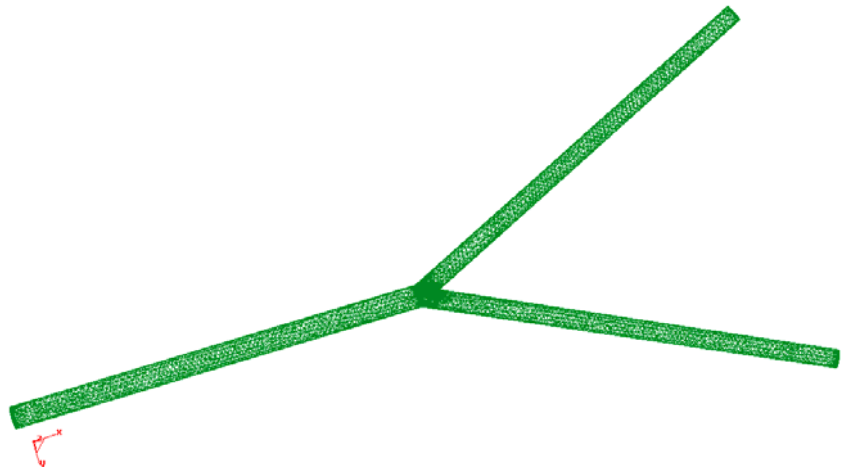


Figure 51 1D-3D geometry representation

The one-dimensional program gives the possibility to solve velocity and pressure in every points of the cardio-vascular system, allowing to use that results (wave shapes) in three-dimensional simulations like first approximation. The calculated pressure was used in the extremity of the external and internal carotid, like initial boundary condition of the three-dimensional blood fluid problem.

This process allows to study the movement of the pressure wave along the time and we can measure that value in every position of the trajectory. In the anterior cases where null-pressure conditions was used, the pressure values wasn't physiological due to the fact that no point in humane been has null-pressure value.

General dimension (m)	Surfaces dimension (m)	Number of triangle	Number of tetraedras
0.002	0.0007	12848	56926

	Initial Aorta (m)	Bifurcation (m)
Radio	0.00946	0.00764
Length	0.177	0.174

11.2. Conditions

To realize this simulation was used simple sinusoidal profile like initial boundary condition in the section were the flow come in (Carotid artery), here all the surface has the same value of velocity. This condition is approved because the velocity profile can stabilized itself before to come at bifurcation point, due that the length of the carotid is quite large respect the diameter dimension.

For the exit conditions was used a variable pressure field. Solved pressure was obtained with the one-dimensional fluid program, and the data was used to fix the pressure in the extremity of the internal and external carotid. To calculate that pressure, the same conditions had the same geometry were used, the velocity condition in the enter section was the same sinusoidal flow of the precedent cases, so we can simulate the same three-dimensional case. Putting the same velocity values of the one-dimensional problem, it is possible to have a preview of the behaviour at the of the blood in the carotid fundamental points, like the bifurcation or the exit. It is also possible to know how the pressure evolves its profile along the time during the simulation using those values in the three-dimensional test.

Density	1024	Kg / m ³
Viscosity	0.0035	Kg / m · s
Compressibility	0.0	s ² / m ²

The lateral vessels have the no slip boundary conditions. The flow takes the properties that usually are found in scientific literature.

Velocity (m/s)	Dynamic pressure (m² / s²)
$0.135 \cdot (1 + \sin(\pi \cdot t))$	$(P - (0.5 \cdot \rho \cdot (0.135 \cdot (1 + \sin(\pi \cdot t)))^2)) / \rho$

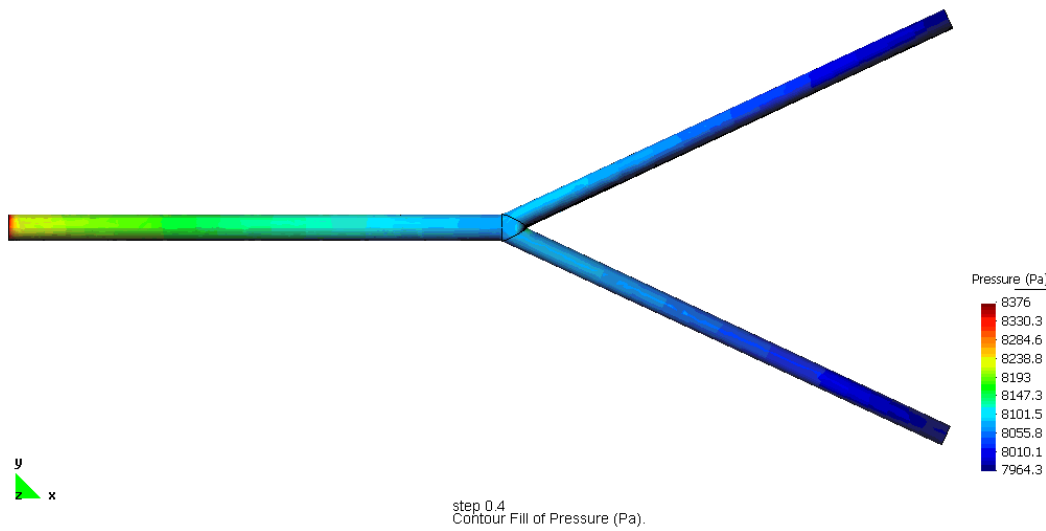
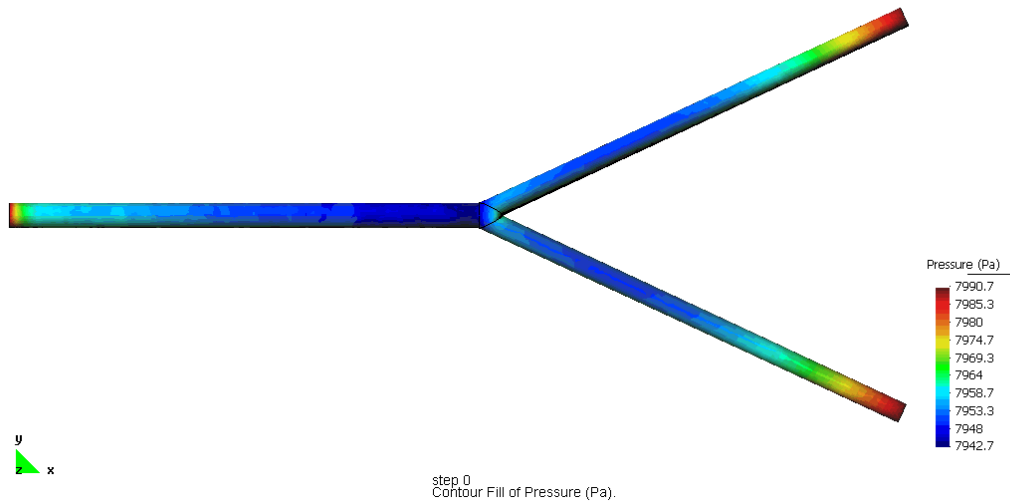
Where P is the initial pressure and ρ is the fluid density.

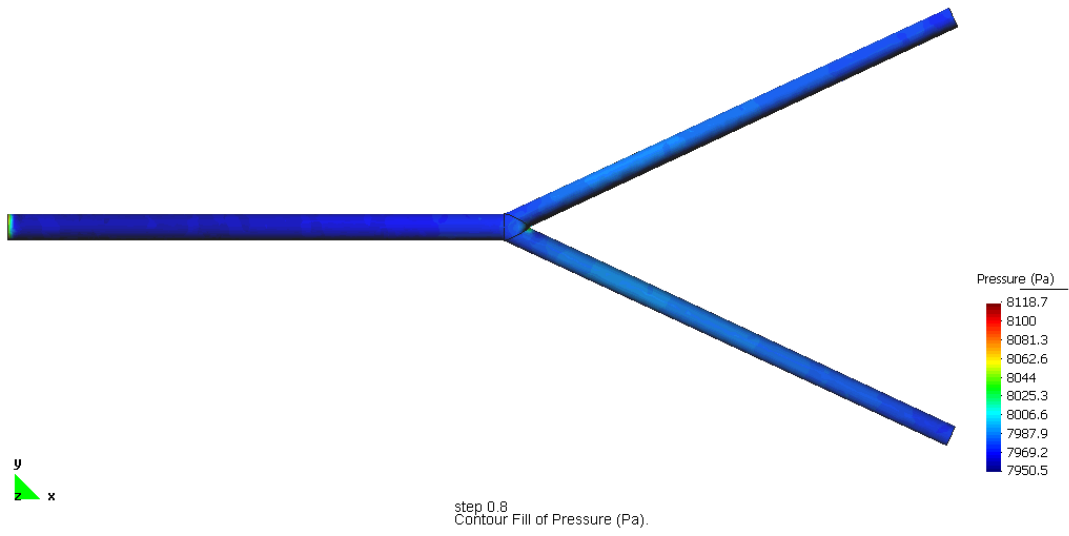
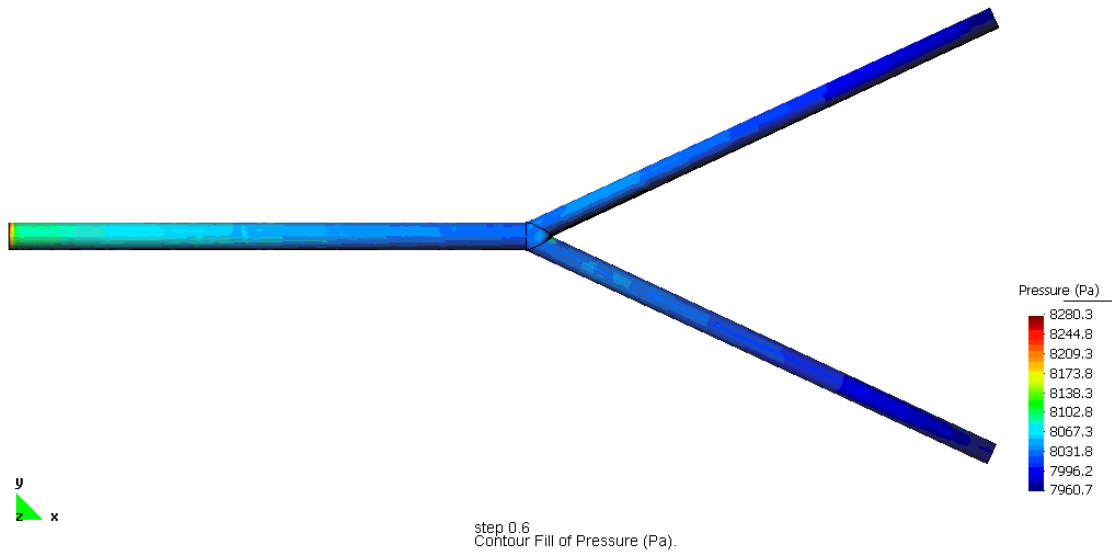
The simulation is realized in a time period that allows the full study of 4 sinusoidal cycles.

11.3. Results

The results show that the variable pressure allows the movement of the pressure wave along the carotid body.

Following are showed the pressure results for different time values.





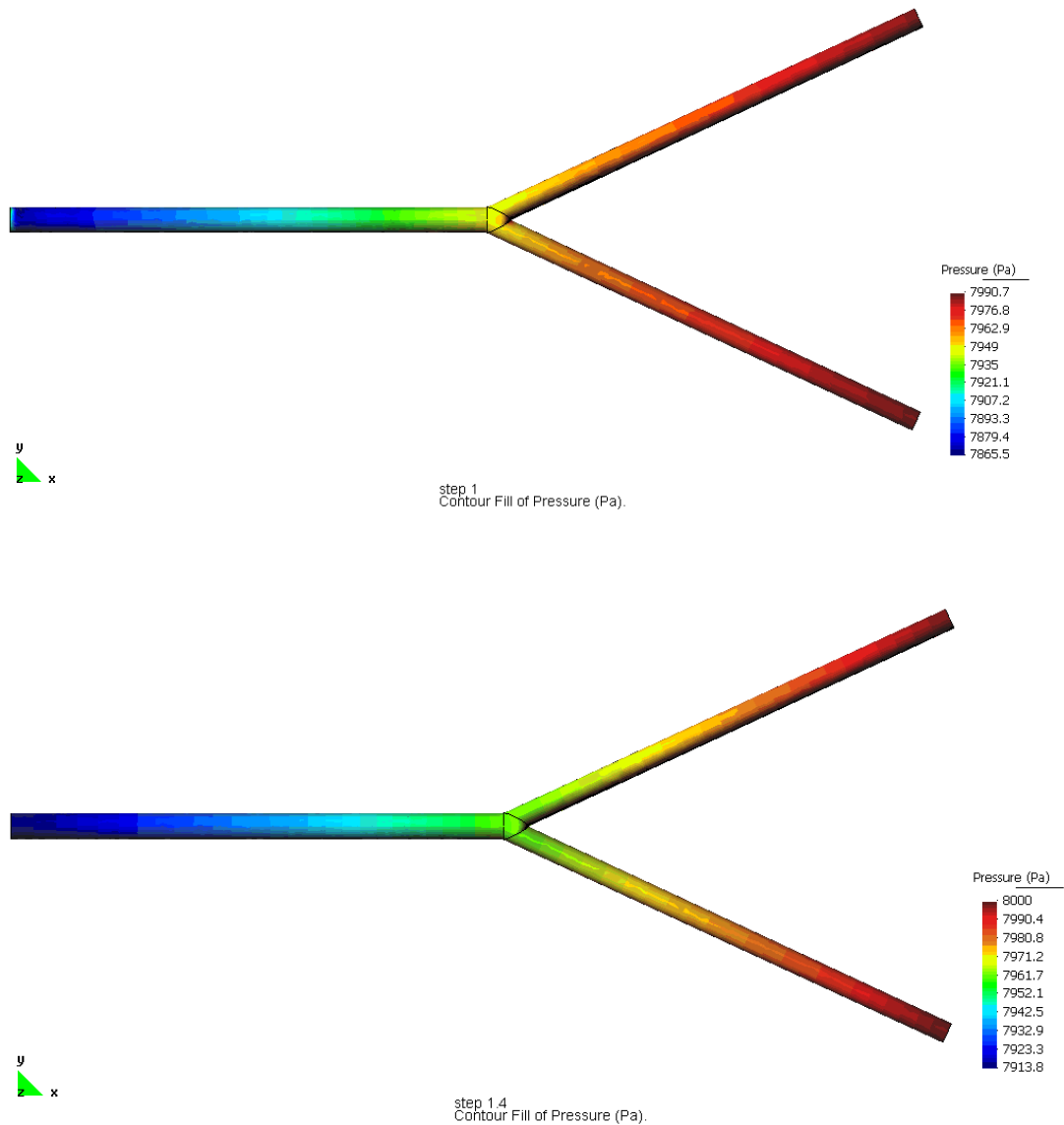


Figure 52 Pressure Wave displacement at different time steps

Like showed in the pictures the pressure wave produces a displacement of the minimum pressure point, that correspond at pick of velocity.

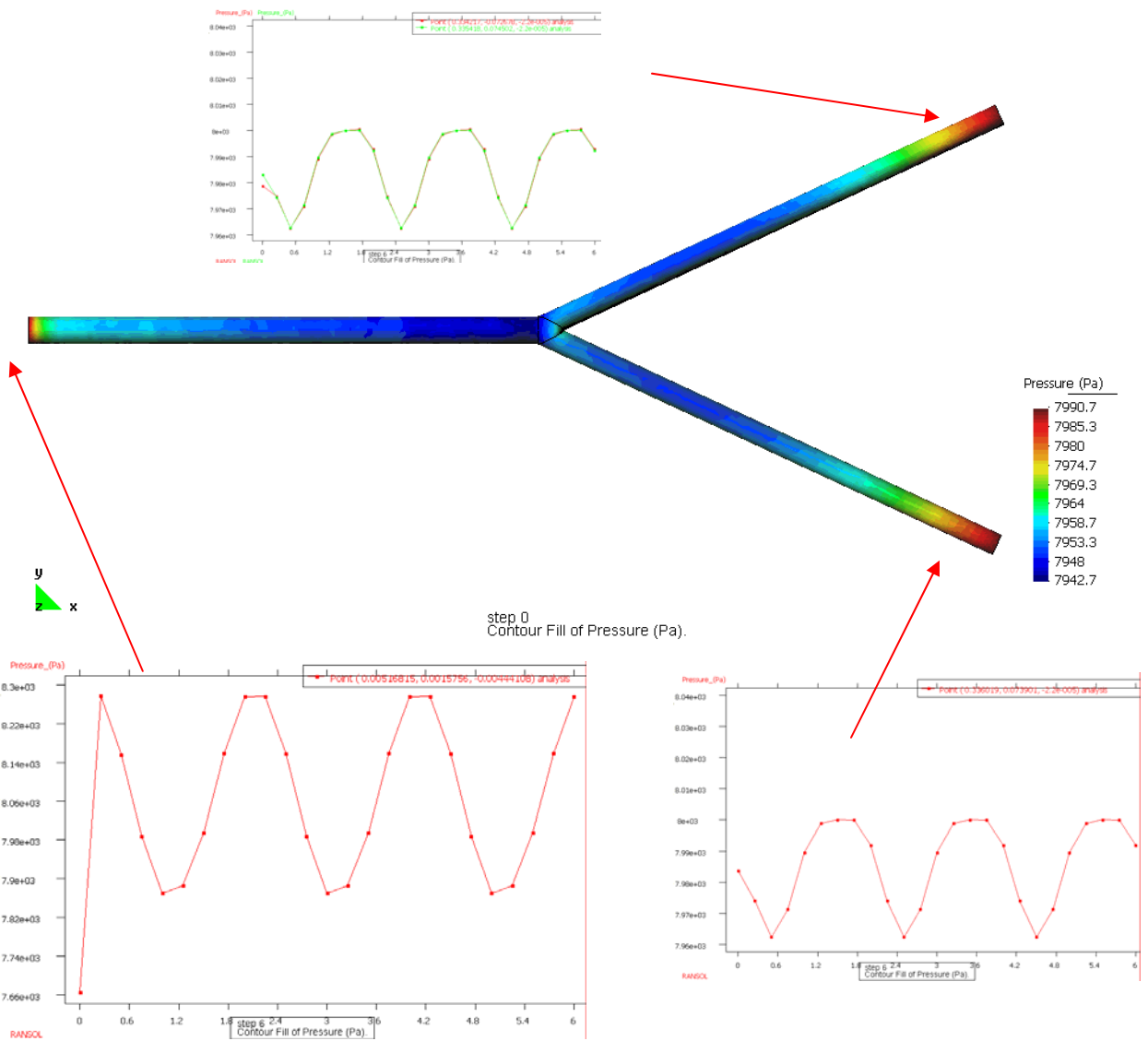


Figure 53 Pressure profiles in different sections of the geometry

These results are the bases of the future testes that will be run to study the fluid-structure interaction.

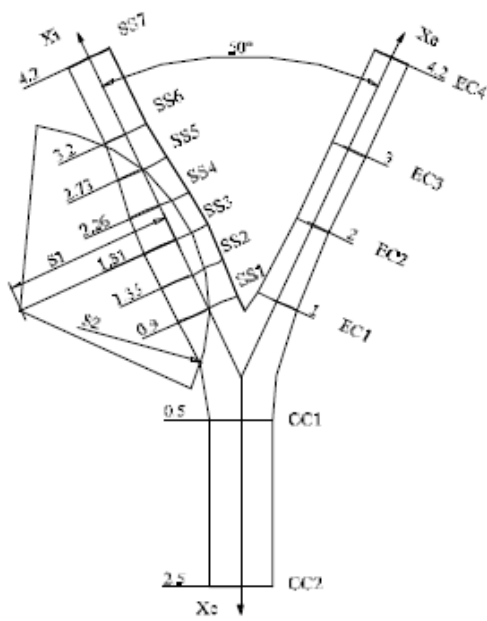
12. Bifurcacion Carotidea

The experiment explained here is the starting point of the coupling between the software that solve fluid problems and the structure solver one. This is very important because the possibility to use boundary conditions with pressure variation may the experiment nearer to the real scenario.

12.1. Geometry, Data and Mesh

The geometry utilized was the one showed in the next picture.

Every section has thought like a perfect circle and the bifurcation zone take an ondulated shape due to the fact that TDyn can joint and do an intersection between several surfaces, creating a unique and continuous surface.



Sección	Diámetro [cm]	
CC1	0.74	
CC2	0.74	
SS1	0.77182	
SS2	0.8214	
SS3	0.8214	
SS4	0.76368	
SS5	0.6364	
SS6	0.5254	
SS7	0.5254	
EC1	0.51356	
EC2	0.42032	
EC3	0.42032	
EC4	0.42032	
Referencias (estenosis)	Medida [cm]	
	80%	95%
S1	2	1.5
S2	2.20535	1.835

Figure 54. Geometry description

The constructed and meshed geometry takes this structure:

72240 tetraedras

10814 triangles

15000 nodes

With elements having mean dimension of 0.0008 meters

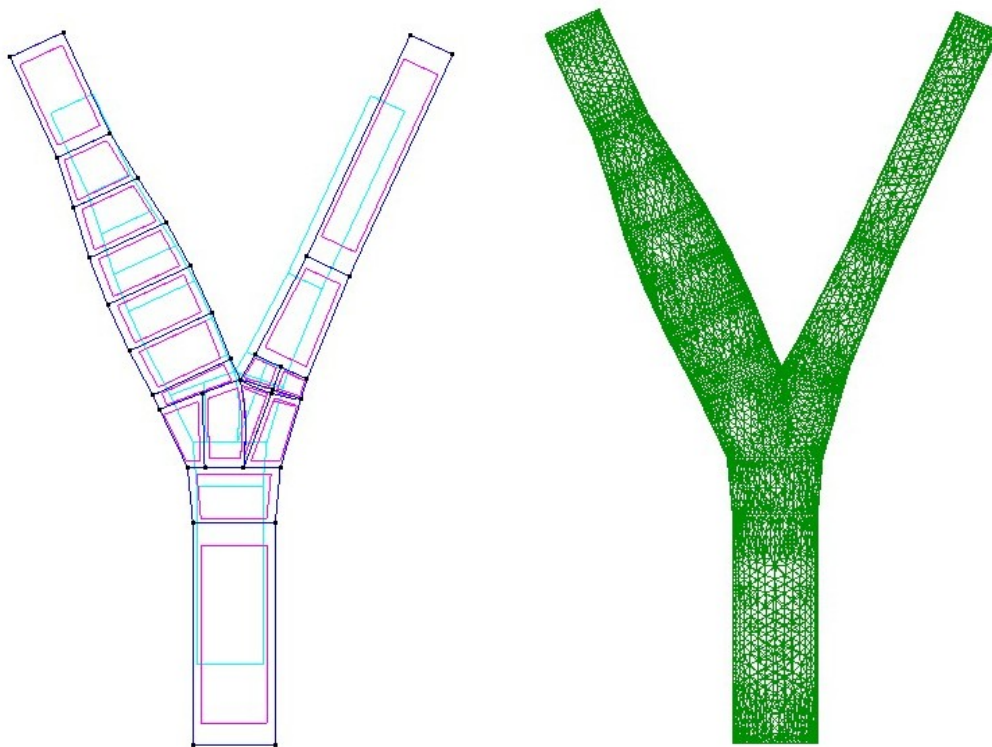


Figure 55 Geometry and mesh visualizations

The fluid properties that in this case is the blood are the usually encountered in literature and they have these values:

Density	1050	Kg / m ³
Viscosity	0.0035	Kg / m · s
Compressibility	0.0	s ² / m ²

At the lateral vessels the “No Slip Boundary Condition” is applied and in the enter section of the carotid, the lower one, we impose velocity conditions, at the exit sections instead of the velocity were used time variable pressure characteristics, fundamental thing for the task of this study.

The polynomial expression that govern the pressure wave in the exits is:

$$0.25 * ((-324810 * t^5 + 519790 * t^4 - 111590 * t^3 - 183520 * t^2 + 86640 * t) / 4 + 7350) / 1024$$

For the inner velocity the polinomy is:

$$2*(1-(x^2+z^2)/(0.0037^2))*(-1357*(t)^9+7443*(t)^8-17099*(t)^7+21255*(t)^6-15356*(t)^5+6379*(t)^4-1368*(t)^3+97*(t)^2+6*(t))$$

Step time chosen to run this test is 0.001 sec and 1000 steps were calculated with a maximum of 3 iterations to solve the problem.

No changes were effectuated in the measure unity, respect the default ones.

12.2. Results

The results obtained show the possibility of create a pressure wave that can displace itself along the geometry that follow a real vein model.

The velocities do not take big variations respect the precedent testes run with stables pressure, the pressure results reach optimal values and they seem to the values that we can record in a in vitro or in vivo test, with real vessel and blood.

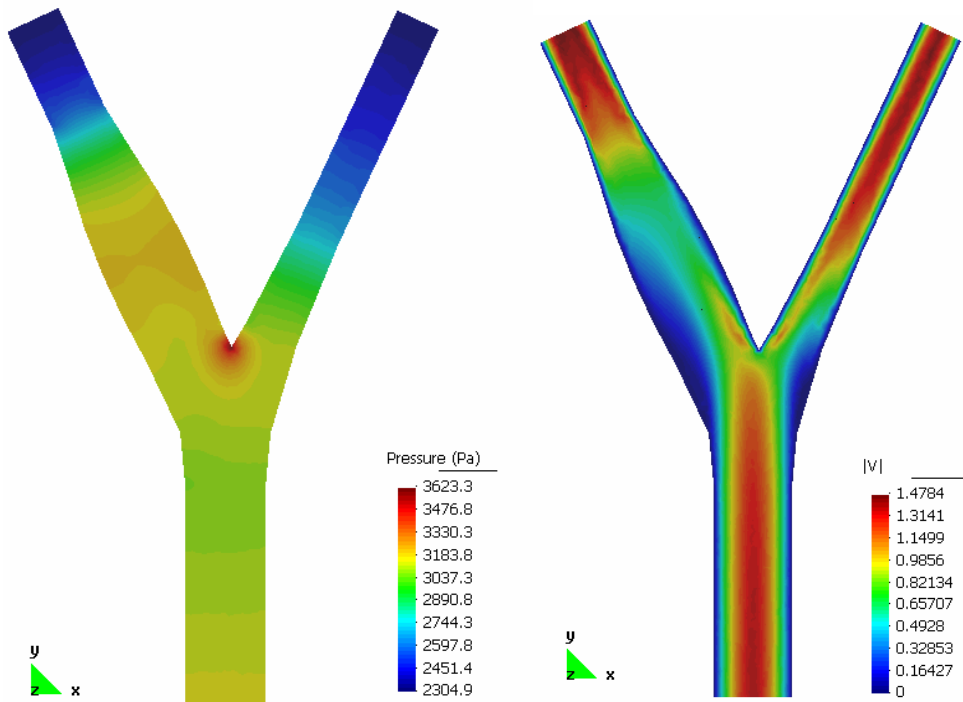


Figure 56 Pressure and Velocity results at 0,1 sec

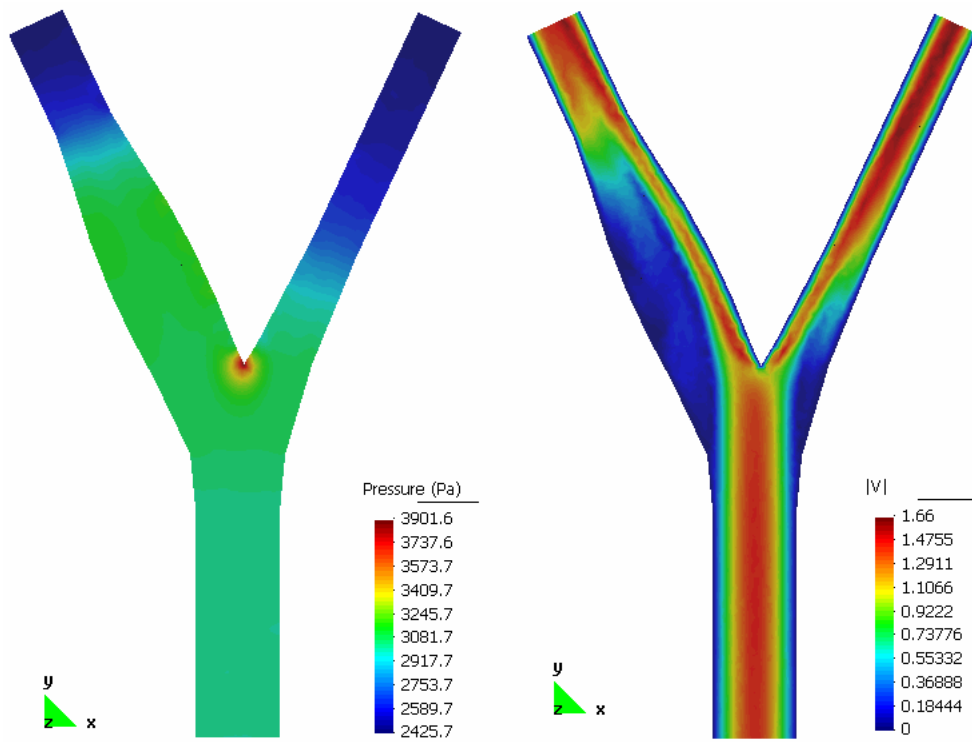


Figure 57 Pressure and Velocity results at 0,15 sec

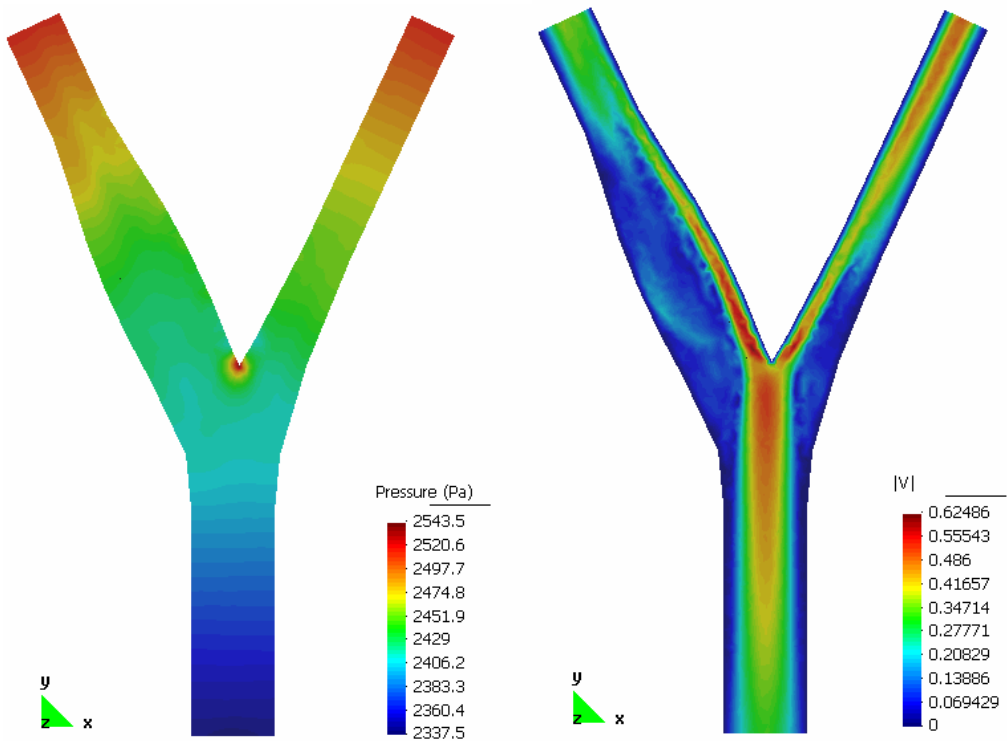


Figure 58 Pressure and Velocity results at 0,3 sec

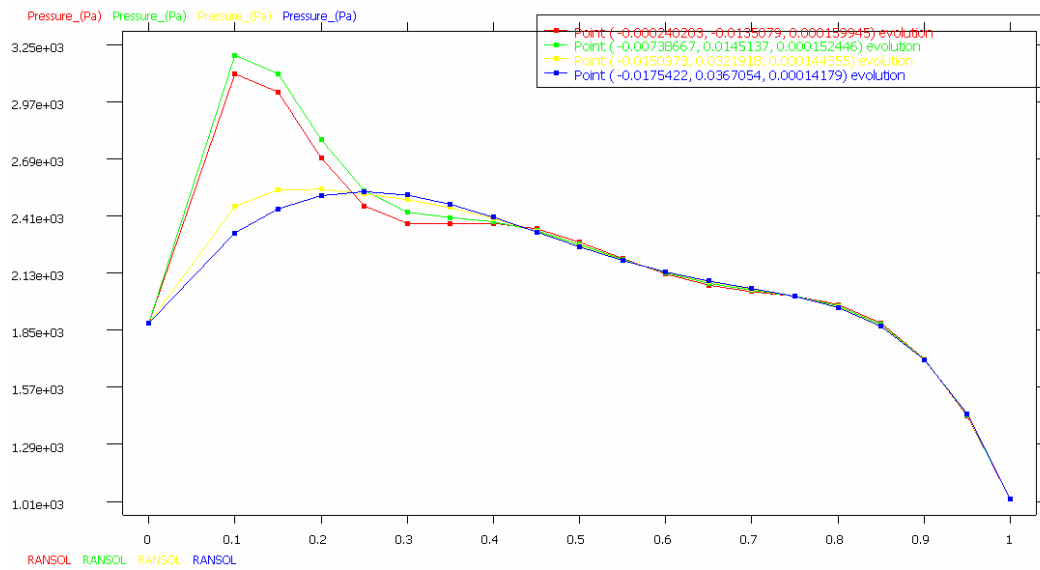


Figure 59 Pressure time evolution at the enter section (red line), at bifurcation point (green line), at right exit (yellow line) and at left exit (blue line)

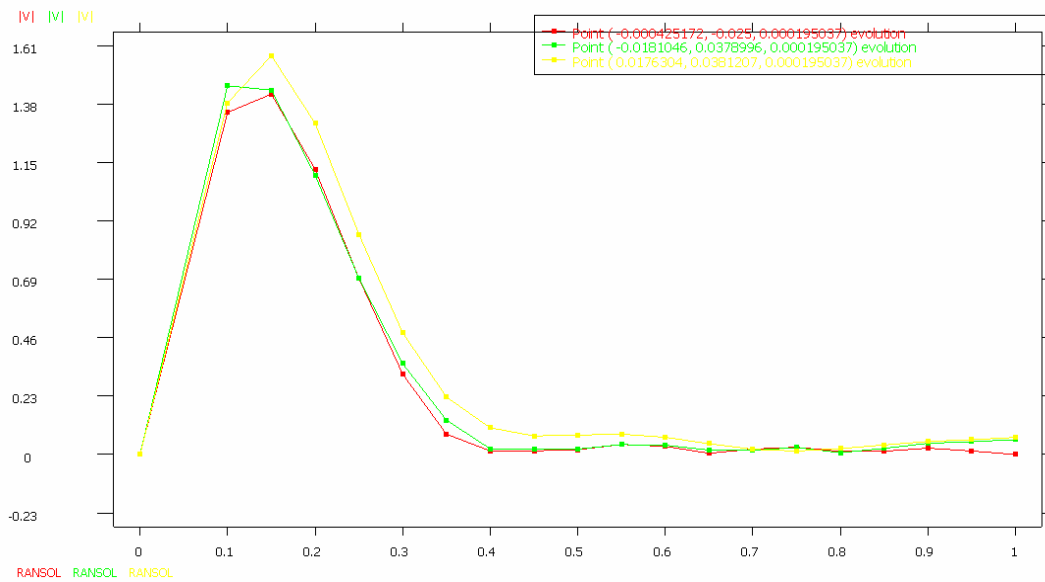


Figure 60 Velocity time evolution at the enter section (red line), at right exit (green line) and at left exit (yellow line)

13. Conclusions

Hemodynamic conditions, including velocity, pressure, shear and all the measurable variables, play an important role in the modulation of vascular adaptation and localization of vascular diseases. Understanding the hemodynamic factor and environment in a region of the vascular system, is consequently important field of research.

As we enter the information age, it is probable that the use of computer models to understand vascular blood flow, vessel deformation, mass transport, stress on the walls and vascular remodelling will increase dramatically. Increasing the data of the model the resolution maybe rise in difficulty; so is very important spent time in the right way to construct the model, and the right conditions used or imposed.

The results obtained give us the hope of good possibilities to develop the investigations about the hemodynamic field. The testes effectuated were the starting point of a bigger project, with the intention to simulate more complicated real cases.

Another step that we want to perform is the study of more realistic conditions of blood flow: the imposition of null pressure at the outgoing section doesn't emulate the real

physiologic condition, but is a good approximation to study the development and the behaviour of the flow in human or animal vessel. This approximation is it used, because the experiments were only focused in the study of the velocity. Now are yet in study models and variation of the yet used models with different values or condition in the pressure field, so that we can find a good response in the study of the propagation of the pressure waves in a cardiac pulsation. The study focused on the aneurysm and the variation of the vessel geometry; permit us to start a plan of study than can consider the vessel and circulatory diseases, like the ateroma plate or the same aneurysms.

Another step that we propose us is the coupling with models 1D that maybe can resolve some problems in way of the boundary condition of pressures or velocities. Some 1D models are yet studied and the next task is to make the 1D and 3D models joinable. This simplification will give us the possibility of the study of harder cases one of these may be the modelling and the flow simulation of an atherosclerosis troubles, or other diseases linked to the modifications of vessels elastic or physiological properties.

Appendix A. MatLab Programs

To develop these testes were necessary to use MatLab software to calculate some solution or to plot the data in the way that best show the target that we want to due. Here is presented the program that permit to compare the result of the first experiment with the theoretical ones

The work with MatLab represents the implementation of Womersley solution of velocity profile in a long and straight tube.

The program is set with all variable of default, but we have the possibility to change one of theme like we want with the instruction:

“womersley(t,R,period,prec,Nfin) “

Where t is the time that we want to analyze, R the radius, period the periodicity of the pulsation, prec is the precision of the computation, Nfin the last element of the sommatoria.

The principal function call a subroutine called *womersley2.mat*, that plot all the results of velocity and error calculated by the other two function “*Womvel.mat* “ and “*errperc.mat*”.

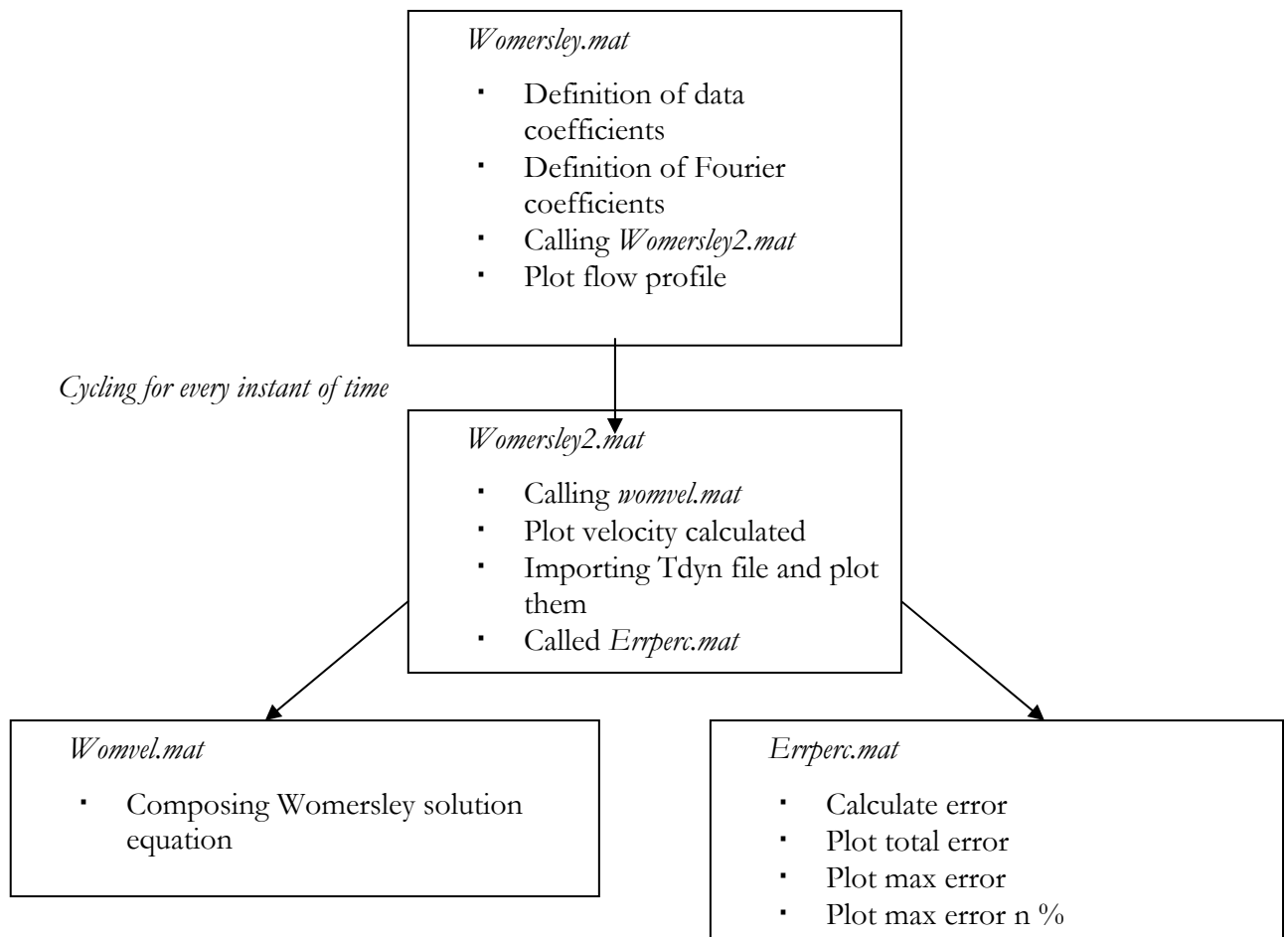
i) Program structure

The MatLab program is organized in four different functions.

The main function that we have to call to run the program is *WOMERSLEY.MAT*, this one call a subroutine function called *WOMERSLEY2.MAT* for all the time instants that we analyze.

The *WOMERSLEY2.MAT* function calls also two other subroutine functions: *WOMVEL.MAT* and *ERRPERC.MAT* that do all the computational steps and calculate all that need for the analysis and for the results plotting. The structure of the program is simple and is easily explicable with a flow diagram.

The next flow diagram shows the program structure, in every box is shown the computations of the function. After we have a description of the fundamental points of computation of every function.



ii) Womersley.mat

This function calculates the exact solution written by Womersley. It computes all the coefficients B_n , of Fourier's transformed, required to calculate the summatory inside the solution; we have composed this summatory, ending at a prefixed step with only 4 elements, because adding other coefficients cannot improve the performance of the solution. ^[5]

Here we also fix the coefficients of anatomical and fluid dynamic data. Finally it plots the wave of the blood flow; we also have to impose here the sinusoidal profile of the flow, like before written:

$$Q(t) = V_{media} * A_{vessel} * (1 + \text{sen}(w*t))$$

The signification of the symbols is the same of the ones used in the chapter 4.

iii) Womersley2.mat

This function recalls the sub functions womvel.mat and errperc.mat and plots the solutions derived by these, in all the four instant of time that we selected in the principal function Womersley.mat

This function plots the theoretical velocity profile together with the fem analytical solution, in the same plot, posed in the results chapter.

We do this to comparate better the results derived from the two different way of solution, and appreciate the difference of amplitude that come to them.

iv) Womvel.mat

Here we construct the Womersley's solution starting by Fourier's coefficient and calculating other parameters derived by fluid dynamic and anatomical ones.

v) Errperc.mat

This function is constructed to calculate the errors between the numerical and exact solution.

We plot 4 graphic (figure 2, 3, 4, 5), the first shows the percent error, between the two results, for all the length of the diameter and the 4 different step of time.

The second plot (figure 3) shows the error in absolute value. This is important because we can see where the error come to the max values and pose the attention in the right place of the first plot.

In the third one we plotted the max error in unity of measure (m/sec) recordable for the 4 instants of time.

The ultimate figure plots the bigger error expressed in percent ratio.

The entire ratio are composed by the difference between the two solutions in absolute value and reported to the exact solution.

The necessity to chose the exact solution like numerator come from the necessity to have numbers different to zero, F.E.M. solution instead go to zero in the extreme positions of the diameter.

vi) The interpolation

Many problems run need a function that follow a pulsatile flow, the simplest way o obtain it was to record the data of the flow and construct a interpolator polinomy that can emulate the behavior of the real flow or velocity.

The data were taken by a second function that permits us to construct a bi-dimensional array starting to graphical informations like a plot. So we convert the data in the range of value of our problem and so we can dispose of data that can reconstruct the wave form that we want to reproduce.

This file now is put in a function (**polifit.mat**) that can interpolate with a polinomy the data, we only have to decide the grade of polynomial expression. After this step we only take and use the polinomy expression in the F.E.M. program with the right transformation due to the change of measure unities or change of profile (for example if we impose a paraboloid profile).

Appendix B. TCL Statement

Tcl (Tool Command Language) is a very powerful dynamic programming language, suitable for a very wide range of uses, including web and desktop applications, networking, administration, testing and many more. Open source and business-friendly, Tcl is a mature yet evolving language that is truly cross platform, easily deployed and highly extensible.

Tk is a graphical user interface toolkit that takes developing desktop applications to a higher level than conventional approaches. Tk is the standard GUI not only for Tcl, but for many other dynamic languages, and can produce rich, native applications that run unchanged across Windows, Mac OS X, Linux and more.

Here is presented the code of the statement used in the fifth experiment realized, this is a file with .tcl extension. This code is used by Tdyn to implement other functions, and is possible, in the latest version, to enable a field, so introducing the correct address of the statement calculate contemporary other solution, different to the standard one of Tdyn.

The TCL-TK extension is the way to create script files to automatize any process created with GiD. With this language it is possible to add new windows or new functionalities to the program.

For more information about the TCL-TK programming language look at www.scriptics.com.

*If such TCL file exists, it must be in the problem type directory; the name of the file has to be the problem type name with the **.tcl** extension.*

```
# Open file "caudal_entrada" ...
cd {C:\Documents and Settings\maurizio\Mis documentos\FEM\Risutati
Modelli\AortaEdu}
```

```
# ... opening file .txt with the nodes and the elements, set the program variables to
calculate
```

```
set f [open entrada.txt r+]
set normal [gets $f]
set readnode 1
while {[eof $f]} {
    set feed [gets $f]
    if {$feed == "Elements"} {
        set readnode 0
        set feed [gets $f]
    }
    if {$readnode} { # if readnode is 1 it do the process
        set nodeid [lindex $feed 0]
        set node($nodeid) [lrange $feed 1 end]
        # puts $fileid "$node($nodeid)"
    } else {
        set elemid [lindex $feed 0]
        set elem($elemid) [lrange $feed 1 end]
        # puts $fileid "$elemid=$elem($elemid)"
    }
}
```

```

close $f
# joint the 2 lists of elements and nodes to have a correspondence between elements
and coordinates
set elems [array names elem]
foreach elemid $elems {
    set nodeindex 1
    foreach nodeid $elem($elemid) {
        set elemnodes($elemid,$nodeindex) $node($nodeid)
        #
        puts $fileid
"elemnodes($elemid,$nodeindex)=$elemnodes($elemid,$nodeindex)"
        incr nodeindex
    }
}

proc TdynTcl_FinishStep { } {
    # the calculation of the rate flow is so implemented. taking the baricenter of any
elements

    upvar elem elem
    upvar elemnodes elemnodes
    upvar normal normal

    # Reading Tdyn internal time
    set t [TdynTcl_Time]
    if { $t <= 0.0 } {
        catch { file delete "caudalentrata.txt"}
        set fileid [open caudalentrata.txt a+]
        puts $fileid "Time FlowRate m3/sec\n"
    } else {
        set fileid [open caudalentrata.txt a+]
    }
}

```

```

}
set flowrate 0.0
set elems [array names elem]

# starting calculating flow. the first instruction permite to simplificate the
computation
foreach elemid $elems {
  set velem 0.0
  foreach nodeid $elem($elemid) {
    set velx [TdynTcl_VecVal vx $nodeid]
    set vely [TdynTcl_VecVal vy $nodeid]
    set velz [TdynTcl_VecVal vz $nodeid]
    set veln [expr $velx*[lindex $normal 0]+ \
                $vely*[lindex $normal 1]+ \
                $velz*[lindex $normal 2]]
    set velem [expr $velem+$veln]
  }

  set velem [expr $velem/[llength $elem($elemid)] ]

  for {set i 2} {$i<=[llength $elem($elemid)]} {incr i} {
    set vx([expr $i-1]) [expr [lindex $elemnodes($elemid,$i) 0]-[lindex
$elemnodes($elemid,1) 0]]
    set vy([expr $i-1]) [expr [lindex $elemnodes($elemid,$i) 1]-[lindex
$elemnodes($elemid,1) 1]]
    set vz([expr $i-1]) [expr [lindex $elemnodes($elemid,$i) 2]-[lindex
$elemnodes($elemid,1) 2]]
  }
  set aux [expr pow($vy(1)*$vz(2)-$vz(1)*$vy(2),2)]
  set aux [expr $aux+pow($vz(1)*$vx(2)-$vx(1)*$vz(2),2)]
  set aux [expr $aux+pow($vx(1)*$vy(2)-$vy(1)*$vx(2),2)]
  set area [expr 0.5*sqrt($aux)]
  set flowrate [expr $flowrate + $area * $velem]
}

```



```
}  
puts $fileid "$t $flowrate "  
  
# closing file  
close $fileid  
}
```

Appendix C. Tdyn Graphics

The option **Countur Fill** allows the visualization of colored zones, in which a variable, or a component, varies between two defined values. GiD can use as many colors as allowed by the graphical capabilities of the computer. When a high number of colors is used, the variation of these colors looks continuous, but the visualization becomes slower unless the Fast-Rotation option is used. A menu of the variables to be represented will be shown, from which the one to be displayed will be chosen, by using the default analysis and step selected.

Vectors will be unfolded into X, Y, and Z components and its module. Symmetric matrix values will be unfolded into S_{xx} component, S_{yy} component, S_{zz} component, S_{xy} component, S_{yz} component and S_{xz} component of the original matrix and also into S_i component, S_{ii} component and S_{iii} component in 3D problems or angular variation in 2D problems. Any of these components can be selected to be visualized.

Several configuration options can be accessed via the Options menu.

- **Number Of Colors:** Here the number of colors of the results color ramp can be specified.

- *Width Intervals:* fixes the width of each color zone. For instance, if a width interval of 2 is set, each color will represent a zone where the results differ at the most in two units.
- *Set Limits:* this option is used to tell the program which contour limits should use when there are no user defined limits: the absolute minimum and maximum of all sets or shown sets, for the actual step or for all steps.
- *Define limits:* when choosing this option the ContourLimits window appears (this option is also available in the postprocess toolbar). With this window the user can set the minimum/maximum value that Contour Fill should use. Outliers will be drawn with the color defined in the OutMinColor/OutMaxColor option.
- *Reset Limit Values:* this option resets the values defined in the DefineLimits option.
- *Reset All:* this option sets all Contour Fill options by default.
- *Max/Min Options:* Inside this group, several options for the minimum or maximum value can be defined:
- *ResetValue:* here the user can reset the maximum/minimum value, so that the default value is used.
- *OutMaxColor / OutMinColor:* with this option the user can specify how the outliers values should be drawn: Black, Max/MinColor, Transparent or Material.
- *Def. MaxColor / Def. MinColor:* this option lets the user define the color for the minimum or maximum value for the color scale to start with.
- *Color scale:* Specifies the properties of the color scale:
- *Standard:* the color scale will be the default: starting from blue (minimum) through green until red (maximum).

- *Inverse Standard: the color scale will just be the inverse of the default: starting from red (minimum) through green until blue (maximum).*
- *Terrain Map: a physical-map like color ramp will be used.*
- *Black White: Black for Minimum and White for Maximum, the scale will be a grey ramp.*
- *Scale Ramp: this option lets the user specify how should the ramp change from minimum color to the maximum color: Tangent, ArcTangent or Linear. The default is ArcTangent.*
- *Scale Type: tells GiD how the colors between the minimum color and the maximum color should change: RGB or HSV.*
- *Color window: a window is popped up to let the user configure the colour scale of the contours easily*

References

13.1. Books, newspaper and journal.

1. Charles A. Taylor. *A Computation Framework for Investigating Hemodynamic Factors in Vascular Adaptation and Disease*, 1996.
2. Charles A. Taylor, Thomas J. R. Hughes and Christopher K. Zarins. *Finite Element Modelling of Three-Dimensional Pulsatile Flow in the Abdominal Aorta: Relevance to Arteriosclerosis*. *Annals of Biomedical Engineering*, Vol 26 pp. 975-987, 1998.
3. J. N. Reddy, D. K. Gartling. *The finite Element Method in Heat Transfer and Fluid Dynamics*. Cap 1,2,4.

4. COMPASS *Ingeniería y Sistemas S.A.* Tdyn. **Environment for Fluid Dynamics (Navier Stokes equations), Turbulence, Heat Transfer, Advection of Species and Free surface simulation. Theoretical background and Tdyn 3D tutorial.** March 2002.
5. G. Gilardi. **Analisi Due.** McGraw-Hill, 2^a edizione 1996.
6. G. Gilardi. **Analisi Uno.** McGraw-Hill, 2^a edizione 1995.
7. M. Lei, D. P. Giddens, S. A. Jones, F. Loth, H. Bassiouny. **Pulsatile Flow in an End-to-Side Vascular Graft Model: Comparison of Computations With Experimental Data.** *Journal of Biomechanical Engineering*, February 2001, vol. 123.
8. D. Citrini, G. Nosedà, **Idraulica** (seconda edizione), casa editrice Ambrosiana 1987.
9. Patrick Segers, Pascal Verdonck, **Role of tapering in aortic wave reflection: hydraulic and mathematical model study.** *Journal of Biomechanics* October 1999.
10. S. J. Sherwin, V. Franke, J. Peirò, K. Parker. **One-dimensional modelling of a vascular network in space-time variables.**
11. C. A. Taylor, T.J.R. Hughes, C.k. Zarins. **Effect of exercise on hemodynamic conditions in the abdominal aorta.** *Journal of vascular surgery* volume 29 number 6.
12. C. A. Taylor, T.J.R. Hughes, C.k. Zarins. **Finite Element Modeling of Three-Dimensional Pulsatile Flow in the Abdominal Aorta: Relevance to Atherosclerosis.** *Annals of Biomedical Engineering*, Vol 26 1998.
13. F.Nicoud **Hemodynamic changes induced by stenting in elastic arteries.** *Center for turbulence research , Annual research briefs* 2002.
14. Meena Sankaranarayanan, Leok Poh Chua, Dhanjoo N Ghista, Yong Seng Tan. **Computational model of blood flow in the aorto-coronary bypass graft.** *Biomedical Engineering OnLine* march 2005.

15. Ferdinando Auricchio. **Mechanics of solid materials: theoretical and computational aspects.** October 2003
16. D.E.M. Taylor, A.L. Steven. **Blood Flow theory and practice.** Academic Press.
17. C.M. Müller-Carger, M.Cerroloza, **Biongeniería en Iberoamérica: avances y desarrollos.** CIMNE. Barcelona. Colección de métodos computacionales en ingeniería: teoría y aplicaciones.
18. **GID, the personal pre and postprocessor,** Reference manual version 7

13.2. Web sites

1. <http://www.tesionline.it/default/index.asp>
2. <http://users.rcn.com/jkimball.ma.ultranet/BiologyPages/C/Circulation2.html>
3. <http://www.cardioexpert.it/site/home.asp>
4. <http://www.dica33.it>
5. <http://www.mathworks.com/>
6. <http://www.mathworks.it/>
7. http://it.wikipedia.org/wiki/Pagina_principale